AD_____

CONTRACT NUMBER DAMD17-95-C-5086

TITLE: Retrieval of Water Channels by Endocytosis in Renal Epithelia

PRINCIPAL INVESTIGATOR: Abdul J. Mia, Ph.D.
Thomas Yorio, Ph.D.

CONTRACTING ORGANIZATION: Jarvis Christian College
Hawkins, TX 75765

REPORT DATE: July 1997

TYPE OF REPORT: Annual

PREPARED FOR: Commander
U.S. Army Medical Research and Materiel Command
Fort Detrick, Maryland 21702-5012

REPORT DOCUMENTATION PAGE

Form Approved
OMB No. 0704-0188

1. AGENCY USE ONLY *(Leave blank)*	2. REPORT DATE	3. REPORT TYPE AND DATES COVERED
	July 1997	Annual (5 Jun 96 - 4 Jun 97)

4. TITLE AND SUBTITLE
Retrieval of Water Channels by Endocytosis in Renal Epithelia

5. FUNDING NUMBERS
DAMD17-95-C-5086

6. AUTHOR(S)
Abdul J. Mia, Ph.D.
Thomas Yorio, Ph.D.

7. PERFORMING ORGANIZATION NAME(S) AND ADDRESS(ES)
Jarvis Christian College
Hawkins, TX 75765

8. PERFORMING ORGANIZATION REPORT NUMBER

9. SPONSORING/MONITORING AGENCY NAME(S) AND ADDRESS(ES)
Commander
U.S. Army Medical Research and Materiel Command
Fort Detrick, MD 21702-5012

10. SPONSORING/MONITORING AGENCY REPORT NUMBER

11. SUPPLEMENTARY NOTES

12a. DISTRIBUTION / AVAILABILITY STATEMENT
Approved for public release; distribution unlimited

12b. DISTRIBUTION CODE

13. ABSTRACT *(Maximum 200)*

Combat crew effectiveness is crucial during sustained and demanding military operations. In particular, how soldiers cope with conditions of excess heat and fluid deprivation will ultimately impact on their ability to carry out their stated objectives. If the kidney should become damaged or obstructed, the kidney will fail to respond to the hormone vasopressin, which is responsible for regulating water balance. Understanding the specific mechanisms involved in the regulation of water balance by the kidney will provide information needed to design preventive measures for dealing with potential adverse conditions that may result in water deprivation and decreased renal responsiveness to vasopressin. The present study is designed to determine the cellular mechanisms involved in reduced fluid reabsorption and membrane reorganization following the removal of the actions of ADH. It is proposed that following removal of hormone, proteinaceous water channels, located in the apical membrane, are internalized through a process of endocytosis, delivered to the cytosol as a consequence of changes in intracellular calcium concentrations, PKC enzyme activation and reorganization of the microfilament/microtubule system. These studies may lead to new drug or non-drug treatment regimes that could be used to enhance the kidney's responsiveness to vasopressin or to maintain the level of water reabsorptive capacity of soldiers facing harsh environmental conditions of prolonged exposure to dehydration and water deprivation or impaired renal function from injury. Such preventive measures will be essential for maintaining the performance and combat effectiveness of our military forces.

14. SUBJECT TERMS
Water flow; ADH (vasopressin); Endocytosis; Water Channels; Channel Retrieval; Membrane Retrieval

15. NUMBER OF PAGES
97

16. PRICE CODE

17. SECURITY CLASSIFICATION OF REPORT	18. SECURITY CLASSIFICATION OF THIS PAGE	19. SECURITY CLASSIFICATION OF ABSTRACT	20. LIMITATION OF ABSTRACT
Unclassified	Unclassified	Unclassified	Unlimited

FOREWORD

Opinions, interpretations, conclusions and recommendations are those of the author and are not necessarily endorsed by the U.S. Army.

__X__ Where copyrighted material is quoted, permission has been obtained to use such material.

__X__ Where material from documents designated for limited distribution is quoted, permission has been obtained to use the material.

__X__ Citations of commercial organizations and trade names in this report do not constitute an official Department of Army endorsement or approval of the products or services of these organizations.

__X__ In conducting research using animals, the investigator(s) adhered to the "Guide for the Care and Use of Laboratory Animals," prepared by the Committee on Care and Use of Laboratory Animals of the Institute of Laboratory Resources, National Research Council (NIH Publication No. 86-23, Revised 1985).

__N/A__ For the protection of human subjects, the investigator(s) adhered to policies of applicable Federal Law 45 CFR 46.

__N/A__ In conducting research utilizing recombinant DNA technology, the investigator(s) adhered to current guidelines promulgated by the National Institutes of Health.

__N/A__ In the conduct of research utilizing recombinant DNA, the investigator(s) adhered to the NIH Guidelines for Research Involving Recombinant DNA Molecules.

__N/A__ In the conduct of research involving hazardous organisms, the investigator(s) adhered to the CDC-NIH Guide for Biosafety in Microbiological and Biomedical Laboratories.

Gerald J. Mia 7/1/94

PI - Signature Date

TABLE OF CONTENTS

Nature of Caveolae and Coated Pits and Vesicles in Cells of Toad Urinary Bladders and Endocytosis

Abstract

The morphology and structural identity of caveolae, clathrin- and nonclathrin-coated pits and vesicles were investigated in toad urinary bladder epithelial, endothelial and smooth muscle cells. Transmission electron microscopic techniques using conventional ultrathin sectioning, freeze fracture and immunoantibody labeling techniques were used to determine the distributional patterns, characteristics and morphology of caveolae in toad urinary bladder cells. We found a large population of caveolae arise predominantly along the basal plasma membranes of the granular cells by making invagination as small sacs. Caveolae appear to constitute a major microdomain membrane component in granular cells of toad urinary bladders. Many of these caveolae, becoming free vesicles by detaching from the basal plasma membranes by an endocytic process, migrate to various locations of the cells, including the apical membrane where they are seen to fuse. This process of caveolar transcytosis results in the transfer of membrane components from the basal to the apical plasma membranes. This appears to be unidirectional, as caveolar endocytosis was not observed at the apical plasma membrane domain. Caveolar fusion at the apical plasma membrane increases apical membrane surface area and may deliver key unknown proteins which could play important roles in membrane permeability processes. We also identified clathrin- and nonclathrin-coated pits and vesicles in toad urinary bladder cells. These pits often arise from the basal plasma membrane by membrane invagination, like caveolae, along the same membrane domain side by side with

caveolae and they were similarly found to be involved in transcytosis like caveolae in granular epithelial cells but to a lesser extent. Therefore, three distinct pits and vesicles appear to be involved in transcytosis from basal to apical membranes in toad urinary bladder epithelial cells. This appears to be unique, involving three independent types of pits and vesicles involved in transcellular processes in a single type of cells. Caveolae also occur in the endothelial and smooth muscle cells, where their number could run into thousands per cell. The diameter of the caveolae in toad urinary bladder cells was measured using both horizontal and vertical plots and their diameter was found to be in the range between 45 and 150nm with a mean diameter of ~85nm. Immunoantibody localization carried out using anti-caveolin IgG and protein-A gold particles indicated the membranes of caveolae are enriched with the 22kd protein, caveolin. Gold particles were found to be associated with caveolae present along the basal plasma membranes as well as within the cytoplasm. We also detected the presence of PKCγ using anti-PKCγ IgG and protein-A gold particles which occurred in association with caveolae. These caveolae laced with gold particles give the impression that they traverse through the cytoplasm to the apical membrane for possible fusion. Mucosal HRP labeling indicated little evidence of HRP incorporation into cytoplasmic vesicles other than the multivesicular bodies. Serosal HRP labeling results in the incorporation of HRP into caveolae along the basolateral cellular attachments. Caveolae may be involved in the transport of basal components to the apical membrane. This process may play a role in the regulation of apical membrane permeability.

Introduction

Biological membranes are dynamic cellular structures with the capacity to regulate a variety of cellular functions including the transmembrane osmotic water flow and cellular homeostasis. In the case of the kidney, the distal renal cortical tubular cells reabsorb fluid from the external environment into the systemic circulation to prevent dehydration at times of thirst. This fluid reabsorption process is governed by antidiuretic hormone (ADH, vasopressin), which promotes rapid transmembrane osmotic water flow across renal epithelia and other renal membrane model including the amphibian urinary bladders. The amphibian urinary bladders have been used as important membrane models (Bentley, 1958; Dratwa et al., 1979; DiBona, 1981; Wade et al., 1981; Masur et al., 1984; Kachadorian et al., 1985; Mia et al., 1983, 1987, 1994 and others) for studies on transmembrane osmotic water transport regulated by ADH.

In most classical studies of water transport process, amphibian urinary bladder sacs are always mounted at the end of a glass tubing with the mucosal side facing inward and the serosal side facing outward. An osmotic gradient is then established by 1/10 dilution of mucosal Ringer's solution to enhance water flow from mucosal to serosal solutions under ADH influence. Serosal ADH stimulation causes the insertion of water channels (aquaporins) into the apical membrane by fusion events to enhance water flow. Following ADH stimulation, water flow diminishes within a short period of time and the apical membrane returns to a normal control state by endocytosis of the water channels. A number of studies indicate that during endocytosis, portions of the inserted apical membrane are retrieved as vesicles back into the cytoplasm (Wade et al., 1981; Masur et al., 1984; Harris et al., 1986; Coleman et al., 1987; Ding et al., 1988; Brown et al., 1990; Zeidel et al., 1992, 1993; Coleman and Wade, 1994 and

others). It was also reported that aggrephores or aggrephores-like clathrin-coated vesicles are endocytosed and may contribute in the restoration of the apical membranes to the pre-hormone normal cellular state. Several other workers (Franki et al., 1986; Ding et al., 1988; Hays et al., 1994) held that vesicles perhaps coated with clathrin (nonaggrephore-mediated system) were the principal path for particle delivery in frogs and further presented evidence to support that aggrephore and nonaggrephore-mediated systems operate in parallel in toads. We demonstrated that the apical membrane of the granular epithelial cells of the toad urinary bladders internalize by a process of endocytosis during retrieval periods following withdrawal of ADH (Mia et al., 1993, 1994). However, we have not achieved a clear understanding of the nature of endocytosis in the retrieval of water channels (aquaporins) following their insertion at the apical membranes. In addition, we identified a large number of caveolae at the basal plasma membrane in toad urinary bladder epithelia (Mia et al., 1996a, b, c). We found that these caveolae were involved in transcytosis and fusion with the apical plasma membrane. Therefore, this study was designed to evaluate the role of caveolae in ADH sensitive toad urinary bladder cells and to monitor the process of endocytosis using a fluid-phase marker, horseradish peroxidase (HRP), in both mucosal and serosal bathing Ringer's solutions to gain understanding of the nature of endocytosis across each membrane surface.

Materials and Methods

Experimental Tissues:

Tropical toads *Bufo marinus* and Northern grass frogs *Rana pipiens* were purchased from either NASCO, Ft. Atkinson, WI, or Carolina Biological Supply Company, Burlington, NC, and were placed in an aquatic environment at 23^{0}C with

continuous irrigation of running tap water. They were fed live crickets biweekly.

Materials:

Supplies for the current experimental investigations were obtained from the following sources and biochemical companies: Monoclonal anti-caveolin IgG was purchased from Santa Cruz Biotechnology (Santa Mateo, CA), monoclonal anti-PKC γ IgG from Seikagaku America (Rockville, MD), 8-Arginine vasopressin (ADH), BSA, horseradish peroxidase (HRP, type II), diaminobenzidine (DAB) tetrahydrochloride and H_2O_2 from Sigma Chemical Co., (St. Louis, MO) and protein A-gold probes from EY Laboratories (San Mateo, CA). The concentration of ADH used in the current series of experiments was 100 mU/ml and was added to the Ringer's solution on the serosal side of the toad urinary bladders.

Experimental Protocol:

Control hemibladder sacs surgically removed from doubly pithed toads were quickly submerged in 2% glutaraldehyde made in PIPES buffer (0.02M). Other control and experimental hemibladder sacs upon surgical removal from doubly-pithed toads, were placed in aerated isotonic Ringer's solution. The bladders were suspended individually at the ends of glass tubes and then equilibrated 20 min in continuously aerated Ringer's solution (Bentley, 1958; Mia et al., 1983, 1987, 1991a). Identical hemibladder pairs from individual animals were used as control and experimental tissues. Several experiments were performed for studying either ADH effects or incorporation of HRP into bladder cells through mucosal and serosal sides of the bladder sacs. In one set of experiments, bladder sacs both inside and outside were bathed in full-strength isotonic Ringer's solution with no imposed osmotic gradient.

The experimental bladder sacs received serosal stimulation with 100 mU/ml ADH for 10 or 15 min but the control sacs (no hormone) were retained in normal Ringer's solution. We emptied the mucosal solution from both control and ADH-stimulated bladder sacs and replaced with 1/10 Ringer's solution containing HRP (5mg/ml). Following three quick serosal buffer rinses of both control and hormone-stimulated sacs, the bladder sacs were placed in full-strength Ringer's solution and allowed 20 or 30 min retrieval for endocytosis prior to tissue fixation. In the second set of experiments, both sides of bladder sacs were bathed in full-strength Ringer's solution, and therefore with no osmotic gradient. Control bladders received only HRP in the serosal bathing solution and the experimental bladders received HRP and ADH, and allowed 10 min stimulation for incorporation of HRP through the serosal side of the bladders before tissue fixation was accomplished. We also carried out identical experiments using Con-A-gold conjugated with HRP. In experiments with mezerein (MZ), MZ at a concentration of 10^{-6}M was added to the mucosal side of the sac. Control and experimental tissues following treatments for 15, 30 or 60 min under identical experimental conditions processed for electron microscopy.

Tissue Preparations for Electron Microscopy:

Following experimental procedures, bladder sacs, still suspended at the ends of glass tubes, were transferred to pre-cooled Ringer's solution on ice and bladders rinsed internally with cold deionized water containing 5.7% sucrose solution (Harris et al., 1986). The bladders were emptied and fixed internally with 2% cold glutaraldehyde in PIPES buffer and then externally using the same fixative. Fixation was carried out for 1 hr. Following buffer rinses at room temperature, the bladders were exposed to DAB using 2mg/ml plus 2 ml of 1% H_2O_2 in PIPES buffer for 30 min for producing

HRP reaction products. The bladder sacs were buffer rinsed, minced and postfixed in 1% osmium tetroxide for an additional hr. These tissues received thorough washes with deionized water and processed for embedding in epon resin for transmission electron microscopic (TEM) studies (Mia et al., 1994). Tissue blocks were polymerized overnight in an oven at 60°C. In other studies, urinary bladders sacs were removed from the ends of the glass tubes, emptied and dropped into 2% glutaraldehyde in PIPES and allowed fixation for 1 hr at room temperature. Following buffer rinses, urinary bladder tissues were separated into individual tissue samples according to need for scanning and transmission electron microscopic (SEM, TEM) preparations. Tissues retained for SEM were dehydrated through exchanges of acetone and liquified Peldri II for critical point drying (Mia et al. 1994), whereas the tissues for TEM studies were minced in PIPES buffer and separated for conventional TEM, freeze fracture and immunogold labeling. For TEM preparations, minced tissues were dehydrated through a mixture of ethanol and propylene oxide for casting into individual epon blocks. Tissue blocks were polymerized overnight in an oven at 60°C. Ultrathin sections showing silver to light gold interference color were made using a diamond knife. These sections were taken on bare copper or nickel grids and then exposed to uranyl acetate and lead citrate for viewing in the TEM. Some grids containing HRP tissue sections were kept without staining with heavy metals for identifying HRP reaction products. Electron micrographs were taken at X31,500 in cases where necessary for comparison.

Freeze Fracture Preparations:

For freeze fracture preparation, tissues received no postfixation with osmium tetroxide, but cryoprotected with 30% glycerol (Mia et al., 1989). Small pieces of cryoprotected bladder tissue were placed on copper holders and then frozen by

plunging into liquid freon at -190^{0}C in a liquid nitrogen bath. Tissues were then transferred into Balzers 400T apparatus and fractured at -100^{0}C with a metal knife cooled with liquid nitrogen. The fractured surfaces were allowed to etch for 5 or 10 min prior to shadowing with evaporated platinum at 35^0 and then coated with evaporated carbon at 0^{0}C. The replicas thus made were removed quickly and coated with a drop of 1% collodion while the tissues were still frozen and then digested with 2.5% Na hypochlorite solution. The replicas were washed and taken on bare copper grids for TEM observations.

Immunoelectron Microscopic Preparations:

Localization of Anti-caveolin and Anti-PKC isozyme γ:

For immunogold labeling, tissues received fixation with 2% glutaraldehyde in PIPES buffer with no postfixation with osmium tetroxide, but dehydrated through exchanges of graded ethanol and L. R. White and then cast into blocks in L.R.White (Mia et al., 1991a,b). Tissue blocks were polymerized at 60^{0}C in closed gelatin capsules for 15 hours in a vacuum oven. Tissue blocks were trimmed and sliced with a diamond knife and the ultrathin sections were taken on pre-cleaned bare nickel grids to perform procedures for localization of caveolin (Rothberg et al., 1992; Lisanti et al., 1994) and PKC isozyme γ (Mia et al., 1991b, 1992) using anti-caveolin IgG and anti-PKCγ IgG antibodies and protein-A gold probes. The anti-caveolin and anti-PKC were diluted separately in freshly prepared 0.1% BSA in PBS and then filtered through 0.2 μm Millipore filter. Ultrathin sections were pre-absorbed with 0.1% BSA for 10 min prior to immunoantibody and gold labeling. These sections were then exposed separately to anti-caveolin or anti-PKCγ monoclonal antibodies (dilution 1/25 using 0.1% BSA in PBS) for 2 hrs and then buffer rinsed for labeling with proteins A-gold

particles (dilution 1/25 using 0.1% BSA) for additional 2 hrs. Control tissues were pre-exposed to either 0.1% BSA or monoclonal antibodies and then to protein A-gold particles. Each grid received extensive rinses 5 min each in 10 drops of filtered 0.1% BSA in PBS between treatments. The grids were then exposed to uranyl acetate and lead citrate for increasing contrast to view in the TEM (Mia et al., 1991a,b, 1992).

Results

Cellular Composition of Toad Urinary Bladder:

The toad urinary bladder is composed of a thin layer containing cell types that include granular, mitochondria-rich, goblet, smooth muscle and endothelial cells. Of these, only the granular, mitochondria-rich and goblet cells, forming a coherent sheet of mucosal epithelium, face the urinary lumen whereas the smooth muscle and endothelial cells along with collagen fibrils form the supporting matrix beneath the mucosal epithelium. A diagrammatic view (Fig. 1) is presented to show the relative distribution of cells in toad urinary bladder tissue. The epithelium of toad urinary bladder is composed of nearly 80% granular cells (Choi, 1963). These cells respond to ADH similar to that of the mammalian kidney cortical cells (Hays et al., 1987) with an insertion of water channels, aquaporins, (Chevalier et al., 1974; Kachadorian et al., 1977, 1985; Mia et al., 1989 and others) and in conformational changes (DiBona et al., 1969; Mia et al., 1983, 1987, 1988) to enhanced reabsorption of fluid from the urinary side into the systematic circulation. Figure 2 represents a low power electron micrograph of toad urinary bladder to demonstrate the distribution of cell types as shown in the diagram (Fig. 1). As can be seen, the granular (G), goblet (J) and mitochondria-rich (R) cells line up the mucosal side of the bladder sac facing the urinary cavity (L). The collagen fibrils (F), smooth muscle (M) and the endothelial

cells (E) surrounding the blood capillary occur on the serosal side remote from the mucosal cavity of the urinary bladder.

Origin of Caveolae in Toad Urinary Bladder Tissues:

In a recent report on the experimental induction of endocytosis involving apical plasma membrane internalization and remodeling in toad urinary bladders, we described the occurrence of a type of coated vesicles in the granular epithelial cells (Mia et al., 1994). These coated vesicles are now determined to be caveolae. Caveolae in amphibian urinary bladder granular epithelial cells commonly originate by invagination of the basal plasma membranes of the granular cells. They can be identified by their small size and flask-shaped morphology appearing at the basal plasma membranes from which they originate. Upon separation from the basal plasma membranes, while retaining their small size, they assume a rounded shape as they diffuse to various locations of the cytoplasm. A low power transmission electron micrograph is represented in figure 3 to show granular cells with the position of the apical plasma membranes (AM) in relation to the basal plasma membranes (B) where caveolae are most frequently localized (arrows). A higher TEM view is presented in figure 4 to depict the presence of caveolae at the basal plasma membranes (B) of granular cells of toad urinary bladders fixed in glutaraldehyde in situ with no stimulation with ADH. As can be seen in this figure a large number of flask-shaped caveolae (arrows) of various sizes are present along the basal plasma membranes (B) immediately inner to the basal lamina (W) of a granular cell. As in endothelial and other cells, caveolae in toad urinary bladder cells arise by inpocketing of the basal plasma membranes of the granular cells regardless whether such cells appear attached to smooth muscles or along collagen fibrils. Figure 5 represents a glancing ultrathin

section cut across granular cells (G), collagen fibrils (F) and a smooth muscle cell (M) showing the composite view of the presence of a large number of caveolae (arrows) along the plasma membrane of these cells. Freeze fracture replica preparations following deep etching revealed the distribution of many caveolae (arrows) along the basal plasma membrane and deep in the cytoplasm of a granular cell (Fig. 6). Most commonly caveolae occur as single units as in figure 4 (arrows) and in figure 7 (short arrows) from the basal plasma membrane surfaces but at times, they may form clusters through invagination of the plasma membranes (Fig. 7, arrows). However, some of the clustered caveolae as seen at or near the basal plasma membranes may merely represent their sectional views because of the existence of a circular remnant of the basal lamina within the caveolae clusters (Fig. 7, fine arrows). It is likely that these caveolae clusters are the results of glancing sections of the toad bladder sacs which have extensive infoldings on the serosal side of the membrane. SEM images taken from the serosal sides of the urinary bladder sacs following critical point drying and platinum and carbon coatings revealed such extensive infoldings (Fig. 8). Clustered caveolae as seen in the ultrathin sections with rosette configuration (Fig. 7) can also be observed in freeze fractured replica preparations showing similar rosette distribution of caveolae along the plasma membrane (Fig. 9, arrows). Although the vast majority of the caveolae are localized at the basal plasma membranes (Fig. 4, arrows; Fig. 11, short arrows), they may at times be seen originating from the basolateral membranes (arrows) which is recognized by the presence of desmosomes (D, Figs. 10, 11) at the attachments of two neighboring cells . We never observed their occurrence from the apical plasma membranes of the granular cells. In addition, we also found no evidence of caveolae in the mitochondria-rich or goblet cells which occur side by side of the granular cells and similarly face the urinary lumen.

The plasma membranes from which the caveolae originate may likely undergo priming for the initiation and eventual development of caveolae. As a result, the basal plasma membranes (B) along with the basement membranes (W) may undergo some degree of thickening showing deep electron density as vividly seen in figure 4 (fine arrows) with associated caveolae. The chemical nature of the caveolar coating has been shown to be caveolin (Rothberg et al; 1992). Such caveolar coatings in transmission electron micrographs appear to contain light striations along the caveolar membrane domains (Figs. 6, 10, 12). In freeze fractured preparations, when the fracture line passes through the middle of the caveolae, these fine striations appear as dots (Fig. 6, fine arrows). In instances, where fracture line occurred over the caveolar flasks, these dotted coatings appear in circular orientation.

Determination of the Diameter of Caveolae:

A morphometric analysis was carried out to determine the diameter of caveolae using TEM taken at a magnification of X31,500. To analyze their diameter, we took the measurements of those caveolae which occurred only at the basal plasma membrane surfaces for maintaining uniformity in measuring their size as well as avoiding possible introduction of measuring errors. These measurements were taken from caveolae at random from over 100 of these microdomain structures and estimated their diameter to be as small as 48nm and as large as 150nm with a mean diameter of ~85 nm.

Dynamics of Caveolae in Toad Urinary bladder Epithelia:

Although the vast majority of the caveolae reside along the basal plasma membranes, many may detach from the native plasma membranes to defuse to other destinations of the cells including the apical area of the cytoplasm and at the apical

plasma membranes. These caveolae once they detach and mingle with other cytoplasmic vesicles of similar appearance, and though at times may present some degree of difficulty to identify, can still be distinguished by their size and distinct physical flask-shaped morphology with fine coatings over their membrane surfaces. Figure 12 is an ultrathin TEM presented to demonstrate the identification of a number of caveolae (arrows) within the apical cytoplasm mixed with other cytoplasmic vesicles (V). In addition, a complementary freeze fracture replica is secured to demonstrate the presence of oval to rounded caveolae within the apical cytosol (Fig. 13, small arrows), two of which appear in transition for fusion with the apical plasma membrane (Fig. 13, arrow). We have also taken a number of TEMs which clearly demonstrate the close relationship of caveolae with the apical plasma membranes. Figures 14, 15 and 16 illustrate TEM images of caveolae in the apical cytoplasm of granular cells (arrows) in positions as if they are about to fuse with the apical plasma membrane. Several caveolae (fine arrows) in these electron micrographs show fusion with the apical plasma membrane.

How caveolae, once they detach from the basal plasma membrane, migrate to various locations of a cell or across the cytosol to the apical membrane is a matter of much speculation (Hays et al., 1994). During our investigation, we observed, in many instances, close associations of caveolae with microfilaments and microtubules suggesting their possible roles in the translocation of caveolae from one area to other. In one instance, we secured a TEM of a number of caveolae at the ends of a bundle of microfilaments indicating their involvement in propelling the caveolae through the cytosol (Fig. 17, arrows). Additional TEMs as presented in figures 4 and 12 display the presence of caveolae in close contacts with microfilaments and microtubules which

indicate that these cellular constituents may be involved in the translocation of the caveolae across the cytosol to various locations of the cell, including the apical plasma membrane.

Caveolae in Endothelial and Smooth Muscle Cells:

In toad urinary bladder tissue, we observed the occurrence of a large number of caveolae within the endothelial cells (Mia et al., 1996b). As described earlier, and presented in diagram (Fig. 1), the granular (G), mitochondria-rich (R) and goblet (J) cells forming a coherent sheet of mucosal epithelium face the urinary lumen (L) whereas the endothelial (E) cells (Fig. 2) along with collagen fibrils (F) have no exposure to the urinary lumen but rather form the supporting matrix beneath the mucosal epithelium. A transmission electron micrograph image of an endothelial cell appearing on the side of a red blood cell (O) is shown to present the general cytoplasmic composition of these cells as well as the presence of many single and clustered caveolae (Fig. 18, arrows) and a clathrin-coated pit (fine arrow) along the endothelial cell plasma membrane. Endothelial cells also contain a number of microtubules as in figure 19 (arrows), along the caveolae, which may indicate their involvement in intracellular translocation of the caveolae and other organelles. In addition, a number of tubular structures (Fig. 20, arrows), reported to be common in endothelial cells, were seen to occur in toad urinary bladder endothelial cells. These tubular structures appear narrower than the diameter of the caveolae, and therefore may not likely be the extensions of the caveolae to serve as channels for intracellular macromolecules. Although most of the caveolae are seen localized along the cytoplasmic side of the plasma membrane, many of them may also appear localized deep within the cytoplasm. The endothelial cells in toad urinary bladders often contain

multivesicular bodies (Fig. 18, short arrow). Figure 21 is an ultrathin cross-sectional view which captured a group of endothelial cells (E) surrounding a blood capillary and a leucocyte (LC) containing many specific granules with polyhedral crystals (arrows). A count of the caveolae from the cross section of a large single endothelial cell indicated the presence of over 75 caveolae along the cell border in addition to those present within the deeper region of the cytoplasm. This could represent thousands of caveolae per endothelial cell when considering its length and diameter.

Large number of caveolae also occur in the smooth muscle cells in toad urinary bladders. Smooth muscle cells are distributed beneath the granular cells and along the collagen fibrils (Figs 1, 5). These cells can be identified by the presence of numerous microfilaments with longitudinal orientation along the long axis of these cells. Figures 5 and 22 show the longitudinal sectional views of the smooth muscle cells of the toad urinary bladders containing numerous longitudinally oriented microfilaments within the cells and the predominant distribution of caveolae (arrows) along the plasma membranes. In these cells, caveolae also occur within the cytoplasm remote from the plasma membrane (Fig. 22, long arrow). A transverse ultrathin section of a smooth muscle cell also demonstrates the presence of many caveolae along the plasma membrane (Fig. 23, short arrows) and deep within the cytoplasm (long arrows) surrounded by numerous microfilaments which appear as minute dots in transverse sections. These microdomain structures were found to occur also in the frog *Rana pipiens* urinary bladders. A freeze fracture preparation with the fracture line passing through the cytoplasm and along the plasma membranes of the smooth muscle cells of frog urinary bladder demonstrates the presence of many caveolar openings and the caveolae along the plasma membrane (Fig. 24, arrows).

Clathrin- and Nonclathrin-coated Pits and Vesicles in Toad Urinary Bladders:

Previously we reported the presence of clathrin-coated and nonclathrin-coated pits and vesicles in toad urinary bladder cells (Mia et al., 1996c). These membrane microdomain structures can be identified by their minute size and distinct structural morphology. Clathrin- and nonclathrin-coated pits, as they are found in other cell types, are decorated with spiny projections and obtuse spikes, respectively (Orci et al., 1986; Robinson et al., 1996). Figure 25 is presented to illustrate an example of a clathrin-coated pit (arrow) with spiny projections as it buds from the basal plasma membranes (B) and away from the basal lamina (basement membrane, W) into the cytoplasmic domain. Similarly, nonclathrin-coated pits with obtuse spikes were seen to originate from the basal plasma membrane by inward invaginations as shown in figure 26 (arrow). Frequently, both clathrin- and nonclathrin-coated pits form elongated necks out into the cytoplasm as shown in figure 25 prior to their release into the cytosol. Occasionally, these coated pits were found to originate from the basolateral plasma membranes (Figs. 10, 11), although not as often as they are seen originating from the basal plasma membranes. We rarely found clathrin-coated pits to originate from the apical plasma membranes (Fig. 27, arrow). Once the clathrin- and nonclathrin-coated pits are released into the cytosol, they are found within the cytoplasm mingled with numerous microfilaments (Fig. 28, arrow), and in trans-golgi compartment (Fig. 29, GL, fine arrows) which may indicate the possible involvement of the golgi bodies in processing these coated vesicles (Robinson et al., 1996). In this figure, several microtubules (short arrows) are also seen in association with golgi body and clathrin-coated vesicles. In addition, many clathrin-coated vesicles are seen within a large multivesicular body (Fig. 29, arrow) indicating that excess and/or unneeded clathrin-coated vesicles are scavenged by multivesicular bodies for possible conversion into

lysosomes for disposal. Clathrin-coated vesicles (Fig. 30, 31, arrows) as well as nonclathrin-coated vesicles (Fig. 32) appear to be transcytosed through the cytosol from the basal plasma membranes, where they most frequently occur, to the apical plasma membranes for fusion.

Immunoantibody and Protein-A gold Labeling of Caveolin:

In our studies of toad urinary bladders, we have made extensive documentation of the presence of caveolae in granular, endothelial and smooth muscle cells. We also found the presence of caveolae in the endothelial-like cells which occur along the serosal lining of the toad urinary bladder sac (Fig. 33, arrows) located within the peritoneal body cavity. However, such observations of caveolae were based on morphology, therefore the presence of a membrane component for identification was needed. Experiments were conducted using specific monoclonal anti-caveolin IgG for detection of caveolin and protein-A gold labeling to determine if caveolin (22kd) was indeed the major membrane protein of the caveolae of toad urinary bladder cells as found in many types of cells including the cultured fibroblasts (Rothberg et al., 1992) and mouse lung tissues (Lisanti et al., 1994). Figures 34, 35 and 36 represent electron micrographs showing the localization of the major protein component caveolin by monoclonal anti-caveolin IgG antibody and by the presence of gold particles (arrows) associated with caveolae. The 10 nm gold particles are localized on caveolae which occurred along the plasma membranes and deep within the cytoplasm of smooth muscle cells as recognized by the presence of many longitudinally oriented microfilaments. Figures 37 and 38 represent electron micrographs to depict the presence of caveolin as determined by binding of several gold particles over the caveolae (arrows) in the granular cells of toad urinary bladder tissues. These caveolae are located in the apical

region of the granular cells. Control bladder tissues blocked by treating the grids with 0.1% BSA in PBS (using no anti-caveolin) for 10 min and then exposed to protein-A gold particles failed to recognize the membrane protein caveolin in toad urinary bladder caveolae (Fig. 39). These results indicate that caveolin is a membrane protein of caveolae in the toad urinary bladder tissues.

Role of Protein Kinase C in Caveolar Transport:

Protein Kinase C, a calcium and phospholipid-dependent protein kinase, exists in various isoforms in a variety of tissues and is known to play a key role in the regulation of a variety of intracellular processes, including calcium signalling (Yoshida et al., 1988) and internalization of caveolae (Parton et al., 1994). In addition, protein kinase Cα was found to be an integral plasma membrane molecular component of caveolae responsible for causing invagination (Smart et al., 1994, 1995). In our previous studies, we demonstrated the presence of PKC isozymes in toad urinary bladder following stimulation with ADH and MZ to indicate that the amphibian urinary bladders also contained a hormone-activated PKC pathway (Mia et al., 1991b, 1992).

These tissues when challenged with MZ, an activator of protein kinase C, 10^{-6}M for 15 min, and later exposed to anti-PKCγ IgG antibody and protein A-gold particles using ultrathin sections, showed localization of gold particles in association with anti-PKCγ, predominantly surrounding the caveolae as shown in figures 40 and 41 (arrows). Figure 40 demonstrates a cluster of caveolae deep into the cytosol as well as at the apical plasma membrane indicating that PKC is associated with caveolae and caveolae may be involved in PKC translocation and for activation. An enhanced view of the clustered caveolae as shown in figure 41 is presented in figure 42 to show the gold

particles laced with caveolae indicating specific association of PKCγ. Unstimulated control tissues exposed to PKCγ isozyme and MZ stimulated tissues exposed only to 0.1% BSA and protein-A gold probes showed no apparent labeling with anti-PKCγ isozyme (Fig. 43).

Nature of Mucosal (Apical) Incorporation of HRP:

We attempted to analyze the possible translocation of the fluid-phase marker HRP and Con-A-gold conjugated HRP from the mucosal as well as serosal surfaces of the intact toad urinary bladder sacs mounted on glass tubes under an imposed osmotic gradient. As can be seen in figure 44 which depicts an electron micrograph of the control toad urinary bladder cell exposed to HRP at the mucosal surface. The HRP reaction products are essentially localized as particles along the apical membrane surface associated with glycocalyx filaments (arrows). There is little evidence to indicate that HRP gained entrance into cellular cytosol through the plasma membrane by a process of endocytosis. The apical region of the cytoplasm contains several secretory granules (S) and empty vesicles (arrows) with no apparent incorporation of HRP. A comparative section of the ADH-stimulated tissue also demonstrated no incorporation of HRP within the cytosolic vesicles, but HRP was found to remain predominantly localized at the apical membrane surface even after 20 or 30 min post hormone washout period (Fig. 45). This is also true with Con-A-gold-HRP. However, we discovered several multivesicular bodies in ADH-stimulated bladder tissues exposed to HRP at the mucosal surface which stained electron dense (Fig. 46, arrows). Upon closer examination of the multivesicular bodies in the electron micrographs, it was revealed that HRP was localized in specific bodies containing fine spiny projections within the multivesicular bodies. These multivesicular bodies containing

spiny structures appear in various locations of the cytoplasm including at the apical plasma membrane surface (Fig. 47, arrow). We also observed large endosomes showing peroxidase reaction products which may likely be lysosomes as shown in figure 48 (arrow). Presence of similar multivesicular bodies labeled with HRP was reported previously in toad urinary bladder granular cells (Masur et al., 1984; Coleman et al., 1987). We also observed presence of a number of multivesicular bodies both in control (Fig. 49, arrows) and ADH-stimulated tissues of toad urinary bladder granular cells (Fig. 50, arrow) with no exposures to HRP. We also found similar multivesicular bodies in granular cells of frog urinary bladders. As seen in these TEM images, these multivesicular bodies also contain specific type of vesicles each of which is decorated with fine spiny structures surrounding a hollow core. A large multivesicular body as seen in ultrathin sections with no peroxidase reaction (Fig. 50) may contain over 50 vesicles and this may account for hundreds of vesicles per multivesicular body when considering its size and diameter. These multivesicular bodies may likely contain endocytic vesicles and other vesicles scavenged from the cytoplasm. These multivesicular endosomes showing HRP labeling may likely originate within the cytoplasm as part of a process of recycling. These endosomes could also represent as lysosomes as they normally contain hydrolytic enzymes for digestion of engulfed substances (Darnell et al., 1986). Additional experiments using antibodies for caveolin and clathrin and protein-A gold probes need to be performed to determine if these endosomes contain caveolae or clathrin-coated vesicles.

Nature of Serosal (Basal) Incorporation of HRP:

Experiments were also performed to demonstrate the nature of serosal HRP labeling of toad urinary bladders. Figure 51 represents an example of control tissues

under an imposed osmotic gradient showing labeling of HRP at the serosal surface (arrows) similar to the mucosal labeling of HRP as in figure 44. The ADH-stimulation of toad bladder sacs under an imposed osmotic gradient demonstrated serosal penetration of HRP deep into basolateral regions and into caveolae along the basolateral membranes (Figs. 52, 53, arrows). Figure 54 represents a high power transmission electron micrograph with no staining with uranyl acetate and lead citrate showing the incorporation of HRP into caveolae (arrows) before the tight junction (short arrow) which may act as barrier for further penetration of HRP into bladder tissues. HRP in the caveolae are localized in particulate bodies (Fig. 55, arrows) which become apparent upon staining of the grids with uranyl acetate and lead citrate. However, caveolae facing the peritoneal cavity were not seen to have HRP incorporation (Fig. 33, arrows), and therefore, the serous membrane facing the peritoneal cavity as expected is impervious to normal fluid penetration.

Discussion and Conclusions

Over the past thirty years, amphibian urinary bladders have been utilized as renal models in experimental investigation of exocytosis (Masur et al., 1984; Mia et al., 1991; Hays et al., 1994 and others), and endocytosis (Harris et al., 1986; Coleman et al., 1987; Mia et al., 1994; Coleman and Wade, 1994) as related to transmembrane osmotic water flow mediated by ADH. These studies have rendered important information pertaining to morpho-cytological, biophysical and biochemical aspects of ADH actions on amphibian urinary bladders. TEM techniques using ultrathin sections and freeze fracture replicas have revealed information dealing with fine structural details of cytoplasmic features as related to the ADH water transport process. ADH induces exocytosis in renal epithelia as well as in amphibian urinary bladders with the

insertion of water channels (aggrephores, aquaporins) to the mucosal membrane surfaces of the granular cells (Chevalier et al., 1974; Muller et al., 1980; Muller and Kachadorian, 1984) during enhanced reabsorption of fluid. The presence of aggrephores (water channels) with tubular configuration adjacent to the luminal plasma membranes showing angular or horizontal orientation for possible apical fusion events has been previously reported (Humbert et al., 1977; Wade et al., 1981; Sasaki et al., 1984; Hays et al., 1987). However, other reports on ADH-induced water transport process in amphibian urinary bladders, especially involving frog urinary bladders, indicated no sightings of water transport vehicles or aggrephores at or around the apical plasma membranes (Ding et al., 1985, 1988; Franki et al., 1986; Hays et al., 1994). Ding et al., (1988) suggested that in frog, some type of vesicles, other than aggrephores, possibly coated with clathrin could be involved in membrane fusion of water channels to facilitate ADH-induced water flow across the apical membranes. They argued that fusion event appeared to be smaller in size than the size of aggrephores and this small size of fusion events was found to correspond with the size of the vesicles. They further suggested that in toads, there may exist two modes of particle delivery systems involving aggrephores and nonaggrephores. Therefore, the mechanism for water channel delivery and the membrane shuttle hypothesis involving aggrephores in amphibian urinary bladder remains unresolved. During our extensive investigations on water transport in amphibian epithelia we have examined numerous ultrathin sections of control and ADH-stimulated toad urinary bladders. No convincing cellular ultrastructures that matched the aggrephore features or description was identified in our micrographs of toad or frog urinary bladders. However, we discovered a large number of caveolae and some clathrin- and nonclathrin-coated pits and vesicles in the toad urinary bladders with or without ADH stimulation. There has

been little attention given to these structures in studies on osmotic water flow in toad urinary bladders and renal epithelia. However, we found the presence of caveolae in toad urinary bladder granular epithelial cells to be more common than aggrephores, clathrin- and nonclathrin-coated pits and vesicles combined. Interesting, Eggena and Ma (1989) demonstrated that the vasopressin receptor complex in toad urinary bladders is endocytosed together with light vesicles (less than 0.22μm) containing water channel proteins from the basolateral membranes and/or intracellular reservoirs and move to the apical plasma membranes for insertion, thereby making the apical membranes more permeable to water. As these vesicles were not subjected to TEM studies, they failed to identify these vesicles. However, if their contention is considered acceptable, then it is possible that caveolae, having an average diameter of ~85nm, may be a candidate for transcytosis. Our finding that caveolae are present at the apical surface and appear to fuse with the apical membrane indicate that caveolae may serve as transport vehicles, somewhat like aggrephores. Moreover, caveolae contain fine arrays of striated coatings as demonstrated by conventional epon ultrathin sections and by rapid-freeze, deep-etch techniques using fibroblasts (Rothberg et al., 1992). In our studies of numerous ultrathin sections of toad urinary bladders, we made extensive records to indicate the presence of fine striations with unknown chemical composition associated with membranes of caveolae, and in vesicles contained in the multivesicular bodies. It will be necessary to conduct additional studies to determine the chemical composition of the fine striations associated with caveolar membranes. Could these striations represent proteins that may have properties of water channels (aquaporins) particularly as these caveolae are found to fuse with the apical plasma membranes in toad urinary bladder granular cells?

Caveolae are membrane microdomain structures that are formed by invaginations of the plasma membranes and have been reported to be present in many mammalian cell types including endothelial cells, epithelial cells, fibroblasts and smooth muscle cells (Palade, 1953; Yamada, 1955; Severs, 1988; Rothberg et al., 1992; Dupree et al., 1993; Anderson, 1993; Chang et al., 1994 and others). Most of these studies on caveolae indicated that they are involved in a variety of cellular functions including potocytosis (Anderson, 1993), transcytosis (Lisanti et al., 1994; Schnitzer et al., 1994; Predescu et al., 1994, 1997), calcium signal transduction (Fujimoto, 1993) and transport of macromolecules and proteins in endothelial cells (Milici et al., 1987; Presdescu et al., 1997). We have identified a large number of caveolae in the granular epithelia of toad urinary bladders which were found to occur essentially at the basal plasma membranes of the granular cells (Mia et al., 1996a). Since our finding, we further noticed that some of these caveolae detach by fission from the native basal plasma membranes in a process of endocytosis to become free vesicles, and then defuse away to various locations of the cytoplasm and at sites of the apical plasma membranes where they are found to fuse in a process of exocytosis (Figs. 14-16, Mia et al., 1996c). In these cells, we never observed formation of caveolae at the apical plasma membranes. These observations strongly suggested that caveolae in toad urinary bladder granular cells traverse unidirectionally from the basal plasma membrane to the apical plasma membrane. It is anticipated that their fusion with the apical plasma membrane will result in the deposition of new membrane components containing unknown protein and macromolecules. Therefore, caveolae in toad urinary bladder granular cells are not engaged in cycling of the membranes as postulated in membrane shuttling hypothesis to recover portions of membranes including water channels (aggrephores, aquaporins), but may present basal membrane components to the apical

plasma membranes. It is not known how the granular cells in toad urinary bladders continue to accept new membranes by caveolar fusions at the apical plasma membranes with no mechanism to recover at least portions of these new membranes that appear to be added to the apical plasma membranes. The membranes from caveolae as deposited at the apical plasma membranes could play a role in modulating apical membrane permeability particularly in response to ADH stimulation.

Our immunocytochemical studies using ultrathin sections, exposed to anti-caveolin and protein-A gold particles demonstrated the presence of a major membrane coat protein caveolin associated with caveolae of toad urinary bladder cells. These techniques have been applied by several workers to identify the major coat protein complexes (Rothberg et al., 1992; Lisanti et al., 1994) in the caveolae of several cell types. Therefore, these procedures can be accepted as standard for identification of caveolin, a 22kd protein of caveolae. Using this immunocytochemical technique, we identified the presence of caveolae in various locations of urinary bladder cells, and further observed that caveolae were not only localized at the basal plasma membrane surfaces but also in association with the caveolae at various locations of the cells including at the apical plasma membranes. In addition, in our previous studies (Mia et al., 1991b, 1992), we demonstrated that presence of protein kinase Cα, β and γ in association with diffused bodies occurring at various locations of the cells, and further identified that some of the bodies to be caveolae (Figs. 40-42). Several workers (Smart et al., 1994; Parton et al., 1994) described protein kinase C association with caveolae in other cells to be important for caveolar functions. Our studies using the conventional epon ultrathin sections as well as using immunocytochemical techniques involving the detection of caveolae in toad urinary bladders, clearly indicate that caveolae are

involved in transcytosis, thereby not only contributing new membrane components to the apical plasma membranes but also carrying cargoes of unknown materials or proteins that are delivered from the basal to the apical membranes.

Clathrin-coated and nonclathrin-coated pits also arise by invaginations predominantly from the basal plasma membranes along with the caveolae of the granular cells of toad urinary bladders (Mia et al., 1996c). They were also seen to be endocytosed primarily from the basal plasma membrane and transported across the cytosol to the apical plasma membrane. However, their number appeared to be insignificant compared to the number of caveolae from which they originate (Mia et al., 1996c). Occasionally, only clathrin-coated pits and not the nonclathrin-coated pits were seen to originate by endocytosis from the apical plasma membranes of the granular cells of toads but their number appears too low to have major role in ADH-induced water transport process (Ding et al., 1988). A large body of literature dealing with the origin and role of clathrin-coated pits and vesicles indicates that these pits invariably originate from the apical and/or external plasma membranes and engaged in receptor-mediated endocytosis, pinocytosis, transport of lysosomal enzymes and export of some endogenous proteins (Brodsky, 1988; Robinson et al., 1996). We have not yet determined their role in toad urinary bladder granular cells.

Toad urinary bladder granular cells contain many multivesicular bodies and lysosomes which appeared electron dense, perhaps because of deposition of peroxidase products resulting from the reaction with DAB and H_2O_2. We found no evidence of localization of HRP within any vesicular structures in presence of mucosal HRP in ADH-stimulated toad urinary bladders under an imposed osmotic gradient, and even

after retrieval for 20 or 30 min. However, HRP was found in multivesicular bodies. Several other workers also reported the presence of HRP in multivesicular bodies and in lysosomes (Peachey and Rasmussen, 1961; Masur et al., 1984; Coleman et al., 1987). They found little evidence to infer that HRP was internalized via vesicular structures during retrieval process or by endocytosis. Upon closer examination of the electron images that we prepared, we discovered that HRP reaction products within the multivesicular bodies were essentially localized in small circular bodies with hollow cores and decorated with spiny surface projections around the hollow cores. By morphological criteria, these vesicular bodies resemble caveolae. Multivesicular bodies as found in the granular cells were also found in endothelial and smooth muscles cells which usually contain a large number of caveolae, and we found no evidence of multivesicular bodies containing caveolae in goblet and mitochondria-rich cells in toad urinary bladders. Many caveolae are likely to be internalized into multivesicular bodies by scavenging when they become old and nonfunctioning in order to maintain tissue integrity. It was demonstrated that caveolae in some endothelial cells were scavenged and chemically modified to provide cellular protection and possibly remove deleterious proteins (Steinberg et al., 1989; Schnitzer et al., 1994). We also discovered that some similar multivesicular bodies in toad urinary granular cells were also involved in scavenging clathrin-coated vesicles likely to remove old, excess and unwanted vesicular products with no useful purpose. Whether these multivesicular bodies play a role in water channel and caveolae recycling needs to be determined. Our findings suggest that caveolae may play a role in membrane transport and possibly from shuttling basal membrane components to the apical membrane surface.

References

Anderson, R.G.W. 1993. Potocytosis of small molecules and ions by caveolae. Trends Cell Biol. 3:69-72.

Bentley, P.J. 1958. The effects of neurohypophysial extracts on water transfer across the wall of the isolated urinary bladder of the toad, *Bufo marinus*. J.Endocrin. 17:201-209.

Brodsky, F.M. 1988. Living with clathrin: Its role in intracellular membrane traffic. Science, 242:1396-1402.

Brown, D., Verkman, A.S., Skorecki, K. and Ausiello, D.A. 1990. The cellular action of antidiuretic hormone. Meth. Enzymology, 1991:551-571.

Chang, W.J., Ying, Y.S., Rothberg, K.G., Hooper, N.M., Turner, A.J., Gambliel, H.A., Gunzburg, J.D., Mumby, S.M., Gilman, A.G. and Anderson, R.G.W. 1994. Purification and characterization of smooth muscle cell caveolae. J. Cell Biol. 126:127-138.

Chevalier, J., Bourguet, J. and Hugon, J.S. 1974. Membrane associated particles: distribution in frog urinary bladder epithelium at rest and after oxytocin treatment. Cell Tissue Res. 152:129-140.

Choi, J.K. 1963. The fine structure of the urinary bladder of the toad, *Bufo marinus*. J. Cell Biol. 16:53-72.

Coleman, R.A., Harris, W. and Wade, J.B. 1987. Visualization of endocytosed markers in freeze-fracture studies of toad urinary bladder. J. Histochem. Cytochem. 35:1405-1414.

Coleman, R.A. and Wade, J.B. 1994. ADH-induced recycling of fluid-phase marker from endosomes to the mucosal surface in toad bladder. Am. J. Physiol. 267 (Cell Physiol. 36):C32-C38.

Darnell, J., Lodish, H. and Baltimore, D. 1986. Molecular Cell Biology, Scientific Am. Book, Inc. (W.H. Freeman & Com.), N.Y.

DiBona, D.R., Civan, M.M. and Leaf, A. 1969. The cellular specificity of the effect of vasopressin on toad urinary bladder. J. Membr. Biol. 1:79-91.

DiBona, D.R. 1981. Vasopressin action of the conformational state of the granular cell in the amphibian urinary bladder. In Epithelial Ion and Water Transport. ed. A.D.C. Macknight and J.P Leader. N.Y. Raven: 241-255.

Ding, G., Franki, N. and Hays, R.M. 1985. Evidence of cycling of aggregate-containing tubules in toad urinary bladder. Biol. Cell, 65:213-218.

Ding, G., Franki, N., Bourguet, J. and Hays, R.M. 1988. Role of vesicular transport in ADH-stimulated aggregate delivery. Am. J. Physiol 255 (Cell Physiol. 24):C641-C652.

Dratwa, M., LeFurgey, A. and Tisher, C.C. 1979. Effect of vasopressin and serosal hypertonicity on toad urinary bladder. Kidney Int. 16:695-703.

Dupree, P., Parton, R.G., Raposo, G., Kurzchalia, T.V. and Simons, K. 1993. Caveolae and sorting in the trans-golgi network of epithelial cells. EMBO J. 12:1597-1605.

Eggena, P. and Ma, C.L. 1989. Vasopressin-induced transfer via light vesicles of receptors and water channels from the basolateral to apical membrane of toad bladder. Biol. Cell, 66:13-17.

Franki, N., Ding, G., Quintana, N. and Hays, R.M. 1986. Evidence that the heads of ADH-sensitive aggrephores are clathrin-coated vesicles: implications for aggrephore structure and function. Tissue Cell, 18:803-807.

Fugimoto, T. 1993. Calcium pump of the plasma membrane is localized in caveolae. J. Cell Biol. 120:1147-1157.

Harris, H.W., Wade, J.B. and Handler, J.S. 1986. Fluorescent markers to study membrane retrieval in antidiuretic hormone-treated toad urinary bladder. Am. J. Physiol. 251: (Cell Physiol. 20):C274-C284.

Hays, R.M., Franki, N. and Ding, G. 1987. Effects of antidiuretic hormone on the collecting duct. Kidney Int. 31:530-537.

Hays, R.M., Franki, N., Simon, H. and Gao, Y. 1994. Antidiuretic hormone and exocytosis: lessons from neurosecretion. Am. J. Physiol. 267 (Cell Physiol. 36):C1507-C1524.

Humbert, F., Montessano, R., Grosso, R., DeSousa, R.C. and Orci, L. 1977. Particle aggregates in plasma and intracellular membranes of toad bladder (granular cell). Experientic Basel, 33:1364-1367.

Kachadorian, W.A., Casey, C. and DiScala, V.A. 1977. Time course of ADH-induced intramembrane particle aggregation in toad urinary bladder. Am. J. Physiol. 234:F461-F465.

Kachadorian, W.A., Soriban-Sohraby, S. and Spring, K. 1985. Regulation of water permeability in toad urinary bladder at two barriers. Am. J. Physiol. 248:F260-F265.

Lisanti, M.P., Scherer, P.E., Tang, Z.L. and Sargiacomo, M. 1994. Caveolae, caveolin-rich membrane domains: a signaling hypothesis. Trends Cell Biol. 4:231-235.

Masur, S.K., Cooper, S. and Rubin, M.S. 1984. Effect of an osmotic gradient on antidiuretic hormone-induced endocytosis and hydroosmosis in the toad urinary bladder. Am. J. Physiol. 247 (Renal Fluid Electrolyte Physiol. 16):F370-F379.

Mia, A.J., Tarapoom, N., Carnes, J. and Yorio, T. 1983. Alteration if surface substructure of frog urinary bladder by calcium ionophore, verapamil and antidiuretic hormone. Tissue & Cell, 15:737-748.

Mia, A.J., Oakford, L.X., Torres, L., Herman, C. and Yorio, T. 1987. Morphometric analysis of epithelial cells of frog urinary bladder. I. Effect of antidiuretic hormone, calcium ionophore (A23187) and PGE_2. Tissue & Cell, 19:437-450.

Mia, A.J., Oakford, L.X., Moore, T.M., Chang, P.H. and Yorio, T. 1988. Morphometric analysis of epithelial cells of frog urinary bladder. II. Effect of ADH, calcium ionophore (A23187) and verapamil on isolated dissociated cells. Tissue & Cell, 20:19-33.

Mia, A.J., Oakford, L.X. and Yorio, T. 1989. Alterations of surface substructures and degranulation of subapical cytoplasmic granules by mezerein (MZ) in toad urinary

bladder epithelia. Proc. Elect. Microscopic Soc. Am. 47:916-917.

Mia, A.J., Oakford, L.X., Cammarata, P. and Yorio, T. 1991a. Modulation of cytoskeletal organization and cytosolic granule distribution by verapamil in amphibian urinary bladder epithelia. Tissue & Cell, 23:161-171.

Mia, A.J., Oakford, L.X. and Yorio, T. 1991b. Role of PKC isozymes in water transport in toad urinary bladder. Proc. Elec. Microscopic Soc. Am. 49: 302-303.

Mia, A.J., Oakford, L.X., Thompson, P.D. and Yorio, T. 1992. Role of PKC isozyme III (alpha) in water transport in amphibian urinary bladder. Proc. Elect. Microscopic Soc. Am. 50:796-797.

Mia, A.J., Oakford, L.X., Hayes, S.C., Davidson, A. and Yorio, T. 1993. Membrane dynamic during endocytosis in toad urinary bladders as visualized by SEM. Scanning 15 Suppl III. 110-111.

Mia, A.J., Oakford, L.X. and Yorio, T. 1994. Surface membrane remodeling following removal of vasopressin in amphibian urinary bladder. Tissue & Cell, 26:189-201.

Mia, A.J., Oakford, L.X., Franklin, J., Berry, N. and Yorio, T. 1996a. Evidence of caveolae and coated pits in toad urinary bladder granular epithelia. FASEB J. 10:A172.

Mia, A.J., Oakford, L.X. and Yorio, T. 1996b. Nature of caveolae in the endothelial cells of toad urinary bladders. Proc. Microscopy and Microanalysis, 934-935.

Mia, A.J., Oakford, L.X. and Yorio, T. 1996c. Possible transcytosis by three distinct coated pits and vesicles in granular cells in toad urinary bladder. Mol. Biol. Cell, 7:226A.

Milici, A.J., Watrous, N.E., Stukenbrock, H. and Palade, G.E. 1987. Transcytosis of albumin in capillary endothelium. J. Cell Biol. 105:2603-2612.

Muller, J., Kachadorian, W.A. and DiScala, V.A. 1980. Evidence that ADH-stimulated intramembranous aggregates are transferred from cytoplasmic to luminal membranes in toad bladder epithelial cells. J. Cell Biol. 85:83-95.

Muller, J. and Kachadorian, W.A. 1984. Aggregate-carrying membranes during ADH stimulation and washout in toad bladder. Am. J. Physiol. 247:C90-C98.

Orci, L., Glick, B.S. and Rothman, J.E. 1986. A new type of coated vesicular carrier that appears not to contain clathrin: its possible role in protein transport within the golgi stack. Cell, 46:171-184.

Palade, G.E. 1953. Fine structure of blood capillaries. J. Appl. Physics, 24:1424.

Parton, R.G., Joggerst, B. and Simons, K. 1994. Regulated internalization of caveolae. J. Cell Biol. 127:1199-1215.

Peachey, L.D. and Rasmussen, H. 1961. Structure of the toad's urinary bladder as relate to its physiology. J. Biophys. Biochem. Cytol. 10:529-553.

Predescu, D., Horvat, R., Predescu, S. and Palade, G.E. 1994. Transcytosis in the continuous endothelium of the myocardial microvasculature is inhibited by N-etheylmaleimide. Proc. Natl. Acad. Sci. USA, 91:3014-3018.

Predescu, S.A., Predescu, D.N. and Palade, G.E. 1997. Plasmalemmal vesicles function as transcytotic carriers for small proteins in the continuous endothelium. Am. J. Physiol. 272 (Heart Circ. Physiol. 41):H937-H949.

Robinson, M.S., Watts, C. and Zeriel, M. 1996. Membrane dynamics in endocytosis. Cell, 84:13-21.

Rothberg, K.G., Heuser, J.E., Donzell, W.C., Ying, Y.S., Glenney, J.R. and Anderson, R.G.W. 1992. Caveolin, a protein component of caveolae membrane coats. Cell, 68:673-682.

Sasaki, J., Tilles, S., Candeelis, J., Carboni, J., Meiteles, L., Franki, N., Bolon, R., Robertson, C. and Hays, R.M. 1984. Electron microscopic study of the apical region of the toad bladder epithelial cell. Am. J. Physiol. 244:C268-C281.

Schnitzer, J.E., Oh, P., Pinney, E. and Allard, J. 1994. Filipin-sensitive caveoale-mediated transport in endothelium: Reduced transcytosis, scavenger endocytosis, and capillary permeability of select macromolecules. J. Cell Biol. 127:1217-1232.

Severs, N.J. 1988. Caveolae: static inpocketings of the plasma membrane, dynamic vesicles or plain artifact? J. Cell Sci. 90:341-348.

Smart, E.J., Foster, D.C., Ying, Y., Kamen, B.A. and Anderson, R.G.W. 1994. Protein kinase C activators inhibit receptor-mediated potocytosis by preventing internalization of caveolae. J. Cell Biol. 124:307-313.

Smart, E.J., Ying, Y.S. and Anderson, G.R.W. 1995. Hormone regulation of caveolae internalization. J. Cell Biol. 131:929-938.

Steinberg, D. and Parthasarathy, S., Carew, T.E., Khoo, J.C. and Witztum, J.L. 1989. Beyond cholesterol: modification low-density lipoprotein that increases its atherogenecity. New Engl. J. Med. 320:9150924.

Wade, J.B., Stetson, D.L. and Lewis, J.A. 1981. ADH action: evidence for a membrane shuttle mechanism. Ann. N.Y. Acad. Sci. 322:106-117.

Yamada, E. 1955. The fine structure of the gall bladder epithelium of the mouse. J. Biophys. Biochem. Cytol. 1:445-458.

Yoshida, Y., Huang, F.L., Nakabayashi, H. and Huang, K.P. 1988. Tissue distribution and development expression of protein kinase C isozymes. J. Biol. Chem. 263:9868-9873.

Ziedel, M.L., Hammond, T., Botelho, B. and Harris, H.W. 1992. Functional and structural characterization of endosomes from toad bladder epithelial cells. Am. J. Physiol. 263 (Renal Fluid Electrolyte Physiol. 32):F62-F76.

Ziedel, M.L., Hammond, T.G., Wade, J.B., Tucker, J. and Harris, H.W. 1993. Fate of antidiuretic hormone water channel proteins after retrieval from apical membrane. Am. J. Physiol. 265 (Cell Physiol. 34):C822-C833.

Key to Figures

Figure 1. Diagram illustrates the arrangement of cells in toad urinary bladder with distribution of caveolae in granular (G), endothelial (E) and smooth muscle (M) cells.

Figure 2. Low power TEM of toad urinary bladder showing the cellular composition with the distribution of granular (G), goblet (J) and mitochondria-rich cells facing the mucosal cavity (L). X2,000.

Figure 3. Low power TEM showing the position of caveolae (arrows) at the basal plasma membrane (B) in relation to the apical plasma membrane (AM). X30,000.

Figure 4. TEM of toad urinary bladder granular cell showing the presence of many caveolae (arrows) at the basal plasma membrane (B) inner to the basement membrane (W) with heavy thickening (fine arrows). X57,500.

Figure 5. TEM of toad urinary bladder showing the presence of caveolae (arrows) in a smooth muscle (M) and in granular (G) cells. X57,500.

Figure 6. Freeze fracture replica of toad urinary bladder showing caveolae (arrows) with decorations as dots (fine arrows) in a granular cell. X67,000.

Figure 7. TEM of toad urinary bladder granular cell showing caveolae (small arrows), caveolae clusters (thick arrows) with remnants of basement membranes (fine arrows) and clathrin-coated pits at the basal plasma membrane inner to the basement membrane. X57,500.

Figure 8. SEM of toad urinary bladder showing numerous folds on the serosal side of the bladder. X1,200.

Figure 9. Freeze fracture replica showing similar circular distribution of caveolae as shown in figure 7. X112,000.

Figure 10. TEM of toad urinary bladder showing the presence of caveolae (arrow) along the basolateral membranes with desmosome (D). X36,000.

Figure 11. TEM of toad urinary bladder showing caveolae (short arrows) on basal

plasma membrane, caveolae on the basolateral membranes (long arrows) with desmosome (D). X57,000.

Figure 12. TEM of toad urinary bladder showing caveolae (arrows) in the apical cytoplasm. X56,000.

Figure 13. Freeze fracture replica showing the presence of caveolae (large arrow) at the apical membrane surface and within the cytoplasm (small arrows). X70,000.

Figures 14, 15 and 16. TEM of toad urinary bladders showing the presence of caveolae (arrows) at the apical membrane surfaces of a granular cells and in positions of fusions with the membrane surfaces (fine arrows). Figs. 14, 15. X56,000. Fig. 16. X94,000.

Figure 17. TEM of toad urinary bladder showing a number of caveolae at ends of a bundle of microfilaments (arrows) indicating their possible involvement in transporting caveolae. X63,000.

Figure 18. TEM of toad urinary bladder showing endothelial cell attached to a red blood cell (O) with many caveolae (arrows), clathrin-coated pit (fine arrow) and a multivesicular body (short arrow). X38,500.

Figure 19. TEM of toad urinary bladder showing caveolae attached to microtubules (arrows) in an endothelial cell. X47,250.

Figure 20. TEM of toad urinary bladder showing tubular structures (arrows) along the caveolae in an endothelial cell. X38,500.

Figure 21. TEM of toad urinary bladder cell tissue showing endothelial cells (E) containing a leucocyte (LC) with many specific granules (arrows) with polyhedral crystals. X12,000.

Figure 22. TEM of toad urinary bladder showing longitudinally-oriented microfilaments in smooth muscle cells with caveolae at the membrane surface (arrows) and within the cytoplasm (large arrow). X56,000.

Figure 23. TEM of toad urinary bladder showing a smooth muscle cell containing caveolae (arrows) and microfilaments in a cross section. X30,000.

Figure 24. Freeze fracture replica of frog urinary bladder showing caveolae and their openings (arrows) in a smooth muscle cell. X30,000.

Figure 25. TEM of toad urinary bladder showing caveolae at the basal plasma membrane along with a clathrin-coated pit with long neck (arrow). X56,000.

Figure 26. TEM of toad urinary bladder showing a nonclathrin-coated pit with obtuse coat (arrow) along with caveolae on the basal plasma membrane. X63,000.

Figure 27. TEM of toad urinary bladder showing the presence of a clathrin-coated pit (arrow) at the apical plasma membrane of a granular cell. X56,000.

Figure 28. TEM of toad urinary bladder showing clathrin-coated vesicles (arrow) associated with numerous microfilaments within the cytoplasm. X56,000.

Figure 29. TEM of toad urinary bladder showing many clathrin-coated vesicles (fine arrows) in trans-golgi (GL) network, a large multivesicular body (arrow) and microtubules (short arrows) associated with golgi body. X56,000.

Figure 30. TEM of toad urinary bladder showing two clathrin-coated vesicles (arrow) at the apical cytoplasm of a granular cell. X128,000.

Figure 31. TEM of toad urinary bladder showing of a caveola and a clathrin-coated vesicle (arrow) possibly fusing with the apical plasma membrane of a granular cell. X57,500.

Figure 32. TEM of toad urinary bladder showing of a nonclathrin-coated vesicle (arrow) at the apical plasma membrane and a nearby microtubule in a granular cell. X56,000.

Figure 33. TEM of ADH-stimulated toad urinary bladder showing many caveolae (arrows) along the serosal membrane of an endothelial-like cell which is impervious to fluid-phase marker HRP. X56,000.

Figure 34. TEM of toad urinary bladder showing detection of caveolin by anti-caveolin and protein-A gold particles over caveolae (arrows) along the plasma membranes. X63,000.

Figure 35. TEM of toad urinary bladder showing detection of caveolin by anti-caveolin and protein-A gold particles (arrow) over a caveola. X63,000.

Figure 36. TEM of toad urinary bladder showing detection of caveolin by anti-caveolin and protein-A gold particles (arrows) over caveolae. X125,000.

Figures 37 and 38. TEM of toad urinary bladder showing the detection of caveolin by anti-caveolin and protein-A gold particles (arrows) over caveolae in the apical regions of granular cells. X63,000.

Figure 39. TEM of toad urinary bladder preabsorbed with 0.1% BSA and then exposed to protein-A gold probes (control tissue) showing no binding of gold particles with caveolae (arrows). X63,000.

Figure 40. TEM of toad urinary bladder showing localization of protein kinase C gamma (PKCγ) by anti-PKCγ and protein-A gold probes in association with caveolae (arrows) in the cytoplasm of a granular cell. X33,500.

Figure 41. TEM of toad urinary bladder showing localization of protein kinase C gamma (PKCγ) by anti-PKCγ and protein A-gold particles in association with a cluster of caveolae (arrow) in the cytoplasm of a granular cell. X33,750.

Figure 42. Same picture as in figure 41 showing enhanced view to show the cluster of caveolae (arrow) laced with gold particles. X53,600.

Figure 43. TEM of toad urinary bladder preabsorbed with 0.1% BSA and then exposed to protein-A gold probes (control tissue) showing no labeling. X67,000.

Figure 44. TEM of control toad urinary bladder showing labeling of HRP at the mucosal surface (arrows), and secretory granules (S) and cytosolic vesicles (short arrows) with no HRP labeling. X70,000.

Figure 45. TEM of ADH-stimulated toad urinary bladder showing little or no HRP labeling at the mucosal surface and secretory granules. X70,000.

Figures 46 and 47. TEM of ADH-stimulated toad urinary bladders showing HRP localization in specific bodies containing spiny structures (arrows) within multivesicular

bodies. X70,000.

Figure 48. TEM of ADH-stimulated toad urinary bladder showing HRP labeling within a multivesicular body (arrow). X70,000.

Figure 49. TEM of control toad urinary bladder showing a number of multivesicular bodies (arrows) each containing many vesicles. X70,000.

Figure 50. TEM of ADH-stimulated toad urinary bladder showing the presence of a large multivesicular body (arrow) containing coated vesicles. X70,000.

Figure 51. TEM of control toad urinary bladder showing HRP labeling at the serosal membrane lining (arrows). X11,000.

Figure 52. TEM of ADH-stimulated toad urinary bladder showing deep serosal HRP penetration through the basolateral membranes and labeling of caveolae (arrows). Section was not stained with uranyl acetate and lead citrate. X12,600.

Figure 53. TEM of ADH-stimulated toad urinary bladder showing serosal HRP penetration through the basolateral membranes and labeling of caveolae (arrows). F-collagen fibrils. Section was stained with uranyl acetate and lead citrate. X17,000.

Figure 54. TEM of ADH-stimulated toad urinary bladder showing HRP labeling of caveolae (arrows) through serosal bathing solution and tight junction (short arrow) restricting possible penetration of HRP across the bladder tissue. Section was not stained with uranyl acetate and lead citrate. X70,000.

Figure 55. TEM of ADH-stimulated toad urinary bladder showing HRP labeling of caveolae (arrows) in particulate bodies which become apparent upon staining with uranyl acetate and lead citrate. X70,000.

OTHER MILESTONES

Full-length project related papers published and submitted:

a) Is protein kinase C alpha (PKCα) involved in vasopressin-induced effects on LLC-PK_1 pig kidney cells? Biochem. Mol. Biol. Intern. 39:581-588 (1996).

b) Mechanism of vasopressin-induced increase in intracellular Ca^{2+} ($[Ca^{2+}]i$) in LLC-PK_1 porcine kidney cells. Am. J. Physiol. 272 (Cell Physiol. 41):C810-C817 (1997).

c) Evidence of basolateral water permeability regulation in amphibian urinary bladder. Biol. Cell (1997).

d) The ATP-depleting reagent "iodoacetamide" induces the degradation of protein kinase C alpha (PKCα) in LLC-PK_1 pig kidney cells. Life Sciences (in press).

Abstracts published and submitted:

a) Nature of caveolae in the endothelial cells of toad urinary bladders. Proc. Microscopy and Microanalysis, 934-935 (1996).

b) Possible transcytosis by three distinct coated pits and vesicles in granular cells in toad urinary bladder. Mol. Biol. Cell, 7:226a (1996).

c) Vasopressin-induced mobilization of intercellular calcium is linked to elevation of cyclic AMP (cAMP). Soc. Neurosci. (1996).

d) Distribution of caveolae in amphibian urinary bladder cells. National Minority Research Symposium. NIGMS, 34 (1996).

e) The ATP-depleting reagent "iodacetamide" induces the degradation of protein kinase C alpha (PKCα) in LLC-PK1 pig kidney cells. FASEB J. (1997)

f) Phosphtidylinositol 3-kinase involved in vasopressin-induced water transport in toad urinary bladder. Intern. Symposium: Molecular Physiology of Water Transport, Paris, France (1997).

g) Presence of caveolae in the granular epithelial cells of rabbit urinary bladder. microscopy and Microbeam Analysis'97 (accepted, 1997).

OTHER ACTIVITIES

Attendance at the Cell Biology Meeting, San Francisco, CA. December, 1996.
Attendance at the FASEB Meeting, New Orleans, LA. April, 1997.
To be attended MSA Meeting, Cleveland, OH. August, 1997.

Training of Students

Three African-American undergraduate students at Jarvis Christian College have been receiving training in biomedical research and career enhancement under the supervision of Dr. Mia. In addition, four of his students graduated from Jarvis in May, 1997. Three students of Dr. Mia, graduated previously from Jarvis have been pursuing graduate studies (Ph.D.) in biomedicine under the supervision of Dr. Yorio at the UNT Health Science Center at Fort Worth. All these students have developed excellent skills in using the computers.

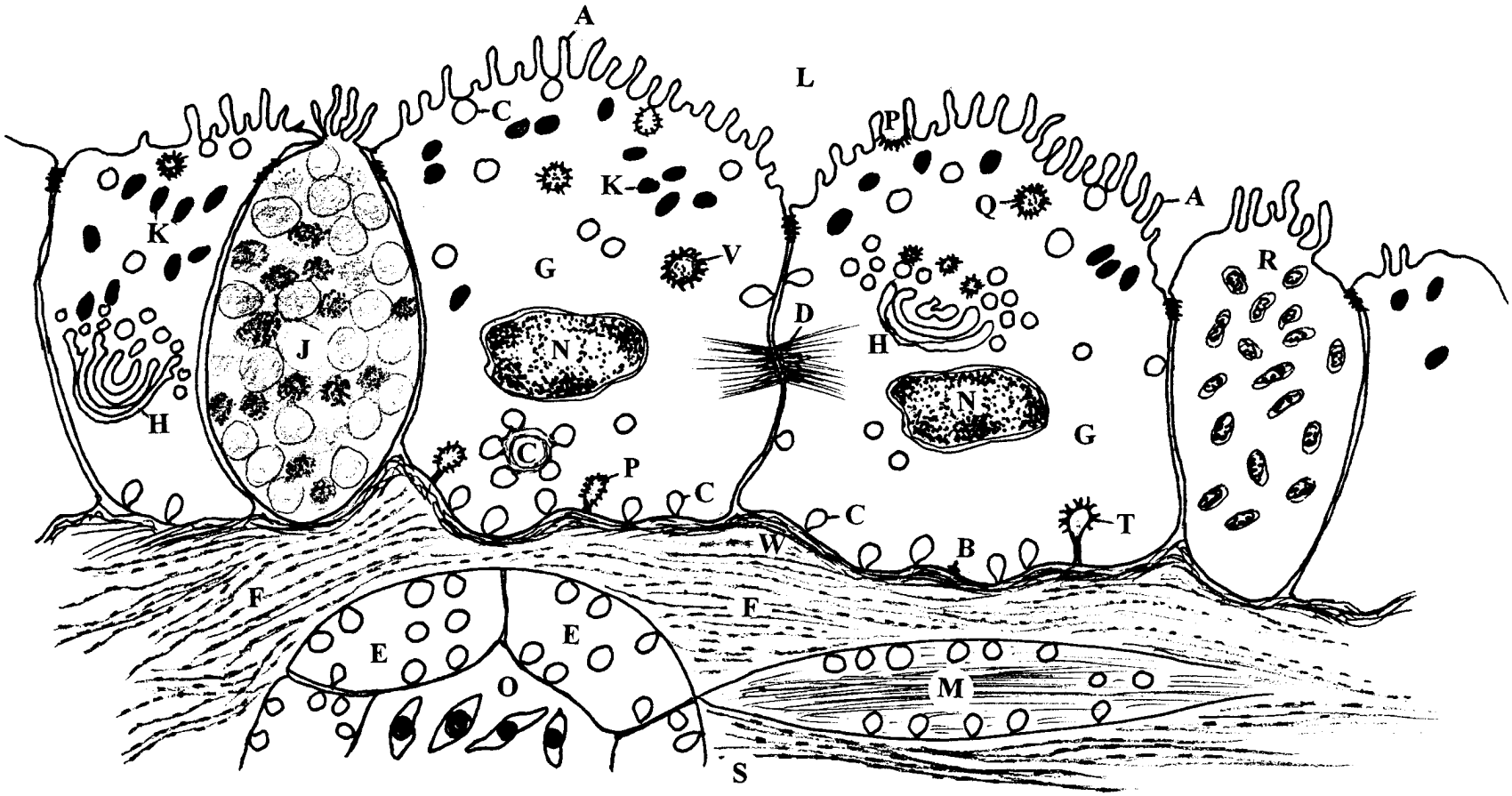

Figure 1. Diagram illustrates the arrangement of cells in toad urinary bladder with distribution of caveolae in granular (G), endothelial (E) and smooth muscle (M) cells.
A, apical plasma membrane B, basal plasma membrane C, caveolae D, desmosome E, endothelial cells F, collagen fibrils G, granular cell H, golgi body J, goblet cell K, secretory granules L, mucosal cavity M, smooth muscle N, nucleus O, red blood cells P, clathrin-coated pits Q, clathrin-coated vesicles R, MR-cell S, serosal cavity T, nonclathrin-coated pits V, nonclathrin-coated vesicles W, basement membrane

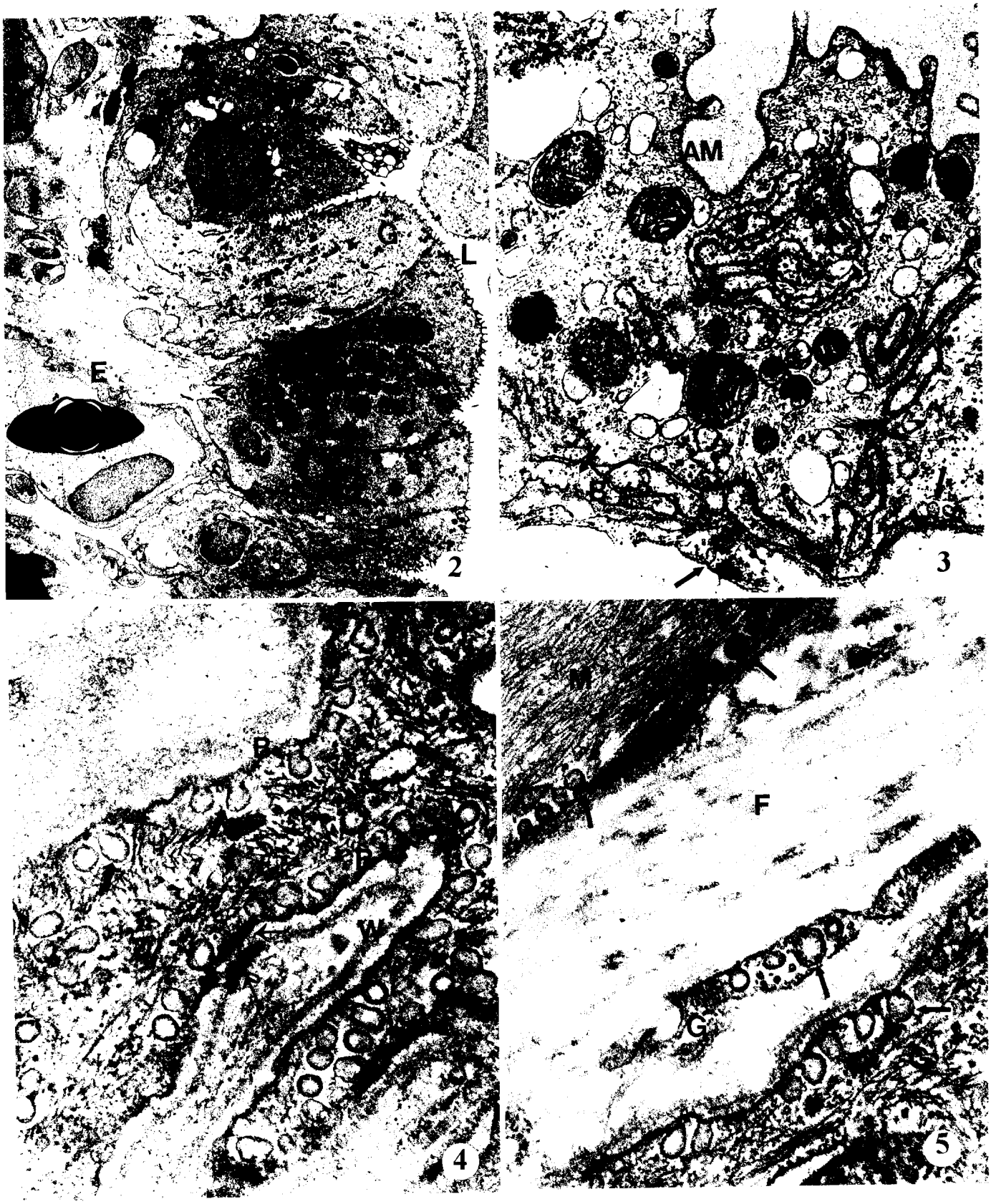
G
L
E
2
AM
3
B
4
F
G
5


6


7

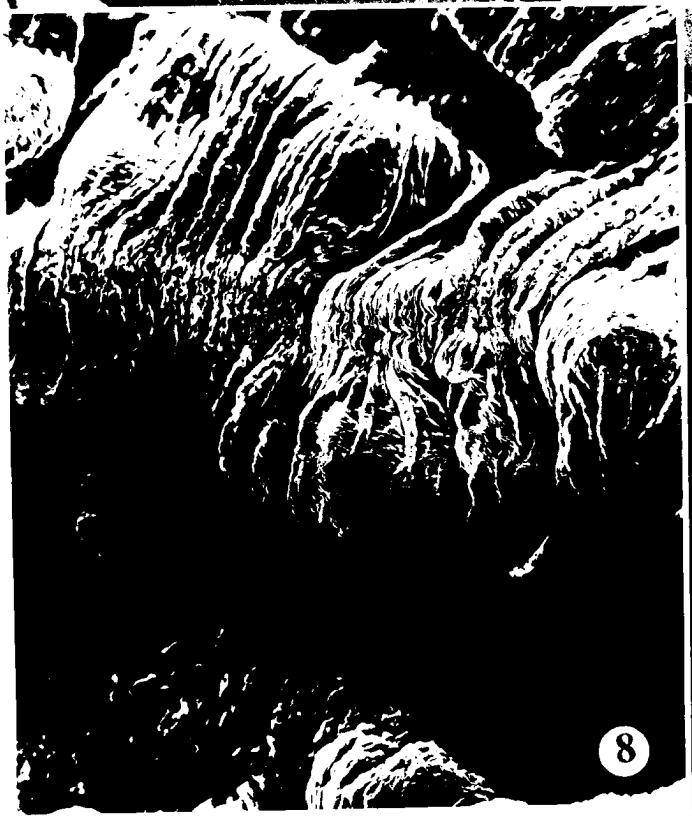
8


9

10

11

12

13

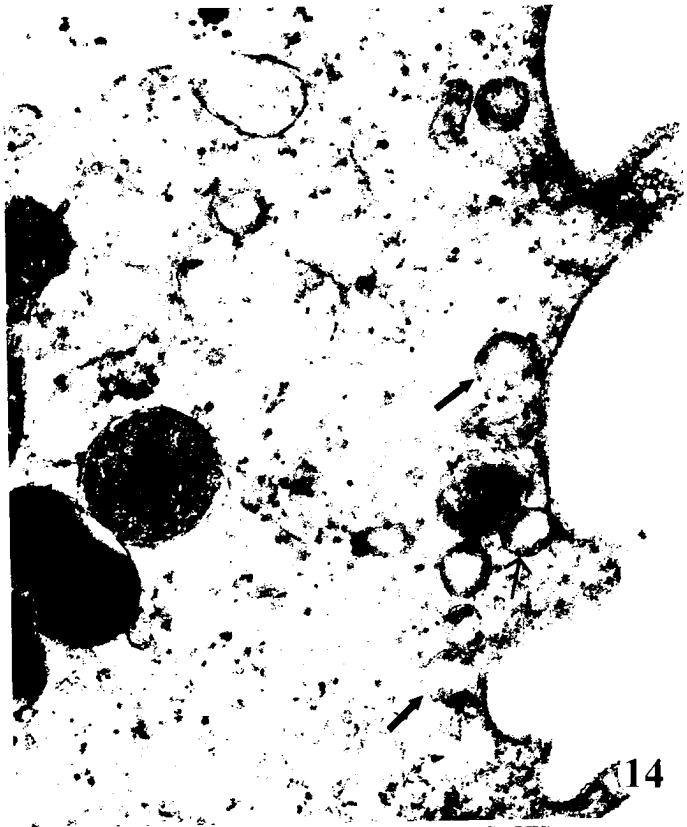

14

15

16

17

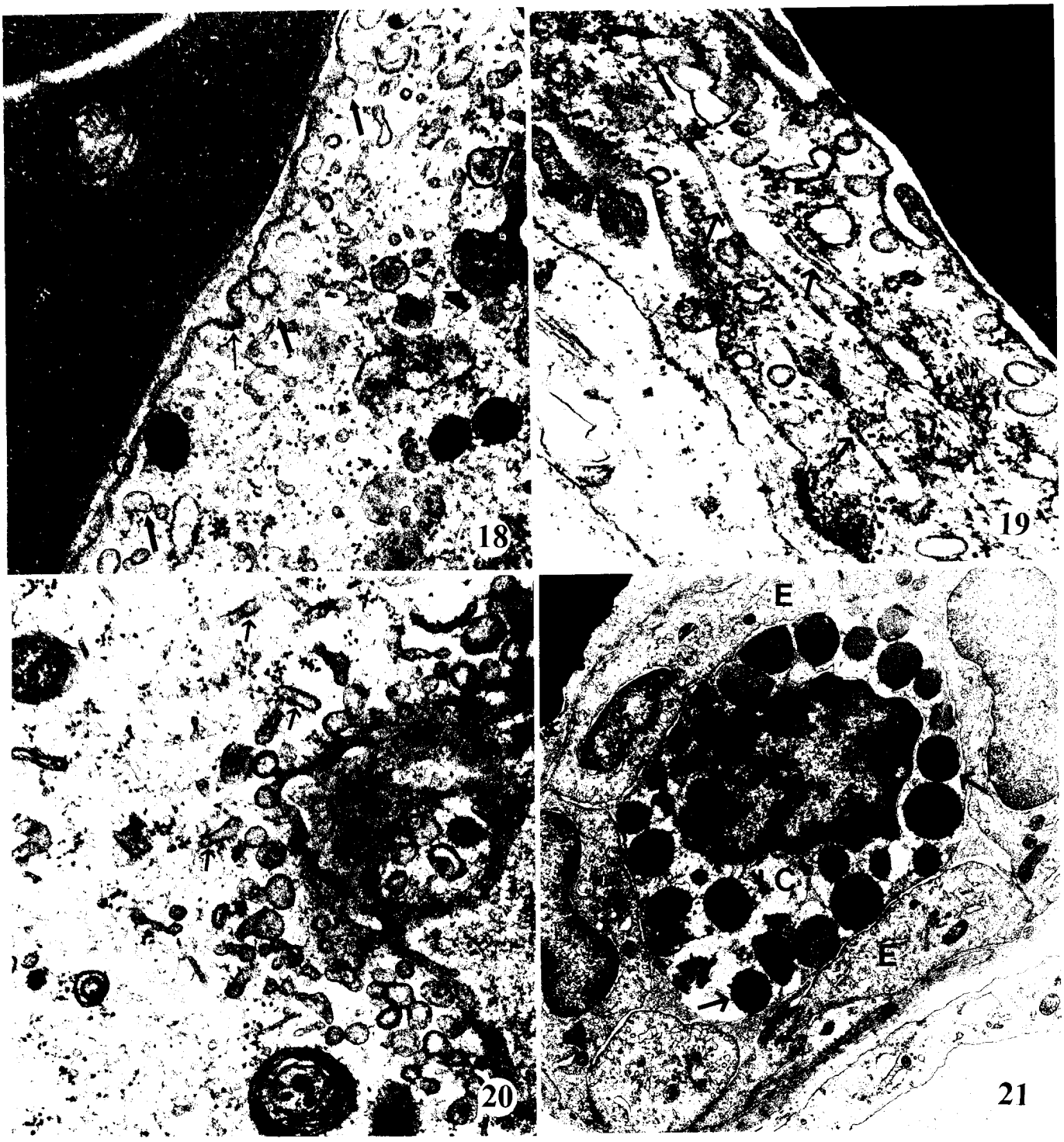
18
19
20
E
C
E
21

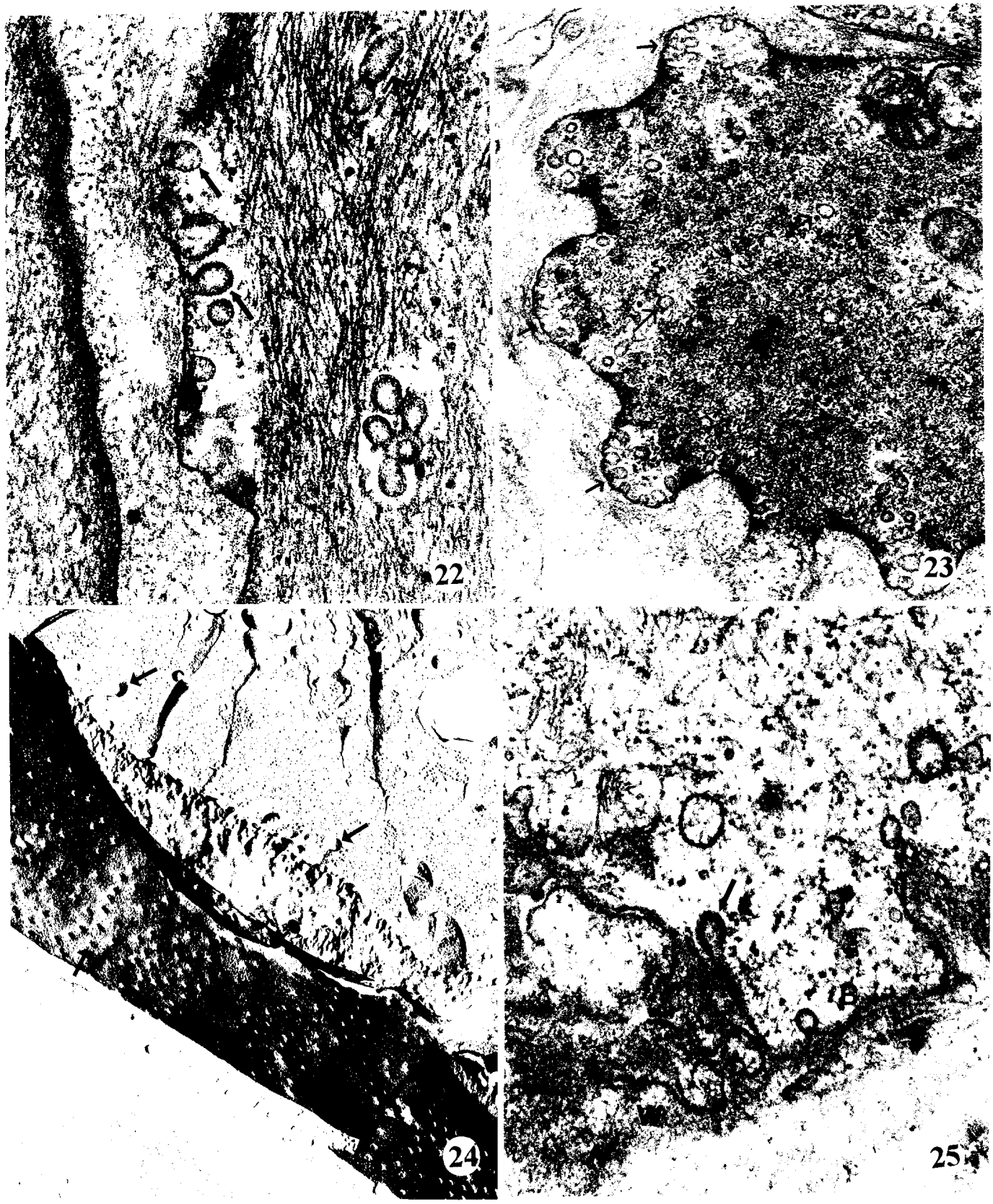
22
23
24
25

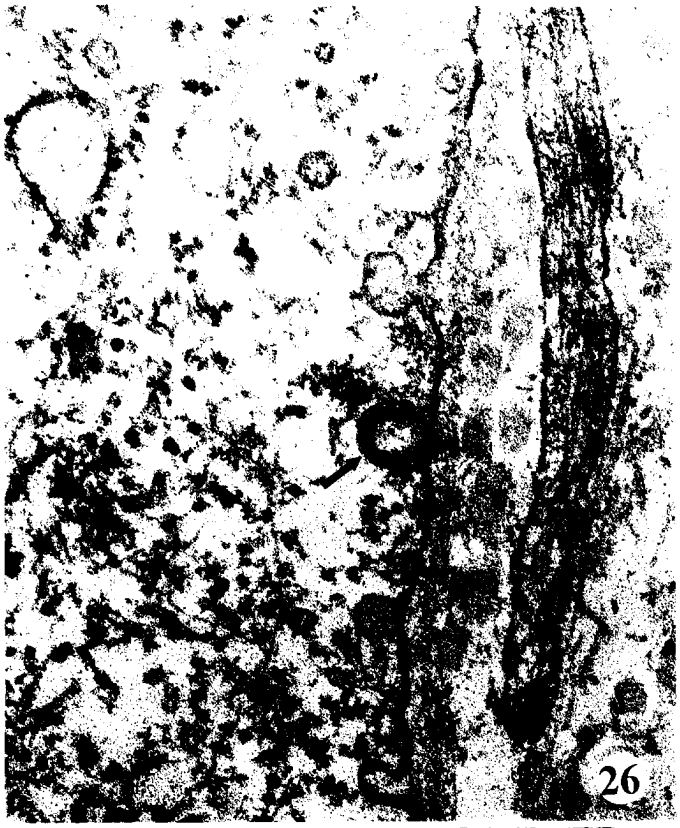
26

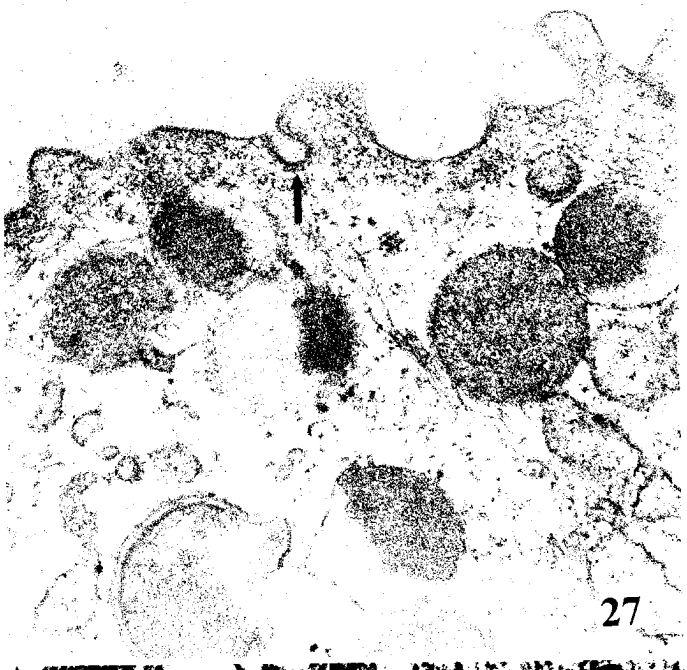
27


28


GL
29

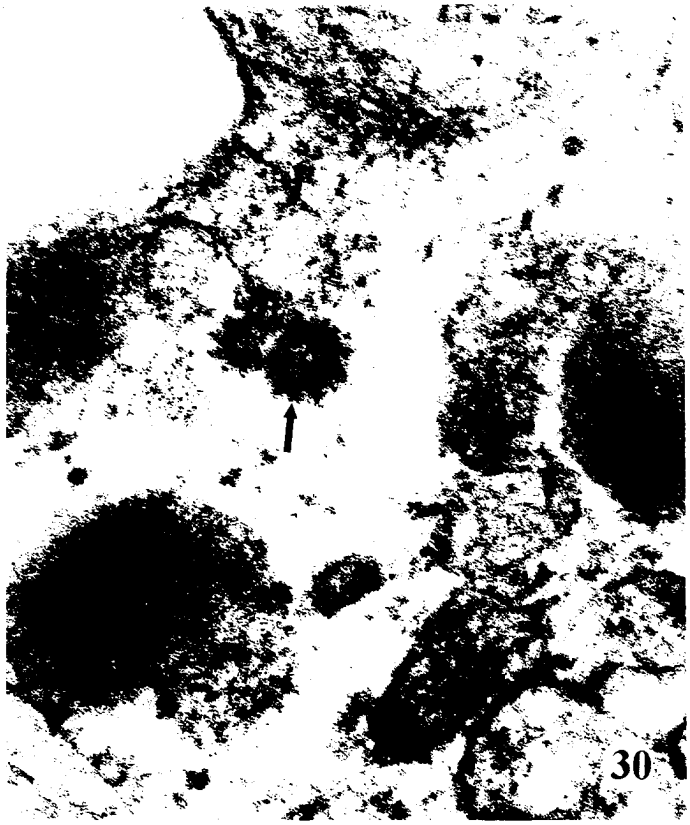
30


31


32

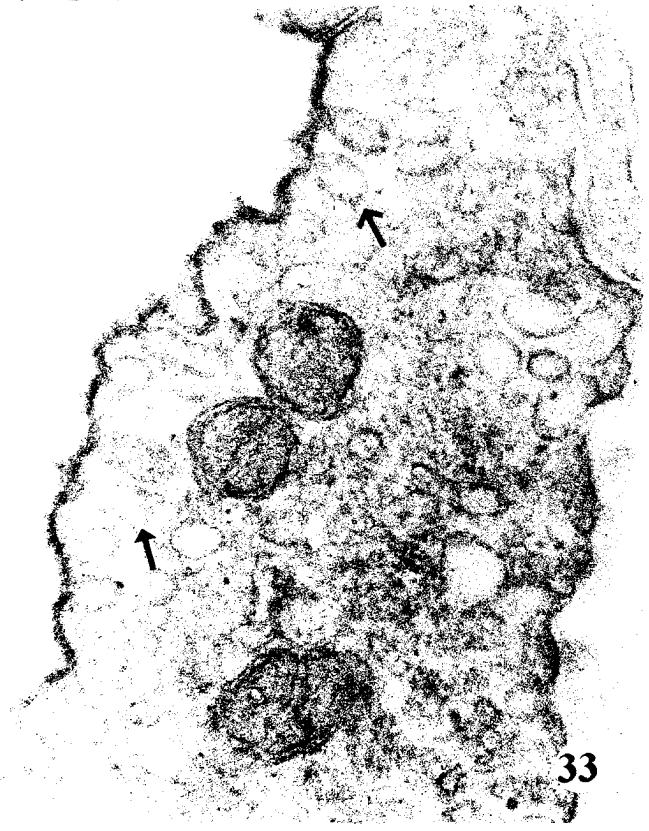
33

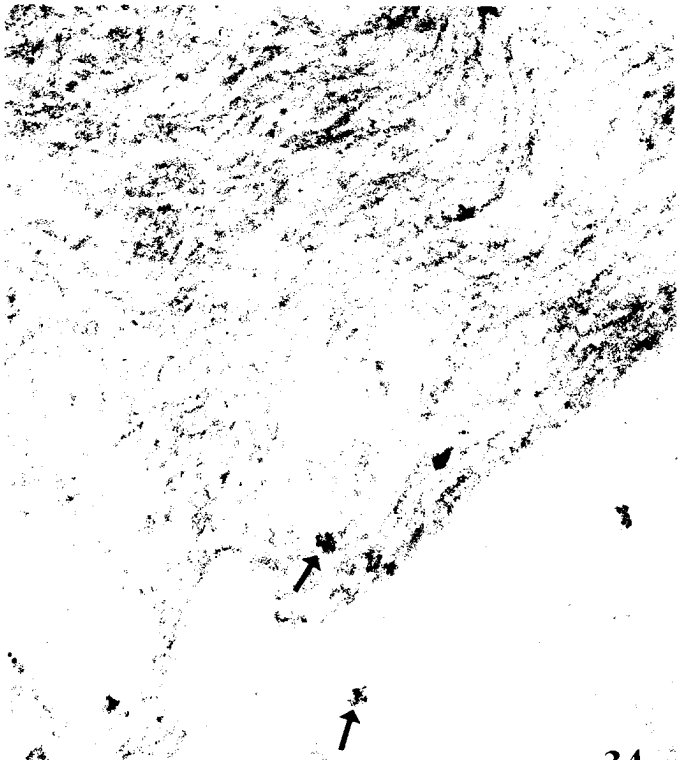

34

35

36

37

38

39

40

41

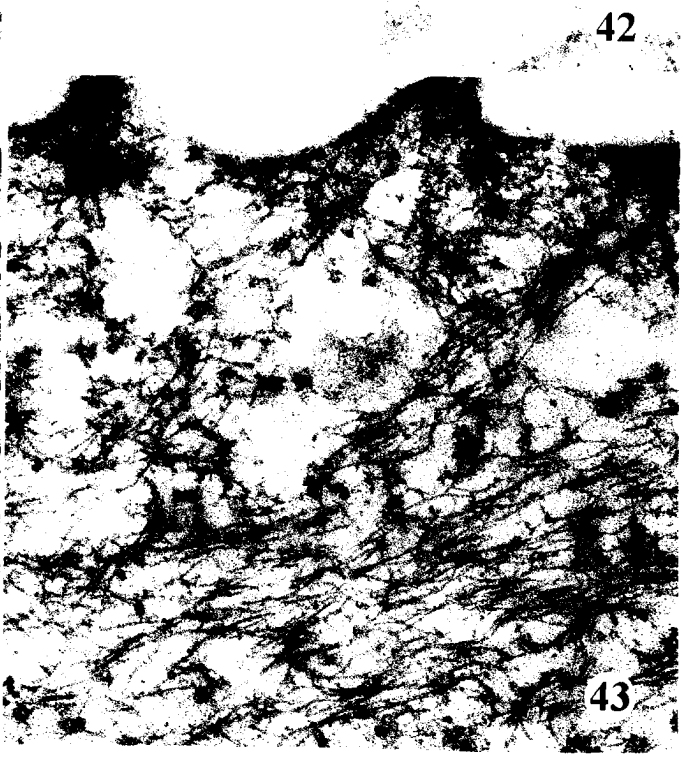

42

43

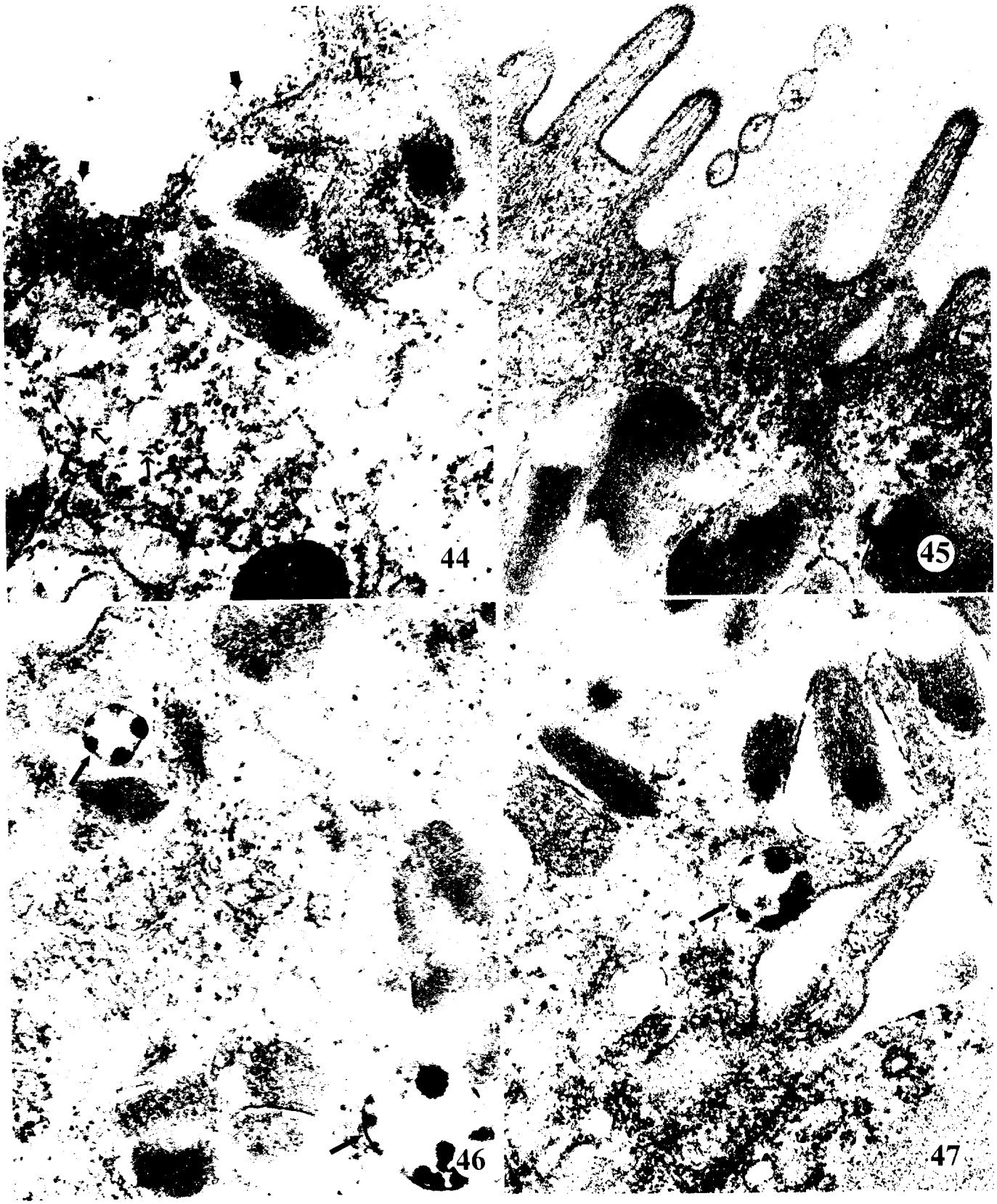
44
45
46
47

48

49

50

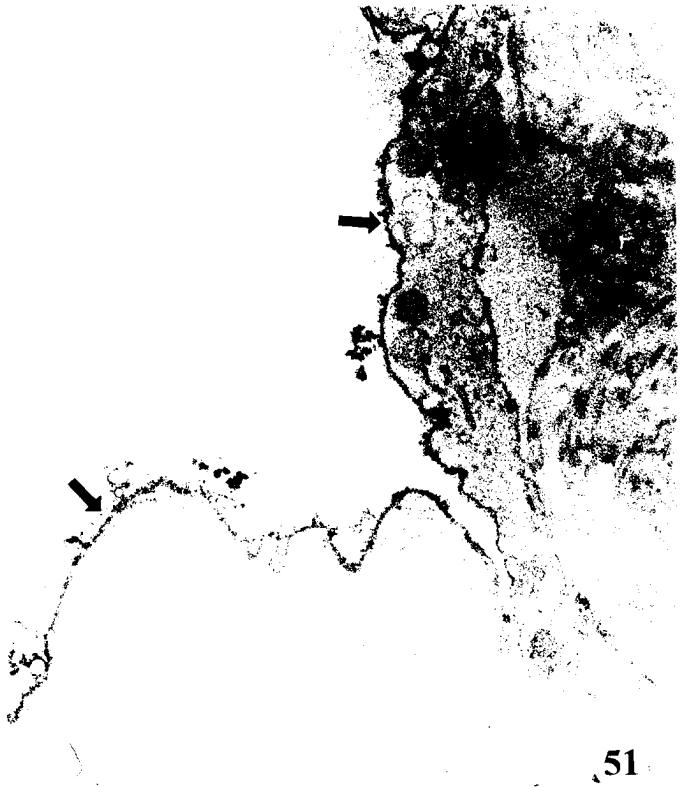

51

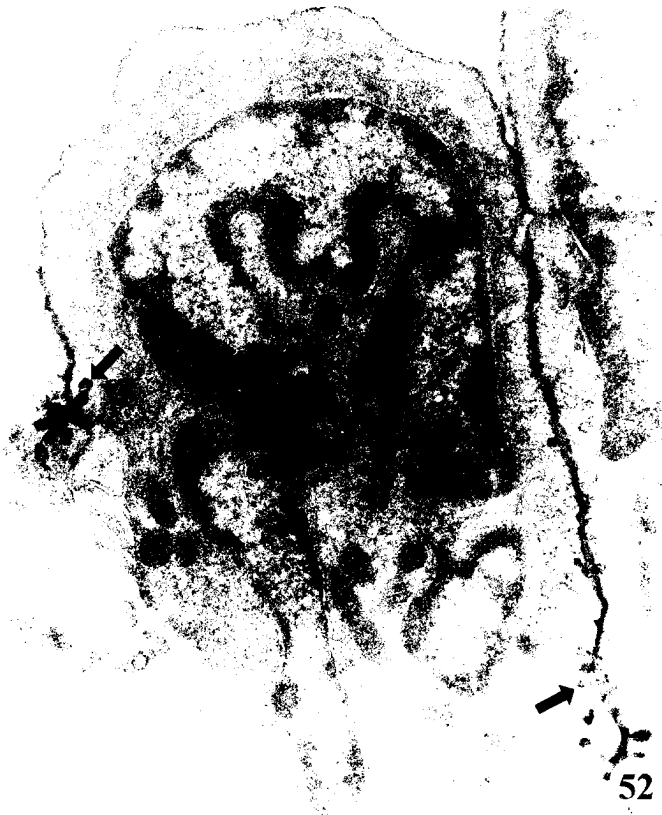

52

53

54

55

APPENDIX

Three Manuscripts

1) Mechanism of vasopressin-induced increase in intracellular Ca^{2+}($[Ca^{2+}]$) in LLC-PK_1 porcine kidney cells. *Am. J. Physiol.* 272: C810-C817 (1997).

2) The ATP-depleting reagent "iodacetamide" induces the degradation of protein kinase C alpha (PKC) in LLC-PK_1 pig kidney cells. *Life Sciences* (In Press).

3) Evidence of basolateral water permeability regulation in amphibian urinary bladder. *Biol. Cell.* (In Press).

Mechanism of vasopressin-induced increase in intracellular Ca^{2+} in LLC-PK_1 porcine kidney cells

ADNAN I. DIBAS,[1] S. MEHDI REZAZADEH,[1] RANGA VASSAN,[1]
ABDUL J. MIA,[2] AND THOMAS YORIO[1]
[1]*Department of Pharmacology, University of North Texas Health Science Center at Fort Worth, Fort Worth 76107; and* [2]*Jarvis Christian College, Hawkins, Texas 75765*

Dibas, Adnan I., S. Mehdi Rezazadeh, Ranga Vassan, Abdul J. Mia, and Thomas Yorio. Mechanism of vasopressin-induced increase in intracellular Ca^{2+} in LLC-PK_1 porcine kidney cells. *Am. J. Physiol.* 272 (*Cell Physiol.* 41): C810–C817, 1997.—Analysis of the signal transduction cascade of vasopressin-induced increase in intracellular Ca^{2+} concentration ($[Ca^{2+}]_i$) in LLC-PK_1 cells was performed. First, a comparison of the effect of vasopressin on $[Ca^{2+}]_i$ in LLC-PK_1 cells with that produced in rat hepatocytes was performed [an intracellular mobilizing mechanism involving a V_1 receptor coupled to the production of inositol 1,4,5-trisphosphate (IP_3)]. Second, the effect of known inhibitors of intracellular Ca^{2+} mobilization on vasopressin Ca^{2+} response in LLC-PK_1 cells was studied. Vasopressin induced a transient increase in $[Ca^{2+}]_i$ in both LLC-PK_1 cells and hepatocytes. In contrast to the single $[Ca^{2+}]_i$ spike seen in LLC-PK_1 cells, vasopressin induced an average of two to three $[Ca^{2+}]_i$ spikes in hepatocytes. The V_1 antagonist (Pmp[1]-*O*-Me-Tyr[2]-[Arg[8]]vasopressin, 1 μM) abolished vasopressin Ca^{2+} response in both cell types. Inhibitors of intracellular Ca^{2+} mobilization, thapsigargin (5 μM) and U-73122 (3 μM), abolished the Ca^{2+} response by vasopressin in LLC-PK_1 cells. The results suggest that vasopressin-induced increase in $[Ca^{2+}]_i$ in LLC-PK_1 cells is mediated via a V_1-like receptor and involves the mobilization of intracellular Ca^{2+} through an IP_3- or thapsigargin-sensitive Ca^{2+} pool.

V_1 receptor; thapsigargin; phospholipase C; U-73122

VASOPRESSIN or antidiuretic hormone is a nonapeptide produced by the brain and released from the neurohypophysis into the blood, where it ultimately acts in the kidney to produce an antidiuretic action (30), and in the liver, where it regulates glucose metabolism (6). In addition, it is transported into the brain, is released from synapses, and affects central regulatory processes including thermoregulation, cardiovascular homeostasis, and learning (3).

Vasopressin can act on at least three different receptors. The vasopressin V_1 receptors are coupled to a phospholipase C (PLC) system (22), in which vasopressin binding to the V_1 receptor induces inositol 1,4,5-trisphosphate (IP_3) production, thus mobilizing intracellular Ca^{2+} concentration ($[Ca^{2+}]_i$), and releases diacylglycerol (DAG), activating protein kinase C (PKC). Unlike the V_1 receptor, the V_2 receptor is coupled to an adenylyl cyclase enzyme in which vasopressin stimulates adenosine 3′,5′-cyclic monophosphate (cAMP) production (13). Although it is believed that the V_2 receptor is the key receptor mediating vasopressin responses in the kidney, V_1 receptors have been detected in renal tubules (4). In addition, a third receptor has recently been reported in the collecting tubules of rabbit but shares no homology to V_1 or V_2 receptors and is termed vascular cell adhesion molecule (VCAM) (5). Vasopressin acting on this novel receptor also increases $[Ca^{2+}]_i$ by stimulating IP_3 production (5).

LLC-PK_1 kidney cells are widely used as a model to characterize vasopressin cellular mechanisms in the kidney (29). These cells exhibit transport properties typical of proximal tubule cells (21), although they respond to vasopressin and calcitonin but not to parathyroid hormones, which suggests a medullary thick ascending limb origin as well (11). Whether LLC-PK_1 cells are of a proximal origin or thick ascending limb origin, a considerable amount of the kidney's Ca^{2+} reabsorption occurs in these nephron sections (55% of total Ca^{2+} reabsorption occurs in proximal tubules, whereas 20% occurs in thick ascending limb; Ref. 9). Weinberg et al. (27) have reported that vasopressin increased $[Ca^{2+}]_i$ in LLC-PK_1 cells. However, a more detailed characterization of vasopressin-induced increase in $[Ca^{2+}]_i$ was needed. Specially, an increase in $[Ca^{2+}]_i$ has been shown to activate Ca^{2+}/calmodulin-dependent protein kinase, which has been shown to phosphorylate the Na^+/H^+ exchanger, resulting in inhibition of Na^+ uptake at the apical membrane of the rabbit proximal tubules (28). Experimental evidence also suggests that Na^+ reabsorption is the driving force for Ca^{2+} uptake in that part of the kidney (9). Therefore a better understanding of intracellular Ca^{2+} release mechanisms by vasopressin may contribute to better comprehension of cellular Ca^{2+} homeostasis. In the present studies, we employed two strategies to further characterize the mechanism of vasopressin-induced increase in $[Ca^{2+}]_i$ in LLC-PK_1 cells. The first strategy was to compare the Ca^{2+} response of vasopressin in LLC-PK_1 cells to another cell type in which vasopressin-induced Ca^{2+} response has a well-understood mechanism. Therefore rat hepatocytes were used, since it has been shown that vasopressin-induced increase in $[Ca^{2+}]_i$ was mediated via a V_1 receptor involving the hydrolysis of phosphoinositide 4,5-bisphosphate to IP_3 and DAG. The effects of potent inhibitors of V_1 and V_2 receptors on vasopressin-induced increase in $[Ca^{2+}]_i$ were tested. The second strategy utilized the new inhibitors of intracellular Ca^{2+} release mechanisms, thapsigargin, an inhibitor of endoplasmic reticular Ca^{2+}-adenosinetriphosphatase (ATPase), and U-73122, a potent inhibitor of PLC (1). Recently, both compounds have been described to be more efficient in testing the involvement of the intracellular Ca^{2+} pool in agonists-induced increase in $[Ca^{2+}]_i$ and were therefore employed. The data obtained in the present report suggest that vasopressin-induced increases in $[Ca^{2+}]_i$ are mediated by a V_1-like-

receptor and involve the release of Ca^{2+} from the intracellular stores.

METHODS

Materials

Phorbol 12-myristate 13-acetate (PMA) and arginine vasopressin were purchased from Sigma Chemical (St. Louis, MO). Nifedipine, 1,2-bis(2-aminophenoxy)ethane-*N*,*N*,*N*′,*N*′-tetraacetic acid (BAPTA) acetoxymethyl ester (AM) and thapsigargin were purchased from RBI (Natick, MA). Fura 2-AM was obtained from Molecular Probes (Eugene, OR). V_1 and V_2 antagonists were purchased from Peninsula Laboratories (Belmont, MA).

Tissue Culture

Rat hepatocytes were a gift from Dr. Thomas Fungwe (Dept. of Biochemistry, University of North Texas Health Science Center). LLC-PK_1 cells (*passages 17–48*) were maintained in Dulbecco's modified Eagle's medium (DMEM) supplemented with 44 mM $NaHCO_3$, 10% fetal bovine serum, and antibiotics. For Ca^{2+} measurements, cells were subcultured onto 25-mm glass coverslips 1–2 days before experimentation. For cAMP assay, cells were plated onto multiwell coated dishes (3 × 4 each) 2 days before experiments.

Intracellular Ca^{2+} Concentration Measurements

All measurements were conducted with a Nikon Diaphot microscope (Tokyo, Japan), utilizing a dynamic single-cell video-imaging technique using an Image-1FL Quantitative Fluorescence System (Universal Imaging, W. Chester, PA). Hepatocytes and LLC-PK_1 cells were loaded with fura 2-AM (5 μM) in a modified Krebs-Ringer solution (Krebs: 115 mM NaCl, 2.5 mM $CaCl_2$, 1.2 mM $MgCl_2$, 24 mM $NaHCO_3$, 5 mM KCl, and 25 mM *N*-2-hydroxyethylpiperazine-*N*′-2-ethanesulfonic acid, pH 7.4) for 30 min at 37°C. Cells were washed with 3 ml of Krebs to remove excess probe, and $[Ca^{2+}]_i$ measurements were determined by monitoring the ratio of fura 2 fluorescence at excitation wavelengths of 340 and 380 nm. Cytosolic Ca^{2+} was calculated according to equations described by Grynkiewicz et al. (12). Calibration was performed in vivo and conditions of high $[Ca^{2+}]_i$ were achieved by adding the Ca^{2+} ionophore A-23187 (1–3 μM), whereas conditions of low $[Ca^{2+}]_i$ were obtained by adding ethylene glycol-bis(β-aminoethyl ether)-*N*,*N*,*N*′,*N*′-tetraacetic acid (4–5 mM).

cAMP Assay

[^{3}H]adenine incorporation. Cells were loaded with [^{3}H]adenine (2 μCi/ml) for 2 h in serum-free DMEM. After adenine incorporation, the medium containing excess [^{3}H]adenine was replaced with a fresh serum-free DMEM containing 0.1 mM of the phosphodiesterase inhibitor, Ro-20–1724. After incubation of cells for 10 min, cells were stimulated with vasopressin, and the incubation was continued for another 10 min at 37°C. The reaction was terminated by aspirating the medium and by adding 1 ml of a stop solution (5% trichloroacetic acid containing 0.5 mM cAMP).

cAMP assay. cAMP was determined by the method of Salomon et al. (23). Thirty minutes after the reaction was stopped, the stop solution from each well was aspirated and transferred to Dowex columns (AG50W-X8, Bio-Rad, Richmond, CA), and the eluate was collected into a scintillation vial. Distilled water (3 ml) was added to each column, the eluate containing [^{3}H]ATP was collected in the same vials and mixed with 10 ml of EcoLume scintillation cocktail (ICN, Costa Mesa, CA), and the radioactivity was counted. The Dowex columns were placed over alumina columns (A950–500, Neutral Brockman, Fisher, Fair Lawn, NJ), and 4 ml of distilled water were added to each column. This transfers the cAMP from Dowex columns to the alumina columns. After both Dowex and alumina columns were allowed to go to a complete elution, the alumina columns were placed over another set of scintillation vials, and 4 ml of a 0.1 M imidazole solution (pH 7.5) were added to each column. The eluate containing both cold cAMP and [^{3}H]cAMP was collected. Three hundred microliters of this eluate were saved for measurement of optical density and calculation of column efficiency. The column efficiency was calculated by measuring the absorbance of cold cAMP in stop solution (at 259 nm) before and after eluting from the column. From these values, the counts for [^{3}H]cAMP were normalized.

RESULTS

Vasopressin Effects on $[Ca^{2+}]_i$ in LLC-PK_1 Cells and Rat Hepatocytes

Vasopressin (83 nM) induced an increase in $[Ca^{2+}]_i$ in LLC-PK_1 cells judged by the increase in the fluorescence ratio of fura 2 (Fig. 1*A*). The increase in $[Ca^{2+}]_i$ was transient where it peaked to 170.9 ± 10 nM (n = 16) and declined rapidly to basal levels (61.2 ± 2 nM, n = 39). In a series of separate experiments, the muscarinic agonist carbachol was added immediately after the addition of vasopressin, and an additional increase in $[Ca^{2+}]_i$ was observed. The muscarinic agonist-induced increase in $[Ca^{2+}]_i$ was transient and was similar to vasopressin's response (with carbachol stimulation, $[Ca^{2+}]_i$ peaked and declined rapidly to basal levels, data not shown). Vasopressin at similar concentrations also induced a transient increase in $[Ca^{2+}]_i$ in hepatocytes (Fig. 1*B*). However, multiple spikes or an oscillation of increased $[Ca^{2+}]_i$ were observed. This phenomenon has previously been reported in hepatocytes with vasopressin stimulation (22). Although vasopressin induced a transient increase in $[Ca^{2+}]_i$ in both cell types, only hepatocytes showed an oscillatory pattern. To verify the involvement of a V_1-like receptor in vasopressin-induced effects on LLC-PK_1 cells, the effect

Table 1. *Summary of effects of different agents on vasopressin-induced increases in $[Ca^{2+}]_i$ in LLC-PK_1 cells and rat hepatocytes*

Cell Type	Ca^{2+} Response	V_1 Antagonist	DBcAMP	U-73122	Thapsigargin
LLC-PK_1	Single spike	Inhibitory	No effect	Inhibitory	Inhibitory*
Rat hepatocytes	2–3 spikes (oscillatory)	Inhibitory	No effect	Inhibitory	Not tested

$[Ca^{2+}]_i$, intracellular Ca^{2+} concentration; DBcAMP, dibutyryl-cAMP. *Ability of thapsigargin to deplete intracellular Ca^{2+} pool and increase $[Ca^{2+}]_i$ prevented vasopressin from producing an additional increase in $[Ca^{2+}]_i$.

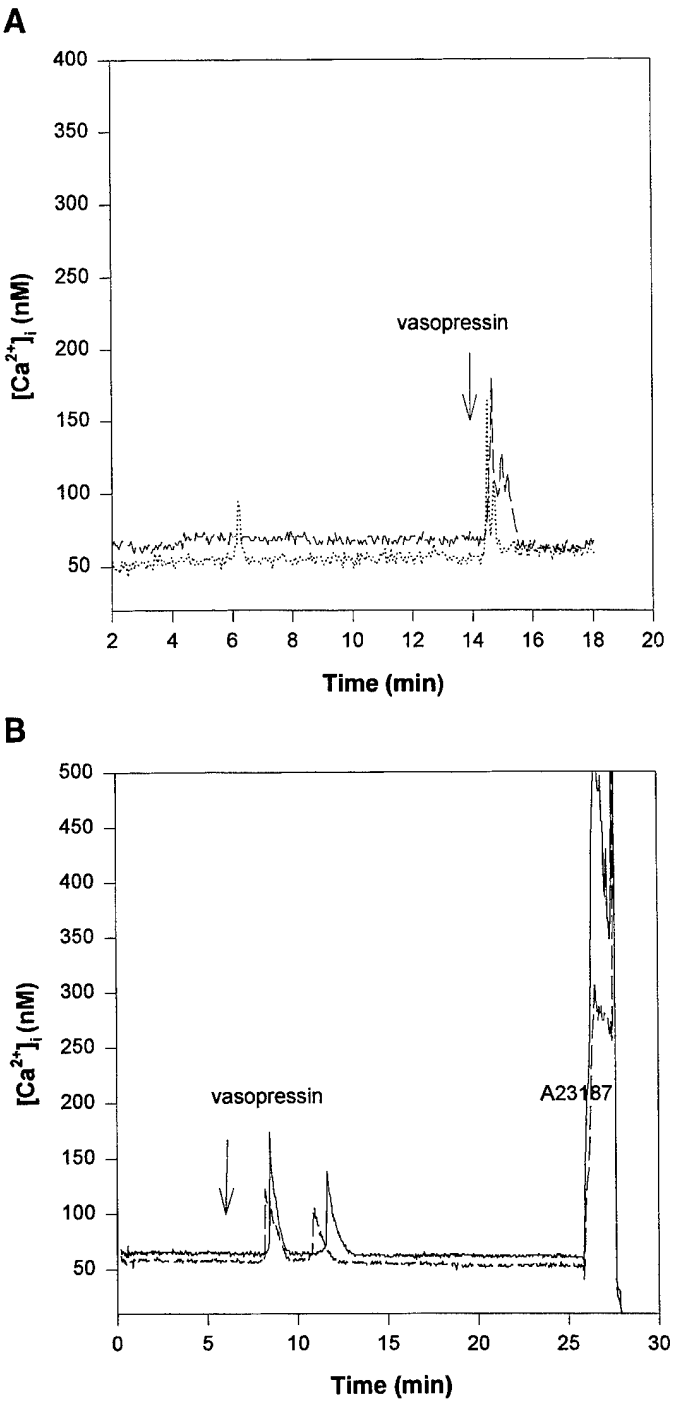

Fig. 1. *A*: vasopressin (83 nM) increased intracellular Ca^{2+} ($[Ca^{2+}]_i$) in LLC-PK_1 cells. LLC-PK_1 cells loaded with fura 2 (5 μM) were treated with vasopressin at time indicated by arrow. As shown, vasopressin induced a transient increase in $[Ca^{2+}]_i$ that showed as a peak, but $[Ca^{2+}]_i$ declined rapidly to basal levels. *B*: vasopressin (83 nM) increased $[Ca^{2+}]_i$ in rat hepatocytes. Rat hepatocytes were loaded with fura 2 as described in METHODS and were stimulated with vasopressin. Vasopressin induced an oscillatory pattern of increased $[Ca^{2+}]_i$.

of a V_1 receptor antagonist (Pmp[1]-*O*-Me-Tyr[2]-[Arg[8]]-vasopressin) was evaluated. As shown in Fig. 2, *A* and *B*, the V_1 antagonist abolished vasopressin-induced increases in $[Ca^{2+}]_i$ in both LLC-PK_1 cells and hepatocytes, respectively. Interestingly, the V_2 receptor has been also suggested to be coupled to Ca^{2+} mobilization in rat inner medullary collecting duct (8). It was therefore of interest to test its potential involvement in vasopressin-induced increase in $[Ca^{2+}]_i$. As shown in

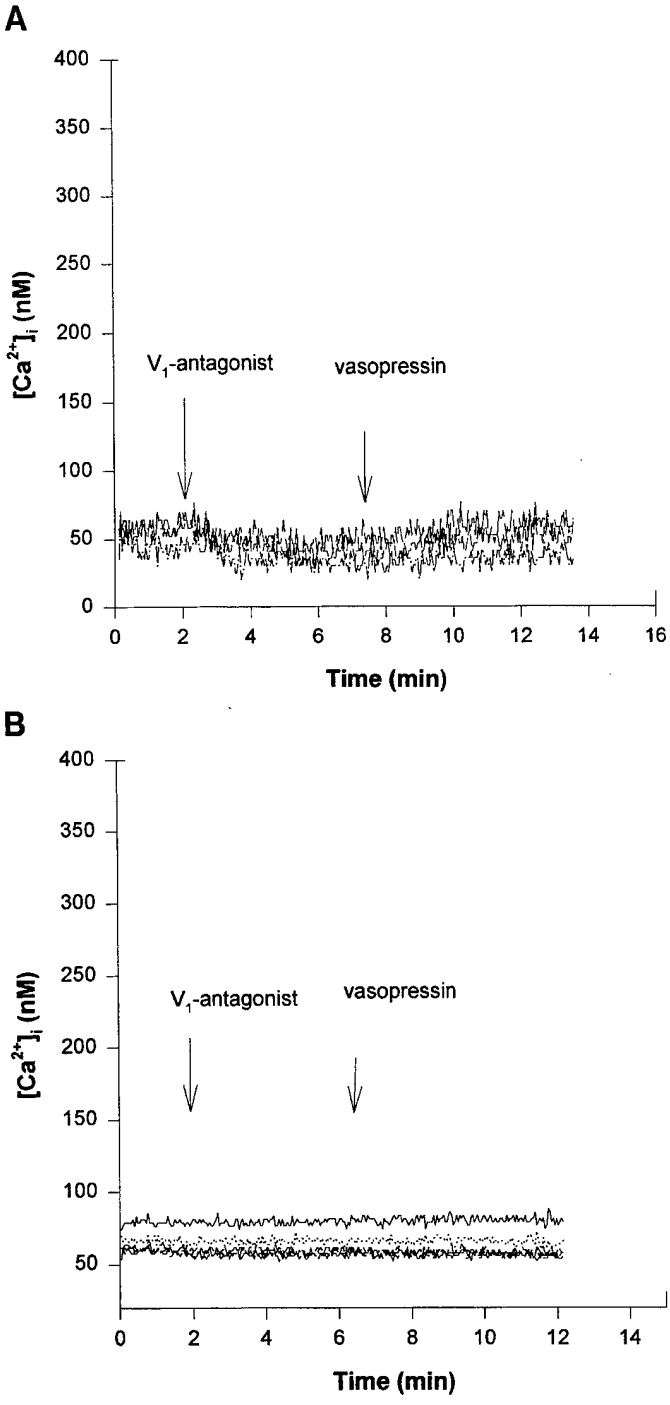

Fig. 2. *A*: V_1 antagonist abolished vasopressin-induced increase in $[Ca^{2+}]_i$ in LLC-PK_1 cells. LLC-PK_1 cells loaded with fura 2 were treated with V_1 antagonist (1 μM) for 2–5 min before addition of vasopressin (260 nM). However, vasopressin failed to increase $[Ca^{2+}]_i$. *B*: V_1 antagonist abolished vasopressin-induced increase in $[Ca^{2+}]_i$ in rat hepatocytes. Rat hepatocytes loaded with fura 2 were treated with V_1 antagonist (1 μM) for 2–5 min followed by addition of vasopressin (260 nM), but no increase in $[Ca^{2+}]_i$ was observed.

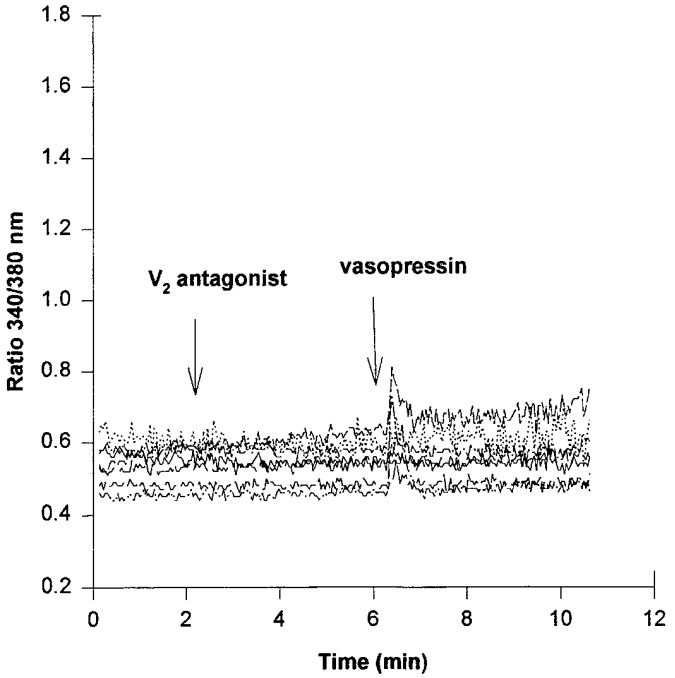

Fig. 3. V_2 antagonist abolished vasopressin-induced increase in $[Ca^{2+}]_i$ in LLC-PK_1 cells. LLC-PK_1 cells loaded with fura 2 were treated with V_2 antagonist (3 μM) for 2–5 min before addition of vasopressin (260 nM). However, vasopressin still increased $[Ca^{2+}]_i$.

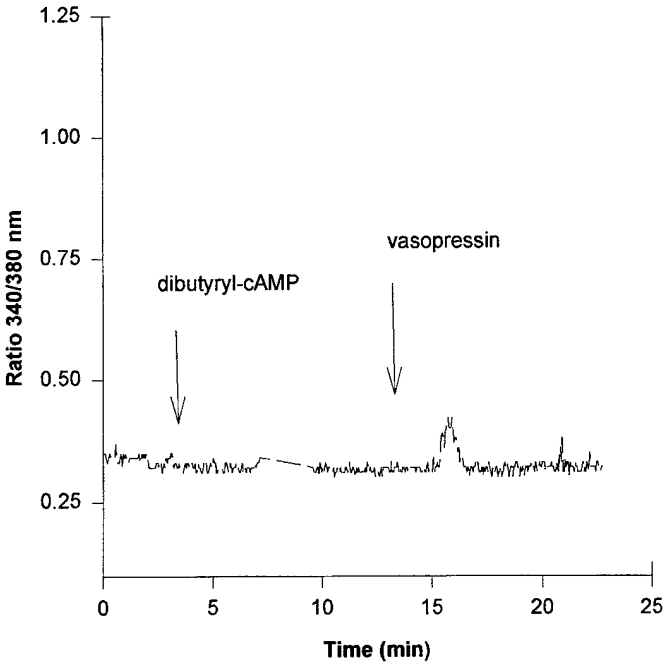

Fig. 5. Dibutyryl-cAMP (DBcAMP), a membrane-permeable analog of cAMP, failed to increase $[Ca^{2+}]_i$ in LLC-PK_1 cells. Addition of DBcAMP (100 μM) to LLC-PK_1 cells had no effect on $[Ca^{2+}]_i$. However, addition of vasopressin induced an increase in $[Ca^{2+}]_i$. $[Ca^{2+}]_i$ measurements were determined by monitoring ratio of fura 2 fluorescence at excitation wavelengths of 340 and 380 nm.

Fig. 3, the V_2 antagonist ([d(CH_2)$_5$,D-Ile^2,Ile^4,Arg^8]-vasopressin, 3 μM) had no effect on vasopressin-induced increase in $[Ca^{2+}]_i$. However, the V_2 receptor was activated by vasopressin as a dose-dependent increase in cAMP levels in LLC-PK_1 cells was observed (concentration eliciting 50% of maximal response = 25 nM, Fig. 4). Furthermore, the addition of dibutyryl-cAMP (DBcAMP, up to 100 μM) had no effect on $[Ca^{2+}]_i$ (Fig. 5). The latter observation further suggests that the V_2 receptor may not be involved in vasopressin-induced increase in $[Ca^{2+}]_i$ in LLC-PK_1 cells.

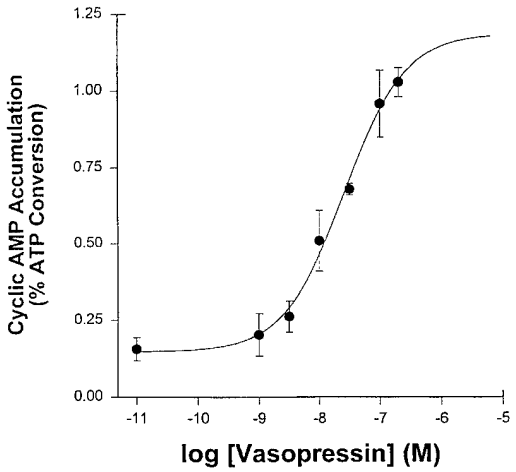

Fig. 4. Vasopressin dose dependently increased cAMP levels in LLC-PK_1 cells. LLC-PK_1 cells were loaded with [^{3}H]adenine as described in METHODS. Vasopressin (1–100 nM) was added to cells (10-min incubation). [^{3}H]ATP and [^{3}H]cAMP accumulated in cells were isolated by Dowex-alumina chromatography and quantitated. Results were normalized and expressed as percent ATP converted to cAMP. Each value represents mean ± SE of at least 3 different determinations.

Source of Ca^{2+} in Vasopressin-Induced Increase in $[Ca^{2+}]_i$ in LLC-PK_1 Cells

In the next series of experiments, the focus of the study was shifted to identify the source of Ca^{2+} involved in vasopressin-induced increase in $[Ca^{2+}]_i$. Thapsigargin (5–10 μM), a potent inhibitor of the endoplasmic reticular Ca^{2+}-ATPase, was used to deplete the intracellular Ca^{2+} pool. As illustrated in Fig. 6*A*, thapsigargin induced a biphasic increase in $[Ca^{2+}]_i$, in which the $[Ca^{2+}]_i$ peaked at 1–2 min and declined to a lower Ca^{2+} level but was maintained above basal levels. Thus a new steady state of $[Ca^{2+}]_i$ was reached. The addition of vasopressin (83 nM) failed to increase $[Ca^{2+}]_i$, suggesting that vasopressin-induced increase in $[Ca^{2+}]_i$ was due to a mobilization of intracellular Ca^{2+}. The depletion of such a pool abolished the vasopressin Ca^{2+} response. The involvement of a thapsigargin-sensitive Ca^{2+} pool has previously been reported (25, 26). However, the sustained increase in $[Ca^{2+}]_i$ observed after thapsigargin suggested a possible influx of extracellular Ca^{2+} similar to the capacitative model proposed by Putney (20). We therefore tested the effect of thapsigargin in the absence of extracellular Ca^{2+}. As shown in Fig. 6*B*, thapsigargin induced a sharp transient increase in $[Ca^{2+}]_i$, which declined to basal levels (after ~3 min), and there was no sustained increase in $[Ca^{2+}]_i$ as previously observed in the presence of extracellular Ca^{2+} (Fig. 6*A*). Interestingly, the introduction of extracellular Ca^{2+} induced an increase in $[Ca^{2+}]_i$ having a

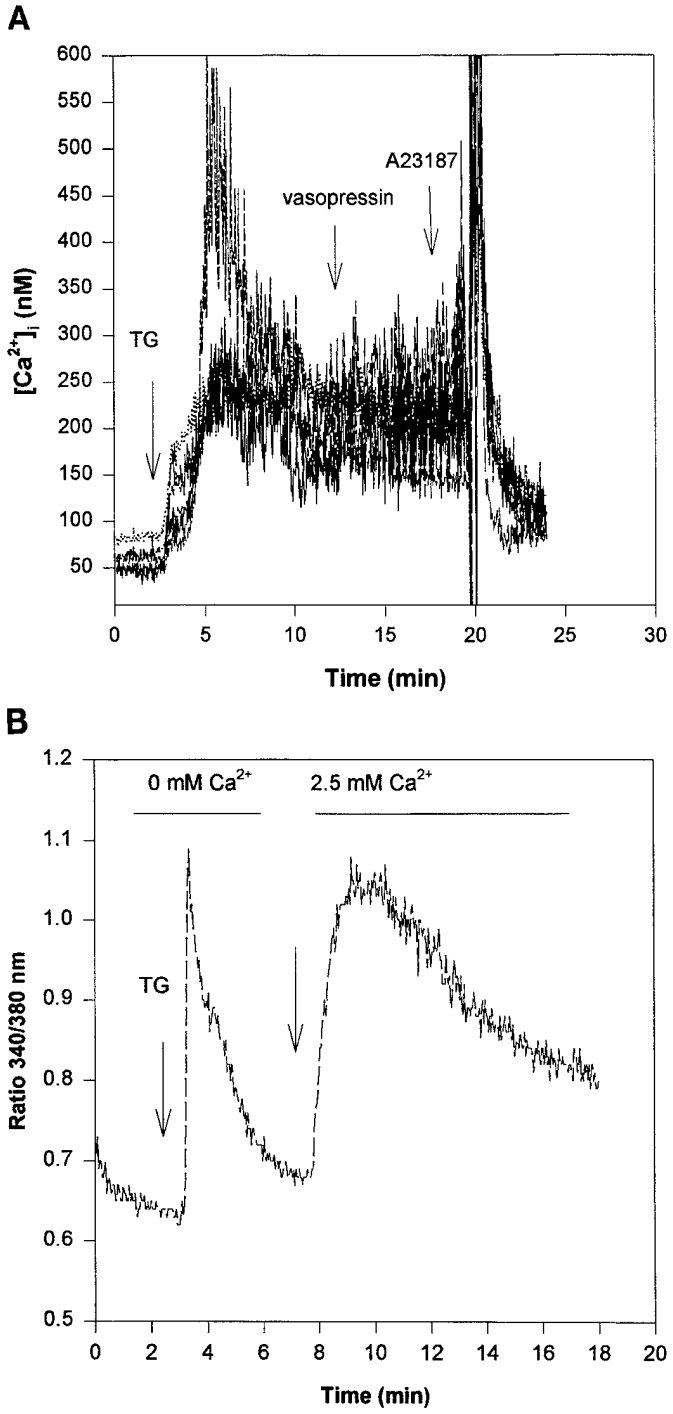

Fig. 6. *A*: depletion of intracellular Ca^{2+} pools with thapsigargin (TG) abolished vasopressin-induced increase in $[Ca^{2+}]_i$ in LLC-PK_1 cells. Treatment of LLC-PK_1 cells with TG (5–10 μM) increased $[Ca^{2+}]_i$, and $[Ca^{2+}]_i$ was maintained above basal levels. Subsequent addition of vasopressin failed to increase $[Ca^{2+}]_i$. *B*: TG induced a transient increase in $[Ca^{2+}]_i$ in LLC-PK_1 cells in absence of extracellular Ca^{2+}. Treatment of LLC-PK_1 cells with TG (5–10 μM) in absence of extracellular Ca^{2+} increased $[Ca^{2+}]_i$. However, increase was transient, and $[Ca^{2+}]_i$ declined to basal levels after ~3 min. Introduction of extracellular Ca^{2+} induced an increase in $[Ca^{2+}]_i$ and response to TG was restored.

bell-shaped pattern, but $[Ca^{2+}]_i$ remained above basal levels as was originally seen in Fig. 6*A*.

The thapsigargin experiment suggests that the depletion of intracellular Ca^{2+} stimulates the influx of extracellular Ca^{2+} and that Ca^{2+} influx contributes to the sustained elevation of $[Ca^{2+}]_i$. To test whether a similar mechanism operated with vasopressin, nifedipine (200 nM), a potent inhibitor of extracellular Ca^{2+} influx by inhibiting voltage-sensitive Ca^{2+} channels, was added before vasopressin. However, nifedipine failed to suppress the vasopressin-induced increase in $[Ca^{2+}]_i$ (Fig. 7).

Finally, to provide direct evidence for the involvement of an IP_3-dependent mechanism in vasopressin's Ca^{2+} response, the effect of U-73122, a potent inhibitor of PLC actions (1) was tested. As shown in Fig. 8*A*, U-73122 (3 μM) abolished vasopressin-induced increase in $[Ca^{2+}]_i$ in LLC-PK_1 cells. Also, U-73122 at a similar concentration abolished vasopressin-induced increase in $[Ca^{2+}]_i$ in hepatocytes (Fig. 8*B*).

In addition, the nuclear IP_3 receptor has been shown to be phosphorylated by PKC in rat liver nuclei (16). The phosphorylation of the IP_3 receptor accelerated Ca^{2+} release by IP_3. It was therefore of interest to test whether PKC would affect vasopressin-induced increase in $[Ca^{2+}]_i$ in LLC-PK_1 cells. The effect of PMA (200 nM; activator of PKC) on $[Ca^{2+}]_i$ was tested. PMA had no effect on $[Ca^{2+}]_i$ (data not shown). A role for PKC in vasopressin-induced increase in $[Ca^{2+}]_i$ was therefore unlikely. It is noteworthy to report that okadaic acid, a phosphatase inhibitor, occasionally augmented vasopressin-induced increase in $[Ca^{2+}]_i$, suggesting the involvement of phosphorylated proteins that activate or potentiate the increase in $[Ca^{2+}]_i$ (data not shown).

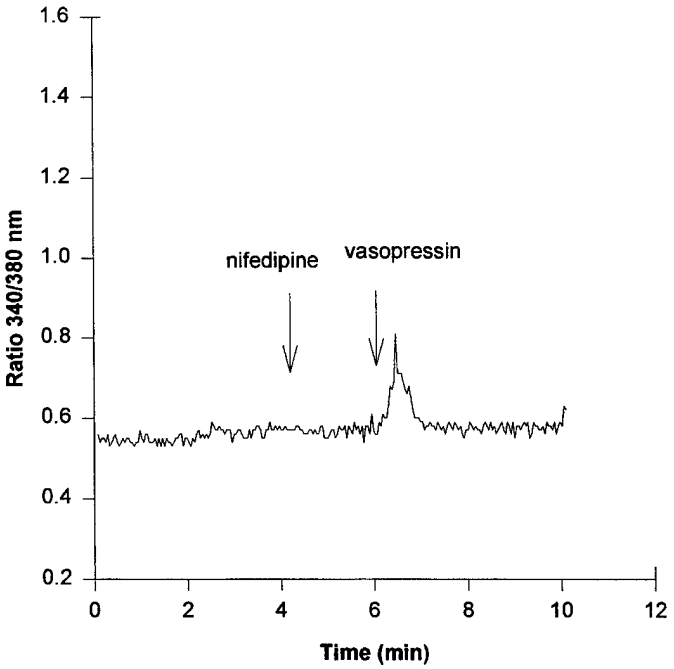

Fig. 7. Nifedipine failed to inhibit vasopressin-induced increase in $[Ca^{2+}]_i$ in LLC-PK_1 cells. Addition of nifedipine (200 nM) 3–5 min before vasopressin did not inhibit vasopressin-induced increase in $[Ca^{2+}]_i$.

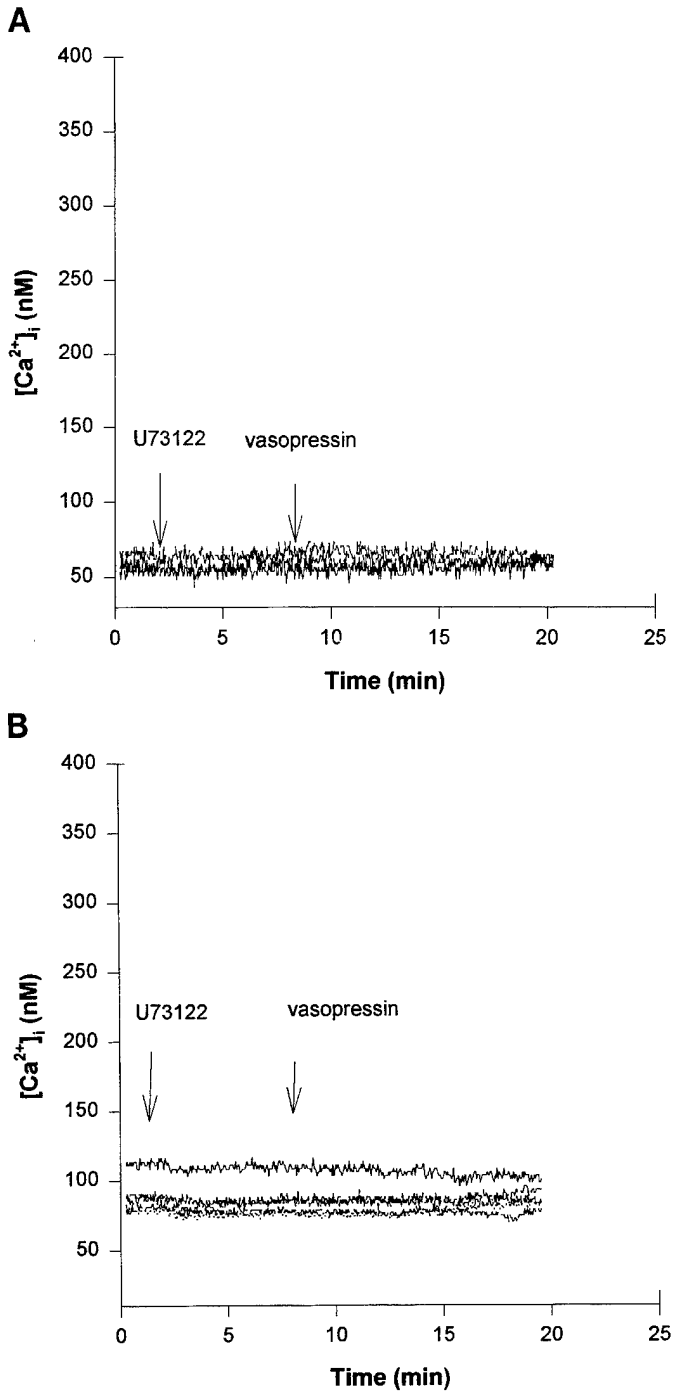

Fig. 8. *A*: U-73122 (3 μM) abolished vasopressin-induced increase in $[Ca^{2+}]_i$ in LLC-PK_1 cells. LLC-PK_1 cells were treated with phospholipase C (PLC) inhibitor U-73122 for 5–7 min before stimulation with vasopressin. However, vasopressin had no effect on $[Ca^{2+}]_i$ under these conditions. *B*: U-73122 (3 μM) abolished vasopressin-induced increase in $[Ca^{2+}]_i$ in rat hepatocytes. U-73122, a PLC inhibitor, abolished vasopressin-induced increase in $[Ca^{2+}]_i$ in rat hepatocytes.

DISCUSSION

The present study characterized the signal transduction cascade of vasopressin in LLC-PK_1 cells, a widely used cell line to analyze vasopressin-induced effects in the kidney. On the basis of the ability of a V_1 antagonist to abolish vasopressin-induced increases in $[Ca^{2+}]_i$ in LLC-PK_1 cells as well as hepatocytes, the vasopressin action appears to involve a V_1-like receptor in LLC-PK_1 cells (radioactive labeling of vasopressin receptors using ^{125}I-Lys-vasopressin did not reveal a VCAM-like receptor in LLC-PK_1 cells; unpublished observations). This conclusion is supported by the observed inhibitory effects of U-73122 (an inhibitor of PLC) on vasopressin-induced increases in $[Ca^{2+}]_i$. The use of U-73122 provided direct evidence for the involvement of an IP_3-stimulated pathway in the release of intracellular Ca^{2+}. Unlike other cell types including hepatocytes and muscle cells which are known to possess only a V_1 receptor, LLC-PK_1 cells appear to express at least two vasopressin receptors. The presence of both V_1 and V_2 receptors in this cell type leads to the question of the physiological significance of a V_1-like receptor in the kidney. It has been shown in kidney and renal-like epithelium that the V_1 receptor response may function to regulate the V_2-cAMP cascade through a "cross-talk" mechanism (4). Increases in $[Ca^{2+}]_i$ in the proximal tubules and thick ascending limb in the kidney may also have alternative actions. For instance, increases in $[Ca^{2+}]_i$ activates Ca^{2+}/calmodulin-dependent protein kinase (detected in proximal tubules; Ref. 28) and has been shown to phosphorylate the Na^+/H^+ antiporter, resulting in inhibition of Na^+ uptake in rabbit apical proximal tubules. It has been also reported that Na^+ reabsorption leads to enhanced Ca^{2+} reabsorption (9) and that the inhibition of the Na^+/H^+ antiporter by phosphorylation results in alkalization of the cytosol and decreases in Ca^{2+} reabsorption. From such observations, Ca^{2+} reabsorption in the lumin would be inhibited by increases in $[Ca^{2+}]_i$, representing another negative-feedback system. Such action would affect ~15% of Ca^{2+} reabsorption that normally occurs through transcellular mechanisms in this nephron site. Therefore the regulation of intracellular Ca^{2+} may play a crucial role in Ca^{2+} reabsorption.

Our present results also suggest that the V_2 receptor, though stimulated (cAMP production was increased in LLC-PK_1 cells), does not play a role in vasopressin-induced increase in $[Ca^{2+}]_i$. This was also confirmed by the lack of inhibitory effects for the V_2 antagonist on vasopressin-induced increase in $[Ca^{2+}]_i$. Nevertheless, this does not rule out a role for cAMP and its potential activation of cAMP-dependent protein kinase A (PKA) in regulating Ca^{2+} homeostasis in LLC-PK_1 cells. We observed that when a pressure was applied in the presence of DBcAMP to LLC-PK_1 cells, a transient increase in $[Ca^{2+}]_i$ was observed, whereas the same pressure applied in the absence of DBcAMP had no effect on $[Ca^{2+}]_i$ (unpublished observations). This phenomenon has been reported by Taniguchi et al. (24) in rabbit collecting tubule cells as well. However, the nature of a pressure-sensitive channel has yet to be identified.

A similar lack of effect of cAMP on $[Ca^{2+}]_i$ has previously been reported in LLC-PK_1 cells (27) and other kidney cell types, including rat renal papillary and collecting tubule (13), rat glomerular mesangial cells (2), perfused rabbit cortical thick ascending limb

(21), and rabbit cortical collecting tubule (4). In contrast, cAMP-induced increases in $[Ca^{2+}]_i$ have also been reported for other kidney cell types, including rat cortical collecting tubule (10), rabbit connecting tubules (3), rabbit proximal tubule (19), porcine renal cortical ascending limb (7), and the amphibian A6 kidney cell line (17). There was no indication in these studies of a pressure-mediated effect for cAMP on $[Ca^{2+}]_i$. The ability of cAMP to increase $[Ca^{2+}]_i$ in different kidney cell types may be of a physiological significance. However, further work is needed to elucidate the importance and the physiological relevance of cAMP-induced increase in $[Ca^{2+}]_i$ in different parts of the kidney as well as to resolve the species differences.

Although vasopressin in the current study induced a transient increase in $[Ca^{2+}]_i$ in both LLC-PK_1 cells and hepatocytes, Teti et al. (25) have shown that vasopressin produced a sustained increase in $[Ca^{2+}]_i$ in LLC-PK_1 cells. Our results were consistent with those reported for hepatocytes but not LLC-PK_1 cells. The reason for such a discrepancy is not known. However, Tshipamba et al. (26) reported that in only 4 of 13 LLC-PK_1 cells did they observe a sustained increase in $[Ca^{2+}]_i$, whereas most showed only a transient increase. This suggests that the population of LLC-PK_1 cells used in their study was heterogeneous. Moreover, the current study does not support a role for extracellular Ca^{2+} in the vasopressin-induced Ca^{2+} response, since nifedipine failed to inhibit vasopressin-induced increase in $[Ca^{2+}]_i$. Such a finding appears to be in contradiction with the capacitative model of Putney (20). Because the magnitude of the vasopressin response was modest, perhaps not all the IP_3 sensitive pool was released. Thapsigargin, used to empty the intracellular Ca^{2+} pools, abolished vasopressin-induced increases in $[Ca^{2+}]_i$. The thapsigargin-induced increase in $[Ca^{2+}]_i$ was identical to that reported by Putney (20) in parotid acinar cells as well as pancreatic β-cells (unpublished observations). These observations are important and suggest that LLC-PK_1 cells possess an intracellular Ca^{2+} pool that is similar to other cell types. Although thapsigargin results clearly validated the presence of the capacitative model in LLC-PK_1 cells, vasopressin results did not. However, to help explain such conflicting results, two key points must be considered. First, the effects exerted by thapsigargin are not exactly mimicked by any agonists mobilizing intracellular Ca^{2+}, since thapsigargin is an irreversible inhibitor of the endoplasmic reticular Ca^{2+} pump. Second, it has been shown that not all the thapsigargin-sensitive Ca^{2+} pools are emptied by IP_3, whereas the opposite is true in LLC-PK_1 cells (i.e., thapsigargin empties all of IP_3-sensitive Ca^{2+} pool; Ref. 26). This was also confirmed in this study by comparing the effect of thapsigargin on $[Ca^{2+}]_i$ in the absence of extracellular Ca^{2+} with that mobilized by vasopressin. The increase in $[Ca^{2+}]_i$ induced by thapsigargin was at least twice that increased by vasopressin (cf. Fig. 6*B* with Fig. 5), although the same experiment also validated the capacitative model in LLC-PK_1 cells, since the increase in $[Ca^{2+}]_i$ was transient in the absence of extracellular Ca^{2+} and an increase in $[Ca^{2+}]_i$ was observed once the extracellular Ca^{2+} was restored to normal levels. It is therefore possible to assume that the complete emptying of IP_3-Ca^{2+} pools by thapsigargin resulted in the influx of extracellular Ca^{2+}, but the partial emptying of some pools by IP_3 released through vasopressin was not sufficient to trigger the influx of extracellular Ca^{2+}. Yet more studies are needed to further clarify such differences in LLC-PK_1 cells.

The observed difference between the LLC-PK_1 cells and hepatocytes in the oscillatory Ca^{2+} response may be due to several reasons. The first is the rate of downregulation of vasopressin receptors in both cells types as well as the internalization of the peptide hormone. For example, Lutz et al. (15) have shown that LLC-PK_1 cells have a unique mechanism for vasopressin peptide internalization that is different from the receptor-mediated endocytosis. In the same study, such a mechanism was absent from A10 smooth muscle cells (known to have a V_1 receptor). The second reason may be the level or isoform type of PLC. Both cell types may have distinct feedback regulation that may limit the production of IP_3. A third possibility may reflect the differences in the efficiency of the Ca^{2+} stores to maintain Ca^{2+} homeostasis in both cell types, i.e., the ability of each cell type to balance the emptying and refilling of Ca^{2+} stores.

In summary, the present study suggests that the vasopressin-induced increase in $[Ca^{2+}]_i$ in LLC-PK_1 cells is mediated via a V_1-like receptor and involves the mobilization of Ca^{2+} from the intracellular stores via an IP_3-dependent pathway. The present study also suggests the presence of at least two vasopressin receptors in LLC-PK_1 cells. The study provides a model for analyzing the signal transduction pathway of specific agonists with an unknown mechanism of action by comparing its effects on other cell types with well-characterized mechanisms. LLC-PK_1 cells may also provide a model for studying the relationship and cross-talk that may occur when both vasopressin receptors are activated.

This work was supported in part by US Army Grant DAMD-17–95–5086.

The views and opinions and/or findings contained in this report are those of the authors and should not be construed as an official Department of Army position, policy, or decision unless so designated by other documentation.

Address for reprint requests: A. Dibas, Dept. of Pharmacology, University of North Texas Health Science Center at Fort Worth, 3500 Camp Bowie Blvd., Fort Worth, TX 76107.

Received 11 June 1996; accepted in final form 26 September 1996.

REFERENCES

1. **Berven, L. A., and G. J. Barritt.** Evidence obtained using single hepatocytes for inhibition by the phospholipase C inhibitor U73122 of store-operated Ca^{2+} inflow. *Biochem. Pharmacol.* 49: 1373–1379, 1995.
2. **Bonventre, J. V., K. L. Skorecki, J. I. Kreisberg, and J. Y. Cheung.** Vasopressin increases cytosolic free calcium concentration in glomerular cells. *Am. J. Physiol.* 251 (*Renal Fluid Electrolyte Physiol.* 20): F94–F102, 1986.
3. **Bourdeau, J. E., and B. K. Eby.** cAMP-stimulated rise of $[Ca^{2+}]_i$ in rabbit connecting tubules: role of peritubular Ca. *Am. J. Physiol.* 258 (*Renal Fluid Electrolyte Physiol.* 27): F751–F755, 1990.

4. **Burnatowska-Hiledin, M. A., and W. S. Spielman.** Vasopressin V_1 receptors on the principal cells of the rabbit cortical collecting tubule. *J. Clin. Invest.* 83: 84–89, 1989.
5. **Burnatowska-Hiledin, M. A., W. S. Spielman, W. L. Smith, P. Shi, J. M. Meyer, and D. L. Dewitt.** Expression cloning of an AVP-activated, calcium mobilizing receptor from rabbit kidney medulla. *Am. J. Physiol.* 268 (*Renal Fluid Electrolyte Physiol.* 37): F1198–F1210, 1995.
6. **Cantau, B., S. Keppens, H. De Wulf, and S. Jard.** Size of vasopressin receptors from rat liver and kidney. *Eur. J. Biochem.* 111: 287–294, 1980.
7. **Dai, L. J., and G. A. Quamme.** Hormone-mediated Ca transients in isolated renal cortical thick ascending limb cells. *Pflügers Arch.* 427: 1–8, 1994.
8. **Ecelbarger, C. A., C. Chou, S. J. Lolait, M. A. Knepper, and S. R. DiGiovanni.** Evidence for dual signaling pathways for V_2 vasopressin receptor in rat inner medullary collecting duct. *Am. J. Physiol.* 270 (*Renal Fluid Electrolyte Physiol.* 39): F623–F633, 1996.
9. **Friedman, P. A., and F. A. Gesek.** Calcium transport in renal epithelial cells. *Am. J. Physiol.* 264 (*Renal Fluid Electrolyte Physiol.* 33): F181–F198, 1993.
10. **Frindt, G., R. B. Silver, E. E. Windhanger, and L. G. Palmer.** Feedback regulation of Na channels in rat CCT. Response to cAMP. *Am. J. Physiol.* 268 (*Renal Fluid Electrolyte Physiol.* 37): F480–F489, 1995.
11. **Golding, S. R., J. M. Dayer, D. A. Ausiello, and S. M. Krane.** A cell strain cultured from porcine increases cyclic AMP content upon exposure to calcitonin or vasopressin. *Biochem. Biophys. Res. Commun.* 83: 434–440, 1978.
12. **Grynkiewicz, G., M. Poenie, and R. Y. Tsien.** A new generation of Ca^{2+}-indicators with greatly improved fluorescence properties. *J. Biol. Chem.* 260: 3440–3450, 1985.
13. **Ishikawa, S., K. Okada, and T. Saito.** Arginine vasopressin increases free calcium concentration and adenosine 3,5-monophosphate production in rat renal papillary collecting tubule cells in culture. *Endocrinology* 123: 1376–1384, 1988.
14. **Jans, D. A., I. Pavo, and F. Fahrenholz.** Oxytocin and cAMP-dependent protein kinase activation and urokinase-type plasminogen activator production in LLC-PK_1 renal epithelial cells is mediated by the vasopressin V_2-receptor. *FEBS Lett.* 315: 134–138, 1993.
15. **Lutz, W., M. Sanders, J. Salisbury, and R. Kumar.** Internalization of vasopressin analogs in kidney and smooth muscle cells: evidence for receptor-mediated endocytosis in cells with V_2 or V_1 receptors. *Proc. Natl. Acad. Sci. USA* 87: 6507–6511, 1990.
16. **Matter, N., M. F. Ritz, S. Freyermuth, P. Rodue, and A. N. Malyivia.** Stimulation of nuclear protein kinase C leads to phosphorylation of nuclear 1,4,5-trisphosphate receptor and accelerated calcium release by inositol 1,4,5-trisphosphate from isolated rat nuclei. *J. Biol. Chem.* 268: 732–736, 1993.
17. **Niisato, N., and Y. Marunaka.** The regulation of Cl^- transport of renal A6 cells by IBMX (Abstract). *FASEB J.* 10: 481, 1996.
18. **Nitschke, R., U. Frobe, and R. A. Greger.** Antidiuretic hormone acts via V_1 receptors on intracellular calcium in the isolated perfused rabbit cortical thick ascending limb. *Pflügers Arch.* 417: 622–632, 1991.
19. **O'Neil, R. G., and L. Leng.** Signaling pathways regulating swelling-activated dihydropyridine-sensitive calcium channels in rabbit proximal tubule cells (Abstract). *FASEB J.* 10: 501, 1996.
20. **Putney, J. W., Jr.** Capacitative calcium entry revisited. *Cell Calcium* 11: 611–624, 1990.
21. **Rabito, C. A.** Sodium cotransport processes in renal epithelial cell lines. *Miner. Electrolyte Metab.* 12: 32–41, 1986.
22. **Rooney, T. A., E. J. Sass, and A. P. Thomas.** Characterization of cytosolic calcium oscillations induced by phenylephrine and vasopressin in single fura-2-loaded hepatocytes. *J. Biol. Chem.* 264: 17131–17141, 1989.
23. **Salomon, Y., C. Londos, and M. Rodbell.** A highly sensitive adenylate cyclase assay. *Anal. Biochem.* 58: 541–548, 1974.
24. **Taniguchi, J., M. Takeda, K. Yoshitomi, and M. Imai.** Pressure- and parathyroid-hormone-dependent Ca transport in rabbit connecting tubule: role of the stretch-activated nonselective cation channel. *J. Membr. Biol.* 140: 123–132, 1994.
25. **Teti, A., R. Paniccia, and S. R. Goldring.** Calcitonin increases free calcium concentration via capacitative calcium influx. *J. Biol. Chem.* 270: 16666–16670, 1995.
26. **Tshipamba, M., H. D. Smedt, L. Missiaen, B. Himpens, B. L. Van Den Bosch, and R. Borghgraef.** Ca^{2+} dependence of inositol 1,4,5-trisphosphate-induced Ca^{2+} release in renal epithelial LLC-PK_1 cells. *J. Cell. Physiol.* 155: 96–103, 1993.
27. **Weinberg, J. M., J. A. Davis, J. A. Shayman, and P. L. Knight.** Alterations of cytosolic calcium in LLC-PK_1 cells induced by vasopressin and exogenous purines. *Am. J. Physiol.* 256 (*Cell Physiol.* 25): C967–C976, 1989.
28. **Weinman, E. J., W. P. Dubinsky, K. Fisher, D. Steplock, Q. Dinh, L. Chang, and S. Shenolikar.** Regulation of reconstituted renal Na^+/H^+ exchanger by calcium-dependent protein kinases. *J. Membr. Biol.* 103: 237–244, 1988.
29. **Wohlwend, A., J. D. Vassalli, D. Belin, and L. Orci.** LLC-PK_1 cells: cloning of phenotypically stable subpopulations. *Am. J. Physiol.* 250 (*Cell Physiol.* 19): C682–C687, 1986.
30. **Zeidel, N. L., K. Strange, F. Emma, and W. H. Harris, Jr.** Mechanisms and regulation of water transport in the kidney. *Sem. Nephrol.* 13: 155–167, 1993.

THE ATP-DEPLETING REAGENT "IODACETAMIDE" INDUCES THE DEGRADATION OF PROTEIN KINASE C ALPHA (PKCα) IN LLC-PK$_1$ PIG KIDNEY CELLS.

*Adnan Dibas[1], Julie Wood[1], Abdul J. Mia[2] and Thomas Yorio[1].
[1]Department of Pharmacology, University of North Texas Health Science Center at Fort Worth, Fort Worth, TX. 76107 and [2]Division of Science and Mathematics, Jarvis Christian College, Hawkins, TX. 75765.

Key words: Iodoacetamide, sulfhydryl modifying reagent.
Protease inhibitor, prevent protein degradation.
Protein kinase C alpha, an 80 Kilodalton isoform of protein kinase C

THE ATP-DEPLETING REAGENT "IODACETAMIDE" INDUCES THE DEGRADATION OF PROTEIN KINASE C ALPHA (PKCα) IN LLC-PK$_1$ PIG KIDNEY CELLS.

*Adnan Dibas[1], Julie Wood[1], Abdul J. Mia[2] and Thomas Yorio[1].

[1]Department of Pharmacology, University of North Texas Health Science Center at Fort Worth, Fort Worth, TX. 76107 and [2]Division of Science and Mathematics, Jarvis Christian College, Hawkins, TX. 75765.

Summary

The alkylating reagent iodoacetamide, a potent inhibitor of sulfhydryl proteases, was found to stimulate the selective degradation of protein kinase C alpha (PKCα) isoform. Treatment of LLC-PK$_1$ cells with iodoacetamide (5 mM) for 30-90 minutes at room temperature followed by western blotting on total cell homogenate, revealed the absence of an 80 KDa protein and the appearance of an 50 KDa band that was still recognized with the antibody. Serine protease inhibitor, metalloprotease inhibitors and leupeptin failed to prevent the degradation of PKCα. The degradation persisted at 4 °C and in the absence of Ca^{2+}. Iodoacetamide had no direct effect on purified PKCα. In conclusion, the degradation of PKCα is a novel phenomenon. The degradation process could not be inhibited by known protease inhibitors or in the absence of Ca^{2+} or at 4 °C and appears to involve interactions with an unknown intermediates.

Iodoacetamide, has been long used to lower ATP concentrations in cells (1). It is also widely used to inhibit sulfhydryl-activated proteases (2). The lowering of ATP concentrations is due to its alkylating effect of glycolysis enzymes, in particular, glyceraldehyde-3-dehydrogenase, and thus inhibiting glycolysis and the supplementing of necessary intermediates for the KREBS cycle (3). The mechanism of iodoacetamide-induced inactivation of enzymes is as a result of its reaction with a cysteine residue at the active site. The mechanism is depicted in the following equation:

$$\underset{\text{active enzyme}}{E\text{-}SH} + \underset{\text{iodoacetamide}}{ICH_2CONH_2} \longrightarrow \underset{\text{inactive enzyme}}{E\text{-}S\text{-}CH_2CONH_2} + HI$$

*To whom correspondence should be addressed: University of North Texas Health Science Center at Fort Worth, Department of Pharmacology, 3500 camp Bowie Blvd., Fort Worth, TX. 76107, Tel: (817) 735-5140, Fax: (817) 735-2091, email address: adibas@hsc.unt.edu

However, it seems to have other diverse uncharacterized effects. In attempt to test the effect of ATP-depletion on PKCα translocation to the plasma membrane, iodoacetamide was used. Surprisingly, a 50 KDa band protein appeared that did not translocate after phorbol-ester treatment. Further characterization of this phenomenon was performed. Surprisingly, none of the known inhibitors of proteases were able to inhibit such degradation. Unexpectedly, it was found that the degradation occurred at 4 °C and even in the absence of Ca^{2+}.

This observed effect of iodoacetamide is unique and could contribute to its inhibitory effects on responses utilizing PKCα. Researchers using iodoacetamide as a method of depleting ATP, need to be aware of such an additional effect. More interestingly, iodoacetamide, which has long been used as a protease inhibitor, stimulated the degradation of PKCα. This paradoxical effect is unique and may provide insight into the process where by PKCα is degraded.

Materials and Methods

Materials: Nitrocellulose membranes were from Schleicher & Schuell (Keene, NH). Aprotonin, leupeptin, soybean trypsin inhibitor and phenylmethylsulfonyl fluoride (PMSF) were purchased from Sigma Chemical Co. (St. Louis, MO). Monoclonal antibodies against PKCα were purchased from Upstate Inc. (NY, NY). Purified PKCα was purchased from Fisher (Houston, TX).

Cell culture: LLC-PK_1 cells (passages 18-35) were subcultured in DMEM medium (Gibco Inc. Gaithersburg, MD) containing 10 % fetal bovine serum and antibiotics. Cells to be used in experiments were starved in serum-free medium overnight.

Preparation of protein samples for western blotting: Cells were washed twice in modified krebs Hanks medium (134 mM NaCl, 2.5 mM $CaCl_2$, 24 mM $NaHCO_3$, 5 mM KCl, 1.2 mM $MgCl_2$ and 25 mM Hepes, pH 7.4) to remove medium and incubated in fresh krebs solution for 15-30 minutes. Iodoacetamide (5 mM) was added to cells and cells were kept at room temperature, 4 °C (on ice) for 30 minutes. To terminate the reaction, cells were pelleted and the medium was discarded. Cells were then sonicated in ice-cold homogenization buffer (20 mM Tris-HCl, pH 7.5, 0.5 mM EGTA, 1 mM EDTA, 2 mM dithiothreitol, 20 μg/ml leupeptin, 20 μg/ml aprotonin, 17 μg/ml PMSF and 20 μg/ml soybean trypsin inhibitor). To test the effect of protease inhibitors on the degradation process, cells were homogenized in homogenization buffer then iodoacetamide (5 mM) was added and the homogenate was kept at room temperature for 30 minutes. The homogenate was centrifuged for 30 minutes at 14,000 x g (4 °C). The resulting supernatant was removed, precipitated with trichloroacetic acid (30 % final concentration). The pellet was resuspended with 40 μl of SDS-sample buffer (62.5 mM Tris-HCl, pH 6.8, 0.1 % (v/v) glycerol, 2 % SDS, 0.05 % β-mercaptoethanol and 0.005 %

(w/v) bromophenol blue) and pH was adjusted using Tris-HCl. Samples were then subjected to gel electrophoresis. Western blotting was performed as described (4).

Results

LLC-PK_1 cells were treated with iodoacetamide as described in Methods. Western blotting analysis on total cell homogenates (utilizing monoclonal antibodies against PKCα) revealed the presence of an 80 KDa protein in control cells (lane 1) and the absence of a such band in iodoacetamide-treated cells (lane 2)(Fig. 1). However, in iodoacetamide-treated cells, a 50 KDa protein was detected (Fig. 1). Since this band was not observed in control cells, it was likely representing a break-down product of PKCα. Therefore, the effect of a number of protease inhibitors on iodoacetamide-induced degradation of PKCα was evaluated. As shown in Fig. 2, the ability of iodoacetamide to promote the degradation of PKCα could not be prevented by all protease inhibitors tested and in the absence of Ca^{2+} (Fig. 2). These included serine protease inhibitors (PMSF, aprotonin and soybean trypsin inhibitor), metalloprotease inhibitors (EGTA, EDTA and phenanthroline), leupeptin. Surprisingly, the effect of iodoacetamide on PKCα occurred at 4 °C (Fig. 3). In addition, we tested the effect of iodoacetamide on purified PKCα. As shown in Fig. 4, iodoacetamide had no direct effect on purified PKCα and no degradation of PKCα was observed. This suggested that the iodoacetamide must be incubated with intact cells in order for this response to be expressed.

Discussion

Activation of protein kinase C results from a cascade of events brought about by receptor signaling mechanisms. There are a number of PKC isoforms present in most cells, each with a unique function in the signaling process. Prolonged activation of PKC by phorbol esters has been shown to result in a decrease in PKCα activity and loss of enzyme following translocation (5). The loss of enzyme has been attributed to PKC degradation (6). The mechanisms associated with PKC degradation are not well-understood. The present report discovered a novel effect for the alkylating reagent iodoacetamide. Although iodoacetamide is a potent inhibitor of sulfhydryl-dependent proteases, it promoted the degradation of cytosolic PKCα. In separate experiments, we were able to show that iodoacetamide-induced degradation also targeted membrane-bound PKC. It is known that phorbol esters induce the translocation of PKC from the cytosol to the plasma membrane. Even in the presence of phorbol ester activated-PKC, iodoacetamide still induced the degradation of PKC. The degradation process of PKCα could not be prevented by known protease-inhibitors or by incubation at 4 °C. This degradation of PKCα was not unique to LLC-PK_1 kidney cells, but was also observed in other cell types (rat hepatocytes, mouse pancreatic β-cells and human epithelial eye cells, manuscript in preparation). This paradoxical effect of iodoacetamide may play a role in

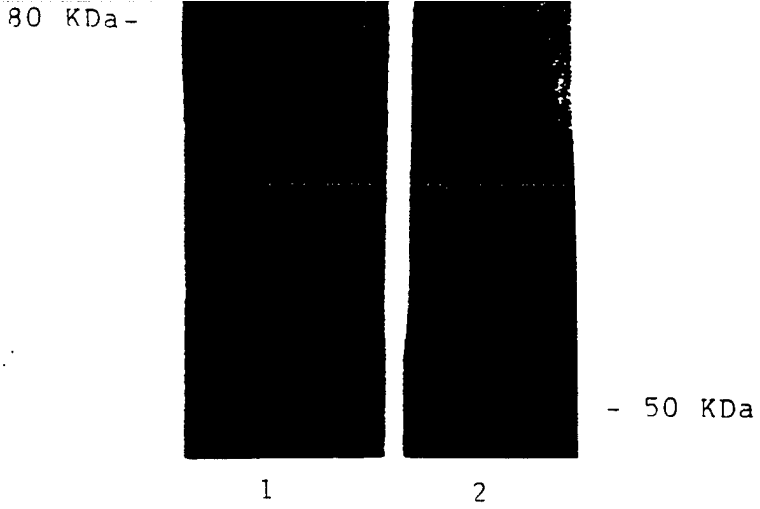

Fig. 1

Treatment of LLC-PK$_1$ cells with iodoacetamide (5 mM) resulted in the appearance of a 50 KDa protein detected by western blotting.

LLC-PK$_1$ cells were treated as described in Methods for 30-90 minutes with iodoacetamide (5 mM) (lane 2) while control cells were treated with the vehicle (lane 1) (dimethylsulfoxide). Immunoblotting revealed the appearance of a 50 KDa band protein and the disappearance of the usual 80 KDa PKCα as observed in control cells.

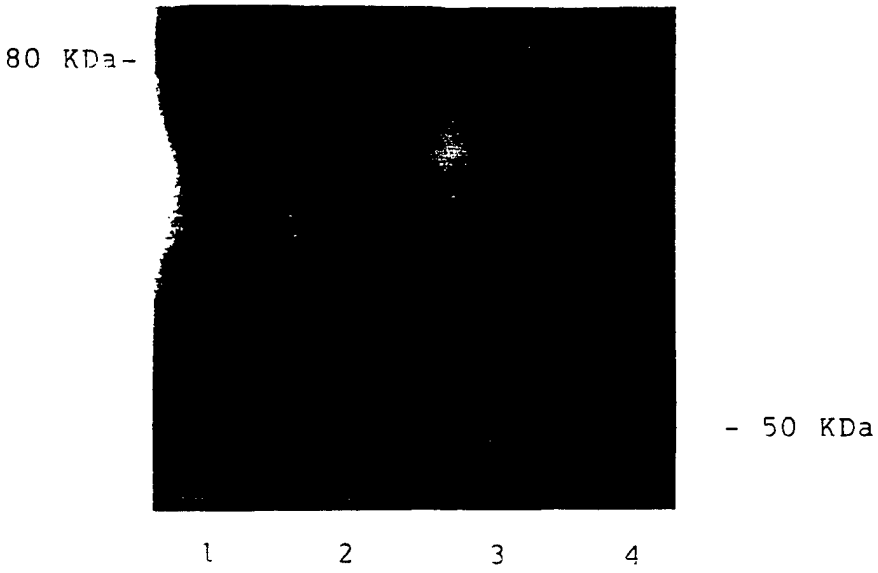

Fig. 2

Proteases inhibitors failed to prevent the iodoacetamide-induced degradation of PKCα LLC-PK$_1$ cells.

The addition of serine protease inhibitors (PMSF), leupeptin, metalloprotease inhibitors (phenanthroline), or aprotonin, failed to inhibit iodoacetamide-induced the degradation of PKCα and the 50 KDa band- protein was still observed (lane 1: control, lane 2: iodoacetamide, lane 3: iodoacetamide + protease inhibitors, lane 4: iodoacetamide + protease inhibitors in the absence of calcium) .

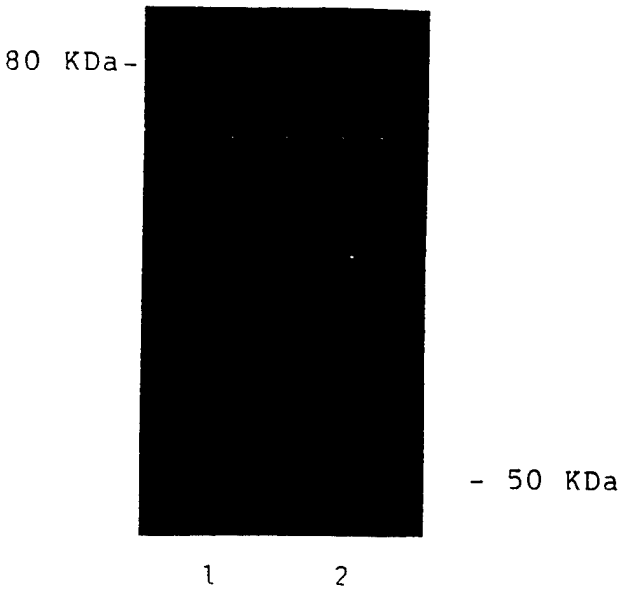

Fig. 3

Iodoacetamide-induced degradation of PKCα was not attenuated by incubating LLC-PK$_1$ cells on ice.
The incubating of LLC-PK$_1$ cells on ice for 10-30 minutes before the addition of iodoacetamide failed to inhibit iodoacetamide-induced degradation of PKCα (lane 1: control, lane 2: iodoacetamide at 4 °C).

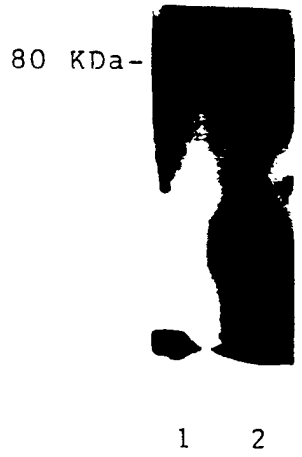

Fig. 4

Iodoacetamide has no effect on purified PKCα
The treatment of purified PKCα (100 ng) with iodoacetamide (5 mM) for 30 minutes did not induce the degradation of PKCα suggesting that the observed iodoacetamide effect was not the result of a direct interaction with PKCα. As shown by western blotting, both PKCα treated and untreated had a molecular weight of 80 KDa (lane 1: control, lane 2: iodoacetamide-treated).

iodoacetamide inhibitory effects on many systems, including those involving the activation of protein kinase C. This response may also provide a tool for probing the degradative pathway of PKCα.

Acknowledgment

This work was supported in part by a grant from USA Army (DAMD, 17-95-5086). The views and opinions and/or findings contained in this report are those of the authors and should not be construed as an official Department of Army position, policy or decision unless so designated by other documentation.

References

1. R. A. LAING, K. CHIBA, K. TSUBOTA, and S. S. OAK, Invest. Opthal. Vis. Sci. 33 3315-3324 (1992).
2. O. ALCAZAR, E. GINE, Z. QIU-YUE, and J. TAMARIT-RODRIGUEZ, Biochem. J. 310 215- 220 (1995).
3. V. SHOSHAN-BARMATZ, S. WEIL, H. MEYER, M. VARSANYI, and L. M. HEILMEYER, J. Mem. Biol. 142 281-288 (1994).
4. A. DIBAS, A. MIA, and T. YORIO, Biochem. Mol. Biol. Int. 39 581-588 (1996).
5. D. H. HONG, J. HUAN, B. R. QU, J. Y. YEH, T. C. SAIDO, P. R. CHEEKE, and N. E. FORESBERG, Biochim. Biophys. Acta. 1267 45-54 (1995).
6. Z. AL, and C. M. COHEN, Biochem. J. 296 675-683 (1993).

EVIDENCE OF BASOLATERAL WATER PERMEABILITY REGULATION IN AMPHIBIAN URINARY BLADDER

Oscar A. Candia[1], Abdul Mia[2] and Thomas Yorio[3]

[1]Departments of Ophthalmology and of Physiology & Biophysics, Mt. Sinai School of Medicine, New York, NY ; [2]Division of Science and Mathematics, Jarvis Christian College, Hawkins, TX; [3]North Texas Eye Research Institute, UNT Health Science Center, Fort Worth, TX.

Oscar A. Candia, M.D.
Department of Ophthalmology
The Mount Sinai School of Medicine
One Gustave L. Levy Place
Box 1183
New York, NY 10029
Phone: 212-241-9607
Fax: 212-289-5945

Summary

It is well known that arginine vasopressin (AVP) produces up to a 40-fold increase (0.1 to 4.0 $\mu\ell/min \cdot cm^2$) in net water flux across the amphibian urinary bladder under an osmotic gradient (mucosal side 10% hypotonic). No AVP effect is observed when the gradient is in the opposite direction (serosal hypotonic). Similar asymmetrical behavior to osmotic gradients occurs in the frog corneal epithelium. This rectification phenomenon has not been satisfactorily explained. We measured net water fluxes in bladder sacs and confirmed that AVP has no effect when the serosal bath is hypotonic. We reasoned that the "abnormal" serosal osmolarity was inducing changes in membrane water permeability, the very parameter being measured. Thus, we studied the effect of solution osmolarity on diffusional water flow (J_{dw}) across the frog bladder using ^3H_2O. As expected, AVP doubled J_{dw} (in either direction from 12 to 24 $\mu\ell/min \cdot cm^2$) when the serosal solution was iso-osmolar regardless of mucosal osmolarity. However, in the AVP-stimulated bladders, hypo-osmolarity of the serosal solution reduced J_{dw} by 16%, an effect that was reversible when normal osmolarity was re-established. Amphotericin B (instead of AVP) was used to irreversibly increase the permeability to water of the apical membrane. Under these conditions, basolateral hypotonicity also reversibly decreased J_{dw} by 32%, suggesting the basolateral membrane as the site where permeability is reduced. SEM of the tissue shows extreme swelling when it was exposed to serosal hypotonicity with or without AVP. We conclude that this swelling may initiate a signaling mechanism that reduces basolateral water permeability. These findings constitute evidence of basolateral water channel permeability regulation, which

can also contribute to cell volume regulation.

Keywords: Vasopressin, water fluxes, rectification, aquaporins

Introduction

The measurement of water permeability across epithelia has acquired renewed importance with the recent discovery of several cell membrane-spanning proteins, the aquaporins [13,22]. These proteins, forming a water permeable channel, contribute to the transepithelial secretion and/or absorption of fluid , a process of fundamental physiological importance. For instance, the permeability to net water flow (P_f) of the toad urinary bladder in the presence of an osmotic gradient is limited due to the low permeability of the apical membrane. Arginine vasopressin (AVP) enhances water flow 20-40 times by the insertion of water channels into the lipid bilayer of the apical membrane [1, 2, 3, 12] . Based on these findings, it was concluded that the apical membrane was rate-limiting for transepithelial water movement. As in the case of ionic translocation, water must also traverse the basolateral membrane. However, the possible restriction imposed by the basolateral membrane to water flow after AVP stimulation has received little attention. It is conceivable that the basolateral membrane could have become rate-limiting after the hormone stimulation and thus, its role in transepithelial water movement can be studied in this or similar conditions in which the apical membrane has been permeabilized.

The most common methods to determine water permeability across epithelia involve the measurement of volume flow (J_v) under an osmotic driving force and diffusional water

flow (J_{dw}) with labelled water (^3H_2O). In principle, permeability is an intrinsic property of the membrane and should be independent of the method used for its determination. However, it is well known that P_f and P_{dw} (both in the presence or absence of AVP) are not equal. This "apparent anomaly" has been attributed to differences between water flow across the lipid bilayer and water channels and has been the subject of numerous analyses and interpretations [9, 14, 19].

Another "apparent anomaly" which has not received equal attention and remains incompletely explained is the rectification observed when measuring water fluxes in the AVP-stimulated amphibian urinary bladder. The 20-40 fold increase in water flow observed in the apical-to-basolateral direction does not occur when an identical osmotic gradient is imposed in the opposite direction. Namely, AVP has little influence on water flow when the serosal bath is the one made hypotonic [8]. In this study, we examine the bases of this rectification phenomenon and show physiological and morphological evidence which indicate that it may be the result of changes in basolateral water permeability. These results are also consistent with regulation of the permeability of the water channels reported to reside at the basolateral membrane of the urinary bladder [21].

Materials and Methods

Experiments were performed on the isolated urinary bladder from the toad *Bufo Marinus* or the frog *Rana Catesbeina*.

Toads were maintained in an aquatic environment at 23°C with continuous

irrigation of running tap water. They were fed live crickets biweekly and were used for the net water flow measurements and scanning electronmicroscopy (SEM). Toads were doubly-pithed and the bladder sacs were surgically removed and placed in aerated Ringer's solution. These bladder tissues were continuously aerated before and during experimental procedures. Identical hemibladder pairs from individual animals were used as control and experimental tissues. In one set of experiments, control and AVP-stimulated urinary bladders were suspended on glass tubing with mucosal side facing inward. In other sets of experiments, urinary bladder sacs were suspended with the serosal side facing inward. The control tissues were retained in Ringer's solution while the AVP-stimulated tissues received 10 mU/μl AVP on the serosal side. An osmotic gradient was established between inside and outside of the bladder sacs using 1/10 concentration of Ringer's solution inside the bladder sacs, (keeping the K^+ and Ca^{2+} concentrations constant) either in the mucosal or serosal bath, and the experiments were run for 30 min for each set of experiments. Water loss from the bladder sacs was measured gravimetrically [1] . The volume flow J_v is expressed in μl/min per sac, and the volume of the sacs was about 4 μl. The osmotic permeability coeffecient, P_f, is expressed in cm/s and can be calculated from the following expression:

$$P_f = J_v/(A \cdot V_w \cdot \Delta C_s)$$

where J_v is in cm^3/s and ΔC_s is the difference in solute concentration (mol/cm^3). For SEM observations, bladder sacs were fixed in 2% glutaraldehyde in PIPES buffer (0.02 M) for 1 hr. A post fixation was carried out in 1% osmium tetroxide for 1 hr prior to tissue processing. The bladder tissues were dehydrated in graded acetone and

processed for critical point drying using Peldri II [7,16]. The dried tissues, mounted on clean aluminum stubs, were gold coated in an argon environment using a sputter coater. The gold coated tissues were subjected to SEM observations and the pictures were taken at X450 magnification for comparative analysis.

Frogs which were used for the unidirectional water flux experiments were obtained from a local supplier and kept in fresh-water tanks. They were double pithed just prior to the dissection of the urinary bladder. The tissue was mounted as a partition between hemichambers. A greased, plastic washer of the thickness of the bladder was placed between the hemichamber to prevent from pressing on the bladder and producing edge damage. The chamber was a modified Ussing-type chamber similar to that used for electrophysiological studies with an 0.5 cm^2 exposed area [4]. The volume of the "hot" side compartment was increased to about 30 ml. This as well as the small area of exposed tissue was necessary to maintain the specific activity of the "hot"side within 10% of its initial value. Typically, at a maximum flux rate of 16 μl/min, the specific activity will decrease by 8% in 3 hr. Nevertheless, periodic samples were taken from the "hot"side and fluxes were calculated based on the activity of the corresponding "hot" samples. Sampling and replacement kept the "cold" side activity below 2% of that in the "hot" side. Vigorous stirring was provided by continuous recirculation with a jet of fluid directed to the surface of the tissue [7]. About 1.3 μCi/ml of ^3H_2O (ICN Biomedicals, Costa Mesa, CA) was added to one side, and samples were taken from the "cold" side every 15 min. At least four flux periods were determined for each experimental condition. A full experiment usually consisted of two

or three conditions of the "before-after" type so that paired comparisons could be made. Unidirectional fluxes were measured in both directions and pooled together for tabulation since there was no detectable difference for the same condition. The chambers also provided the necessary salt bridges for electrical resistance. The electrical properties and response to AVP were within previously reported ranges. In the tables, the diffusional water flux, J_{dw}, is expressed in $\mu l/min \cdot cm^2$. The diffusion permeability coefficient, P_{dw}, is expressed in cm/s and is given by:

$$P_{dw}=J_{dw}/(A \cdot V_w \cdot C_w)$$

where A is the area of the membrane (cm^2). V_w is the partial volume of water (cm^3/mol), C_w is the concentration of water (mol/cm^3), and J_{dw} is the measured flux in cm^3/s.

The Ringer's solution used during the dissection and control part of the experiments had the following composition (in mM): 103.4 Na^+, 2.5 K^+, 1.0 Ca^{2+}, 1.2 Mg^{2+}, 75.0 Cl^-, 25.0 HCO_3^-, 1.8 SO_4^{2-}, 2.0 HPO_4^{2-}, 0.7 $H_2PO_4^-$, 2.0 gluconate, and 26.0 glucose. Amphotericin B was from Squibb, Princeton, NJ and AVP was from Sigma, ST. Louis, MO. When this solution was diluted, it was supplemented to maintain K^+, Ca^{2+} and pH constant, for a final nominal osmolarity of 40 mOsm.

Results

Osmotic water flow across toad urinary bladder is enhanced by AVP. If an osmotic gradient is introduced (1/10 N-Ringers) with the mucosal side hypotonic with respect to the serosal side, net reabsorption of fluid flow increases 10-fold (Table I).

However, if the osmotic gradient is reversed, i.e., serosal side hypotonic with respect to the serosal, a net fluid flow occurs in the serosal to mucosal direction. However, under these conditions the addition of AVP does not enhance water flow, but actually decreases net osmotic water movement (Table I). If the serosal bathing solution is returned to normal Ringer's and the mucosal solution is made hypotonic, then the AVP response is restored (Table I).

Under these serosal hypotonic conditions, scanning electron microscopy of the mucosal surface area depicts generalized cell swelling and strained cell junctions (Figure 2). However, the cells are able to sustain this serosal hypotonicity and there is no further change in cell morphology even in the presence of AVP (Figure 4). When the serosal solution is returned to isotonicity, the cells regain their normal configuration (data not shown). When the mucosal surface is made hypotonic, as under normal conditions, little swelling is observed and cells maintain their normal structure (Figure 1). In the presence of AVP the cells swell slightly and express the typical surface morphology changes seen in response to AVP, i.e., increase in apical microvilli formation from a control microridge structure (Figure 3) [17].

Our measurements of J_v reaffirmed the well known fact that AVP does not elicit a fluid flow when the basolateral (instead of apical) bath is made hypotonic. Although several interpretations have been advanced to explain this result, no one had considered the possibility that it was due to a decrease in water permeability produced by the hypotonic solution. Since AVP also increases J_{dw} when the bladder is bathed in isotonic solutions, we reasoned that J_{dw} should not change appreciably when decreasing the

basolateral bath osmolarity, unless this maneuver affected P_{dw} directly.

Table II summarizes the results of 5 experiments in which J_{dw} was first measured in either direction in isotonic conditions, followed by the addition of AVP. As expected, this produced a significant increase of J_{dw} to 20.2 $\mu\ell/min \cdot cm^2$. Then, in the presence of AVP the tonicity of the basolateral bath was reduced to 40 m0sm by dilution keeping K^+ and Ca^{2+} concentration and pH constant. This change produced a significant 16% decrease in J_{dw} which reverted to the AVP-stimulated value upon restoration of isotonicity into the basolateral bath.

Table III shows the results of similar experiments but with the AVP and basolateral hyposmolarity maneuvers order reversed. On the un-stimulated bladders, basolateral hyposmolarity produced a small increase in J_{dw}, consistent with the similar increase in J_v observed in the volume flow experiments. Addition of AVP in this condition produced (instead of the usual stimulation) a small but significant decrease in J_{dw}. Restoration of isotonicity in the basolateral bath elicited the usual 2-fold increase in J_{dw}. This was a good indication of the reversibility of the basolateral-hypotony effect. To discount the possibility that under basolateral hypotony the AVP-signaling mechanism was ineffective and the apical membrane remained at a low permeability state, this barrier was permeabilized with amphotericin B. As previously reported in toad bladder [9, 15, 20] and also observed in the corneal epithelium [5, 18], the antibiotic increased the value of J_{dw} by 74%, effectively transferring the rate-limiting step to the basolateral membrane. Under this condition basolateral hypotony produced a 33% decrease in diffusional water flow. This decrease could not be ascribed to an

effect at the apical membrane.

Discussion

Compared to non-polarized cells, epithelial cell layers are subjected to extra demands imposed by the transepithelial fluid flow. Not only must these epithelial cells synchronize the fluid flow across the apical and basolateral side, but they must regulate their volume when exposed from the apical and basolateral side simultaneously to solutions of different osmolarity.

This is the case when the isolated urinary bladder is bathed on its mucosal side with a hypotonic solution to test the effect of AVP. It is well known that since the apical membrane has low water permeability, little water flow is observed in the un-stimulated condition and the morphological appearance is normal. On the contrary, hypotonic solutions on the serosal side produce, in the un-stimulated bladder, a swelling of the epithelial cells and an increase in the water flow from serosal to mucosal (from 1.8 to 24 μl/min per sac; Table I). These results can be interpreted as a consequence of the relatively large water permeability of the basolateral side. Water easily flows into the cells from the serosal side, but cannot easily leave across the apical side producing the observed swelling and the morphological distortion which could be responsible for the increase in serosal-to-mucosal J_v. Since the cells do not burst even though the osmolarity of the serosal solution is only $\approx$25 mOsm, a volume regulatory decrease mechanism must be operational in this condition. It should be noted that

while the cell regulates its volume and osmolarity to adapt to that of the serosal bath, it deviates from its own normal osmolarity and from the isotonic solution present in the apical bath. This steady state, with cell osmolarity similar to that in the basolateral bath, is achieved because of the relatively low apical water permeability.

When the mucosal bath is hypotonic and the apical permeability is increased by AVP, the transepithelial flow from mucosal to serosal increases considerably and the cells swell moderately . One can argue that as the apical membrane becomes more permeable, water cell volume increases, but because of the normally high water permeability of the basolateral membrane, water leaves the cell across that surface establishing a high transepithelial flow with a moderately swollen epithelium with cell osmolarity at a value between the 24/240 apical/basolateral bath osmolarity. The preceding analysis has been repeatedly described by many to explain the AVP stimulatory effect on water flux [10, 15, 20] and some of the present experiments are simply confirmatory. However, the failure of AVP to elicit a water flow in opposite but symmetrical conditions (with the serosal bath hypotonic) has not been adequately explained. After all, it would be expected that after the initial swelling elicited by serosal hypotonicity, AVP, by triggering the insertion of water channels in the apical membrane, should establish a large water flow from serosal to mucosal. This expected result does not occur and on the contrary a small inhibition in flow is observed. This anomalous result has been explained as AVP not exerting its effect on the apical membrane for a variety of reasons including diluted cell components, and interference with the signaling mechanism from the receptor onwards [8]. We thought that an

alternative interpretation was that as the cell swelled, its basolateral water permeability decreased to prevent a sudden cell burst, until the conventional volume regulatory mechanisms could cope with the substantial osmotic challenge. The only mechanisms of water permeability regulation so far described are that of insertion/internalization of aquaporin 2 by AVP [2] and Cl^- activation of water channels in the frog corneal epithelium [5]. Thus, it is possible that the membrane-resident basolateral water channels [21] may be regulated by a comparable mechanism. The main appeal of this hypothesis was that it could be tested experimentally by measuring J_{dw} in either direction with or without an osmotic gradient before and after AVP. This was a definite advantage over the measurement of J_v which always requires an osmotic gradient and precludes a comparison of the value of P_f between control and hypotonic conditions. As shown in Table II after the stimulation of J_{dw} by AVP in isotonic conditions, basolateral hyposmolarity produced a statistically significant inhibition of J_{dw}. This could only occur if the permeability of either the apical or basolateral membrane decreased as a consequence of the basolateral bath hyposmolarity. The effect was fully reversible indicating its functional regulatory nature rather than a permanent change in tissue properties. As indicated before, both unidirectional fluxes were equally affected by AVP and basolateral hyposmolarity. Thus, no rectification on J_{dw} was observed but rather a simple decrease in overall permeability. Table III showed basolateral hyposmolarity made the preparation more permeable to water. We can only assume that as the cells were swelling, pressure developed inside the cells which contributed to the larger values of J_{dw}. As water channels were inserted into the apical

membrane, pressure was released, the permeability of the basolateral membrane decreased becoming rate limiting and a decrease of the overall permeability was observed. Again, the effects were fully reversible and identical on both unidirectional fluxes. To ascertain that the inhibition of water permeability by serosal hypotony was an effect on the basolateral membrane we studied its effect independently of AVP by permanently increasing the water permeability of the apical membrane with amphotericin B. As seen in Table IV serosal hypotonicity significantly reduced J_{dw} after it was increased by the permeabilization of the apical membrane. Since the permeability of the apical membrane is permanently increased with the basolateral side becoming rate limiting, the overall decrease in J_{dw} (in both directions) can only be interpreted as a reduction in basolateral water permeability, which is also consistent with the lack of AVP effect on J_v b→a even if the apical membrane permeability was increased by the hormone. This influence of serosal bath tonicity on basolateral water permeability has also been observed in the isolated frog corneal epithelium where a similar rectification of J_v and inhibition of J_{dw} has been reported [6]. It is not surprising that epithelial cells possess mechanisms to control water movement across its membrane as it is the case with ion channels. The finding that "aquaporins" are located on the basolateral membrane of renal epithelia [11], suggest that these water channels may be regulated, in part, by changes in volume or osmolarity. Although the triggering signal seems to be cell volume the signaling mechanisms need to be elucidated.

Acknowledgment

This work was supported by the U.S. Army Medical Research and Development Command under Contract 17-95C-5086 and National Eye Institute grants EY00160 and EY01867. We would like to thank A. Dibas, C. Hulet and A. Zamudio for technical assistance. The views, opinions and/or findings contained in this report are those of the authors and should not be construed as an official Department of the Army position, policy or decision unless so designated by other documentation.

References

1. Bentley PJ (1958) The effect of neurohypophyseal extracts on water transfer across the wall of the isolated urinary bladder of the toad *Bufo marinus. J. Endocrinol* 17, 201-219.

2. Brown D (1989) Membrane recycling and epithelial cell function. *Am J Physiol* 256, F1-F12.

3. Brown D, Katsura T, Kawashima M, Verkman AS, Sabolic I (1995) Cellular distribution of the aquaporins: a family of water channel proteins. *Histochem Cell Biol* 104, 1-9.

4. Candia OA (1972) Ouabain and sodium effects on chloride fluxes across the isolated bullfrog cornea. *Am J Physiol* 223(5),1053-1057.

5. Candia OA, Zamudio AC (1995) Chloride-activated water permeability in the frog corneal epithelium. *J Mem Biol* 143, 259-266.

6. Candia OA, Zamudio AC (1997) Osmotic regulation of water permeability across the frog corneal epithelium. *Invest Ophthalmol Vis Sci* 38 (4), S683.

7. Candia OA, Mia AJ, Yorio T (1993) Influence of filter supports on transport characteristics of cultured A6 kidney cells. *Am J Physiol* 265, C1479-C1488.

8. Eggena P (1972) Osmotic regulation of toad bladder responsiveness to neurohypophysenl hormones. *J Gen Phys* 60, 665-678.

9. Finkelstein A (1987) Water movement through lipid bilayers, pores, and plasma membranes: theory and reality. *Distinguished Lecture Series of the Society of*

General Physiologists, v 4, Wiley-Interscience, New York, 1-228.

10. Hays RM, Leaf A (1962) Studies on the movement of water through the isolated toad bladder and its modification by vasopressin. *J Gen Physiol* 45, 905-919.

11. Ishibashi K, Sasaki S, Fushimi S, Uchida M, Kuwahara H, Saito T, Furukawa K, Nakajima Y, Yamaguchi T, Gojobori, Marumo F (1994) Molecular cloning and expression of a member of the aquaporin family with permeability to glycerol and urea in addition to water expressed at the basolateral membrane of kidney collecting duct cells. *Proc Natl Acad Sci USA* 91, 6269-6273.

12. Jo I, Harris Jr HW (1995) Molecular mechanisms for the regulation of water transport in amphibian epithelia by antidiuretic hormone. *Kidney Int'l* 48, 1088-1096.

13. Knepper MA (1994) The aquaporin family of molecular water channels. *Proc Natl Acad Sci USA* 91, 6255-6258.

14. Levitt, DG (1981) Routes of membrane water transport: comparative physiology. *Alfred Benzon Symp* 15, 248-257.

15. Mendoza SA, Handler JS, Orloff J (1967) Effect of amphotericin B on permeability and short-circuit current in toad bladder. *Am. J. Phys* 213, 1263-1268.

16. Mia AJ, Oakford LX, Yorio T (1994) Surface membrane remodeling following removal of vasopressin in toad urinary bladder. *Tissue and Cell* 26, 189-201.

17. Mia AJ, Tarapoom N, Carnes J, Yorio T (1983) Alteration in surface

substructure of frog urinary bladder by calcium ionophore, verapamil and antidiuretic hormone. *Tissue and Cell* 15, 737-749.

18. Parisi M, Candia O, Alvarez L (1980) Water permeability of the toad corneal epithelium: the effects of pH and amphotericin B. *Pflügers Archiv*, 383, 131-136.

19. Parisi M, Bourguet J (1983) The single file hypothesis and the water channels induced by antidiuretic hormone. *J Mem Biol* 71, 189-193.

20. Singer I, Civan MM, Baddour, Leaf A (1969) Interactions of amphotericin B, vasopressin and calcium in toad urinary bladder. *Am J Physiol* 217, 938-945.

21. Van Der Goot F, Corman B, Ripoche P (1991) Evidence for permanent water channels in the basolateral membrane of an ADH-sensitive epithelium. *J Mem Biol* 120, 59-65.

22. VanOs CH, Deen PMT, Dempster JA (1994) Aquaporins--water selective channels in biological membranes--molecular structure and tissue distribution. *Biochim Biophys Acta* 1197, 291-309.

Figure Legends

Fig. 1 SEM of control toad urinary bladder with a mucosal to serosal osmotic gradient for 30 min. showing distribution of granular cells with smooth surface configuration and cellular demarcation. X450.

Fig. 2 SEM of complementary experimental toad urinary bladder (Fig. 1) with a serosal to mucosal osmotic gradient for 30 min. showing vivid cellular swelling and caving of the basolateral junctions. X450.

Fig. 3 SEM of AVP-stimulated toad urinary bladder with a mucosal to serosal osmotic gradient for 30 min. showing minimal tissue swelling as that of the control tissue (Fig. 1) with some apical membrane invaginations in the AVP-stimulated tissues. X450.

Fig 4. SEM of AVP-stimulated experimental toad urinary bladder with a serosal to mucosal osmotic gradient for 30 min. showing vivid cellular swelling as compared to that of the control tissues (fig.2) with formation of some apical membrane invaginations (fig. 4) X450.

Table I. Water flow across toad urinary bladders under a reversed osmotic gradient

Treatment	Period I Basal Conditions	Period II +AVP	Period III Washout + AVP
Control (M to S gradient)	**1.8** ±0.3	**19** ±1.4	**15** ±0.8
Experimental (S to M gradient)	**24** ±2*	**14** ±1.7*	**25** ±5.1*

Values are water flow in μl/min per bladder sacs.

Results as mean ±SE of six paired experiments. *$p<0.05$ for differences from control.

The osmotic gradient was created by diluting the solution bathing either the mucosal or serosal surfaces of the bladder with 1/10 N-Ringer's solution. In period III the solutions bathing the Experimental bladder were replaced and an osmotic gradient from M to S was established as in the Control bladder tissue.

Table II. Sequential effects of vasopressin and basolateral hypo-osmolarity on diffusional water flux (J_{dw}) across the frog urinary bladder

	Control 240 mOsm both sides	AVP (20mU/$\mu\ell$) basolateral bath	AVP+ Basolateral Hypo-osmol. = 40mOsm	240 mOsm +AVP
Mean ± SE	**12.2** ±1.6	**20.2**** ±3.0	**17.1*** ±5.4	**24.5**** ±5.5

Values are mean ± SE in μl/min·cm^2

n=5

** significantly larger than in preceding condition. P<0.01 as paired data.

* significantly smaller than in preceding condition. P<0.01 as paired data.

Table III. Sequential effects of basolateral hypo-osmolarity and vasopressin of diffusional water flux (J_{dw}) across the frog urinary bladder

	Control 240 mOsm both sides	Basolateral Hypo-osmol. = 40mOsm	AVP (20mU/$\mu\ell$) +Basolateral Hypo-osmolarity	240 mOsm +AVP
Mean ± SE	**9.5** ±0.8	**11.7**** ±1.4	**10.2*** ±1.3	**20.2**** ±2.9

Values are mean ± SE

n=7

** significantly larger than in preceding condition. P<0.01 as paired data.

* significantly smaller than in preceding condition. P<0.01 as paired data.

Table IV. Effects of amphotericin B and basolateral hypo-osmolarity on diffusional water flow across the frog urinary bladder

	Control	Amphotericin B (10^{-5}M Apical)	Basolateral hypo-osmol. = 40mOsm
Mean ± SE	**7.4** ±0.3	**12.9** ±0.9	**8.7*** ±1.0

n=6

* significantly smaller than in previous condition. $P<0.01$ as paired data.

Values are in $\mu\ell/min \cdot cm^2$.

J_{dw} was measured in both directions and the effects of amphotericin B and hypo-osmolarity were similar.

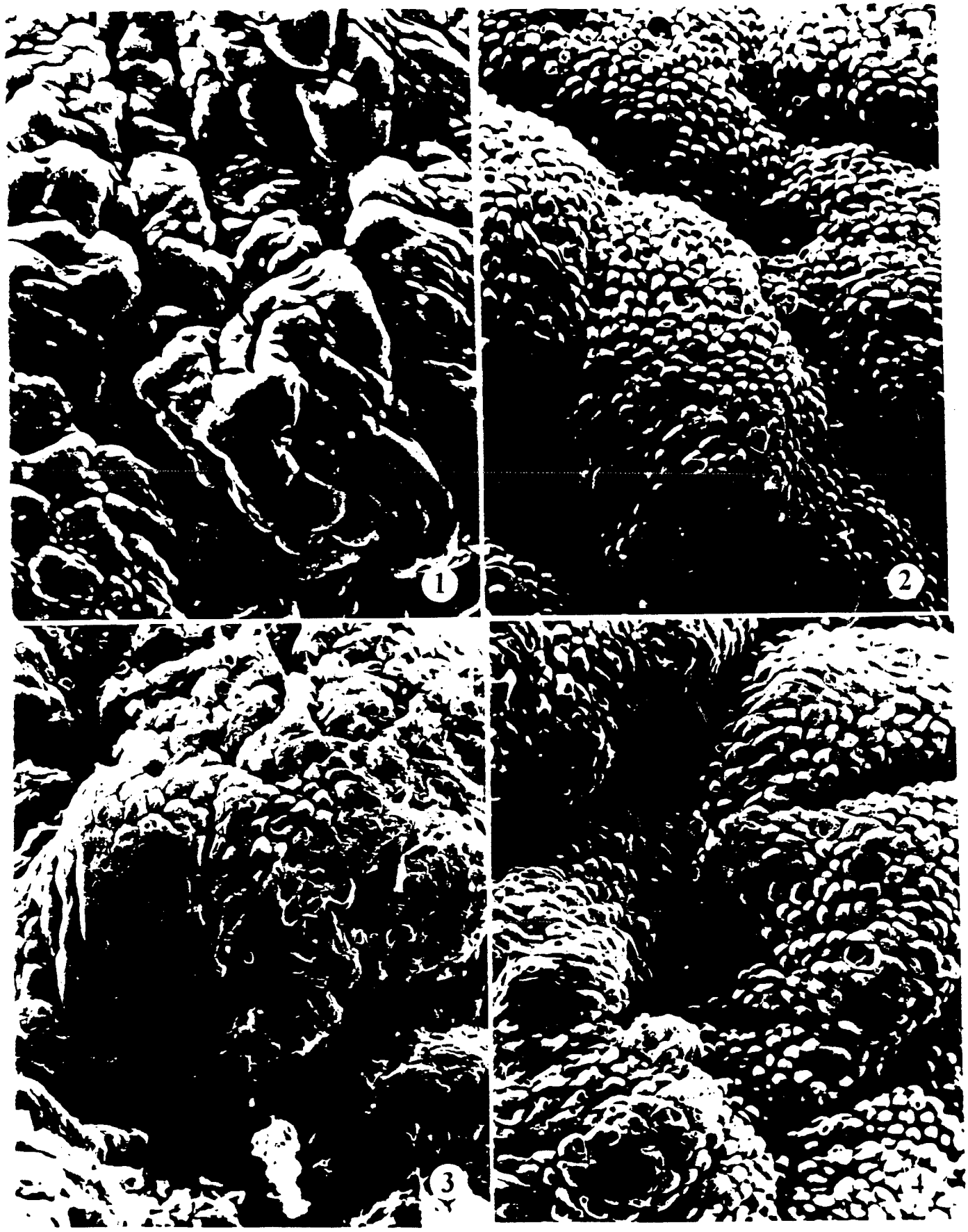
1
2
3